Saroj Thapa

Development of a fossil-free heating system for chicken barns based on heat pumps and thermal storage

July 2023

Master's thesis

NTNU
Norwegian University of
Science and Technology

NTNU
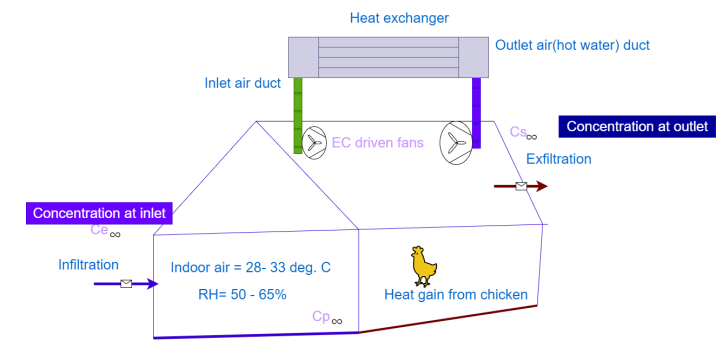
**Norwegian University of
Science and Technology**

Development of a fossil-free heating system for chicken barns based on heat pumps and thermal storage

Saroj Thapa

Preface

This is the Master Thesis of Saroj Thapa written during the final year the of master's study program in Sustainable Energy at the Department of Energy and Process Engineering at the Norwegian University of Science and Technology (NTNU). The research work was carried out during the Fall of the year 2023.

The primary focus of this thesis involved comprehensive literature reviews on the existing techniques for heating the poultry houses, the integration of heat pumps with solar, and thermal storage. This research led to design of potential layouts for poultry house heating, leveraging heat pump technology. An integral part of this thesis was also the creation and utilization of heat pump in Modelica (Dymola) to investigate the energy flow. This thesis also analysis the potential of drying the concrete floor after cleaning the poultry farm.

I would like to take this opportunity to express my deepest gratitude to my supervisor, **Prof. Dr.-Ing. Armin Hafner** and co-supervisor **Dr. Håkon Selvnes,** whose invaluable guidance helped shape this research. I also extend my heartfelt appreciation to **Hanne Laura Pauliina Kauko,** who support allowed me to grasp the fundamental elements of the project. I am grateful to **Professor Dr. Trygve Magne Eikevik** for his invaluable assistance in developing the concept of drying system.

I wish to acknowledge the contribution of **Engin Söylemez,** which was instrumental in the successful completion of the project. I would like to thank Luca Contiero, and Muhammad Zahid Saeed for guiding me to learn Modelica and express my profound gratitude for their motivation and support.

Additionally, I was fortunate to spend my summer as a "sommerorsker" (summer scientists) at SINTEF Energy, where I was part of a project by HighEFF. This assignment, which involved computing the energy needs of an Inderøy Poultry farm owned by Norsk kylling As, to boost its energy efficiency using heat pumps, added significantly to my learning experience in sustainable energy and heat pumping processes and systems.

It is my sincere hope that the findings of this project will contribute to the advancement of sustainable energy practices.

Abstract

As global poultry meat consumption continues its upward trajectory, it casts an inevitable spotlight on its sizable environmental footprint, particularly the considerable CO_2 emissions associated with broiler consumption. To reconcile the growing demand with the need for sustainability, this study proposes the integration of renewable, economically viable heating and cooling systems within the poultry industry, consistent with the European Union's commitment to carbon reduction and energy affordability.

At present, pellets boilers are used to maintain the temperature inside the farm. Energy consumption was conducted to log energy consumption in poultry farms. The resulting uncertainty analysis of energy consumption data demonstrated a low error margin, estimated at 0.41%.

The study then delved into an evaluation of alternative heating and cooling systems, focusing on the performance of a 120 kW CO_2 heat pump. Among the diverse configurations simulated, the system featuring a Flash Gas Bypass Valve (FGBV) and parallel evaporators delivered the most impressive Coefficient of Performance (COP), fluctuating between 4 to 4.6 in response to various source loads. In contrast, the setup utilizing the city water as a source manifested a steady state COP of 3.6.

To assess system efficiency, the calculated drying time for a 2 cm water film on a 2000 m^2 concrete surface. When 50 °C air was uniformly distributed at an air velocity of 1 m/s is 23 hrs. Notably, slow, and steady airflow led to more effective drying than high flow rates, indicating significant potential for energy savings. The process resulted in high relative humidity at the exit, due to moisture absorption from the concrete surface.

Annual energy production was calculated for new and old poultry farms at 145.1 MWh and 73.1 MWh. The new farm exhibited peak monthly energy production exceeding 20 MWh during May, June, and July, with December registering the minimum output.

This research underscores the transformative potential of fossil-free heating and cooling systems. By fusing environmental stewardship with improved productivity and economic viability, these novel systems could herald a new era in sustainable poultry production.

Sammendrag

Mens det globale forbruket av fjørfekjøtt fortsetter sin oppadgående trend, rettes det uunngåelige søkelyset mot den betydelige miljøpåvirkningen, spesielt de betydelige CO_2-utslippene knyttet til konsum av kyllingkjøtt. For å forene den økende etterspørselen med behovet for bærekraft, foreslår denne studien integrasjonen av fornybare og økonomisk levedyktige oppvarmings- og kjølesystemer innen fjørfenæringen, i tråd med Den europeiske unions forpliktelse til karbonreduksjon og rimelig energi.

For øyeblikket brukes pelletskjeler til å opprettholde temperaturen inne på gården. Energiforbruket ble logget for å registrere energiforbruket på fjørfegårder. Den resulterende usikkerhetsanalysen av energiforbruket viste en lav feilmargin, estimert til 0.41 %.

Studien gikk deretter inn på en vurdering av alternative oppvarmings- og kjølesystemer, med fokus på ytelsen til en 120 kW CO2-varmepumpe. Blant de ulike konfigurasjonene som ble simulert, viste systemet med en Flash Gas Bypass Valve (FGBV) og parallelle fordampere den mest imponerende ytelsen, med en effektfaktor (COP) som varierte mellom 4 – 4.6 som svar på ulike belastninger. Sammenlignet med det oppsettet som brukte byvann som kilde, hadde dette oppsettet en stabil COP på 3.6 i likevekt.

For å vurdere systemets effektivitet ble tørketiden for en 2 cm vannfilm på en 2000 m^2 betongoverflate beregnet. Når luft med en temperatur på 50 ℃ ble jevnt fordelt med en luftfart på 1 m/s, var tørketiden 23 timer. Bemerkelsesverdig førte sakte og jevn luftstrøm til mer effektiv tørking enn høye luftstrømningshastigheter, noe som indikerer betydelig potensial for energisparing. Prosessen førte til høy relativ luftfuktighet ved utløpet på grunn av fuktighet som ble absorbert fra betongoverflaten.

Årlig energiproduksjon ble beregnet for nye og gamle fjørfegårder til henholdsvis 145.1 MWh og 73,1 MWh. Den nye gården viste en topp månedlig energiproduksjon på over 20 MWh i mai, juni og juli, mens desember registrerte den laveste produksjonen.

Denne forskningen understreker det transformative potensialet til fossilfrie oppvarmings- og kjølesystemer. Ved å forene miljøansvar med forbedret produktivitet og økonomisk bærekraft, kan disse nye systemene innlede en ny æra innen bærekraftig fjørfeproduksjon.

List of Abbreviations/ symbols

LMTD = Logarithmic Mean Temperature difference

NPK = Nitrogen, Phosphorous and Potassium

GHGs = Greenhouse gases

PV = Photovoltaics

COP = Coefficient of Performance

CFCs = Chlorofluorocarbon's

HCFCs = Hydrochlorofluorocarbons

PFCs = Perfluorocarbons

ODP = Ozone depletion potential

GWP = Global Warming Potential

NBP = Normal Boiling Point

GSHP = Ground source Heat Pump

ASHP = Air source heat Pump

DSM = Demand side management

SAHP = Solar assisted heat pump

TES = Thermal Energy Storage

CTES = Cold Thermal Energy Storage

SMER = Specific Moisture extraction rate

CAD = Computer aided design

MSP = Market selling price

EC = Electronically commutated

ppm = parts per million

Units /Symbols

MT = Megatons

MWh = Megawatt's hour

kWh = Kilowatt hour

m = meter

GJ = Gigajoule

£ = Pound

$ = dollar

NOK = Norwegian kroner

GW = Gigawatt

TWh = Terawatt hour

Mtoe = Megatons of oil equivalent

Subscripts

m_r = mass of refrigerant

h_{2s}, h_1, h_3, h_4 = enthalpy at point2s ,1, 3 and 4 respectively

W_{is} = isentropic work

η_{is} = isentropic efficiency

Q_c = condenser load

Q_e = evaporation load

COP_h = COP of heat pump

COP_r = COP of refrigeration

T_{cr} = critical temperature

P_{cr} = critical pressure

Table of Contents

List of Figures

List of Tables

1   Introduction

This chapter explores the environmental and economic context of the poultry industry, with an emphasis on the need of sustainable heating solutions for poultry farms. It also outlines the rise of in global poultry consumption, the environmental impact of various meat sources, the current heating methods employed by the poultry industry, and the potential benefits of adopting more sustainable and energy-efficient alternatives.

1.1   Background and Motivation

The poultry industry contributes significantly to global meat production, with the per capita supply of eggs doubling and the poultry meat supply increasing sixfold since the 1960s. Poultry is a major source of protein worldwide [1]. Additionally, poultry waste or manure is utilized in crop cultivation as nitrogen, phosphorous, and potassium (NPK) fertilizer. The poultry industry generates approximately 5 kg of manure per chicken per year, which translates to 25731 MT of poultry manure applied to soil annually. This highlights the dual benefits of poultry farming, providing both meat and fertilizer for crops [1].

Global poultry meat consumption increased by 1.4% from 87.8 million MT in 2020. Meat consumption has a direct impact on the environment, with chickens producing less CO_2 than other edible animals. A shift from beef, pork, and other meats to chicken is occurring to reduce global CO_2 emissions. In 2019, researchers determined that producing 1 kg of beef generates 60 kg of CO_2 equivalents, while lamb and pork produce 20 kg and 7 kg, respectively. In comparison, poultry emits only 6 kg of CO_2 equivalents, making its production the most environmentally friendly among sources [2].

In the current context, Norway's meat consumption is transitioning from other meats to chicken for various reasons [3]. Broiler consumption produces 693 tons of CO_2 equivalents, while beef production generates 0.08 MT of CO_2 equivalents in 2021. Therefore, the adoption of renewable, economically viable heating and cooling systems is crucial to meet the growing demand for broiler meat in Norway while minimizing environmental impact [4].

Currently, over 62 million chickens are raised in Norway. Approximately 857 poultry companies operate in the country to meet the demand for meat [5]. Most poultry farms use propane dual-based heating systems, with some relying on bio-pellets, fossil fuels, and oil heaters for broiler house heating. However, these methods are not as cost-effective as heat pumps. Heat pump systems outperform traditional heating systems in terms of efficiency (COP), cost, and payback. For instance, a standard 73 m x 18 m broiler house with 27,000 chickens consumes between 240-266 MWh of heat energy, equivalent to 23,000-26,000 liters of kerosene heating oil and 35,000 kWh of electricity [6]. To reduce payback periods, the introduction of new technology is essential.

The European Union has set goals to reduce CO_2 emissions to achieve sustainable development and curb high energy prices. As a result, transitioning from fossil fuel-based heating systems to fossil-fuel free alternative is crucial. Poultry farms consume significant amounts of energy, leading to considerable greenhouse gas (GHG) emissions. These emissions from broilers and heating systems in poultry farms contribute to air pollution, posing potential risks to farmers, livestock, and nearby residents.

Energy consumption in poultry farms is expected to rise in the coming years due to increased mechanization and automation, aiming to meet the nutritional demands of a growing population. Temperature, humidity, air quality, and lighting control account for a large share of energy consumption in a poultry farm. Enclosed poultry farm buildings require substantial energy for microclimate control. In general, poultry houses consume between 30-130 kWh/m^2 (0.87 to 0.89 kWh per bird) or energy needed to produce meat per kg varies from 0.25 to 0.48 kWh.

Hence, fossil-free heating systems offer potential cost savings and improved energy efficiency for poultry farms. By utilizing renewable energy sources and advanced technology, these systems can provide control over temperature, humidity, and air quality within the farm, resulting in optimized growth conditions for poultry and improved overall productivity.

Furthermore, the implementation of thermal energy storage solutions offers additional advantages. By employing phase change materials (PCMs) and other innovative storage methods, excess heat generated during non-peak hours can effectively be stored and utilized when needed. This ensures consistent thermal comfort for the poultry, reducing energy consumption and associated costs.

Moreover, the integration of renewable energy sources, such as solar power and biogas, contributes to the circular economy. Solar energy can be harvested through photovoltaic cells on the roof of the poultry farm, while biogas generated from chicken manure can be used to power heating systems. Both methods reduce the farm's reliance on fossil-fuels and promote sustainable energy practices.

Lastly, incorporating advanced cleaning and drying processes within the farm can minimize the risk of disease transmission while optimizing drying time and energy savings. Wet cleaning methods, for example, help reduce the aerosolization of viruses and ensure a healthier environment for both poultry and farm workers.

In summary, the motivation for developing fossil-free heating systems and thermal energy storage in poultry farms lies in the pursuit of environmentally sustainable, economically viable, and efficient solutions. These advancements have the potential to revolutionize the poultry industry, reduce its environmental impact, and contribute to a more sustainable future.

1.2 Literature Survey

This deals with study of poultry farm heating using heat pump system, assistance of heat pump with solar, and comparison between the conventional heating systems and heat pumps.

1.2.1 Energy Supply system for Poultry farms

There are very few existing studies evaluating the energy consumption of Norwegian or European farms. However, a couple of international examples were found. A study for the energy inputs and output in a part of Iran is studied. This review will also reflect on an interesting study done about the use of ground-source heat pump for heating farm in Poultry in Korea, as well as similar studies for Syria and Peru.

1.2.2 Convention Fossil-based heating system

M.D. Heidari et al. [7] and his team studied to determine the energy consumption for broiler production in Yazd Province of Iran. They collected the data from 44 farms in January-February 2010. The surveyed farms had a capacity of 18,142 birds per farm, and the average meat production was 2610 kg per 1000 birds. In their study, chicken, human labor, machinery, diesel fuel, feed, and electricity are included as input energy sources, whereas broiler and manure are included as output energy sources. Total energy input and output per 1000 birds were found to be 186.89 GJ and 27.46 GJ respectively. The energy input and output of constituent items are given Table 1.

Table 1 Energy equivalents for input and output of broiler production

A. Inputs/ Outputs	Unit	Quantity per unit (1000 bird)	Total energy equivalent MJ (1000 bird)	Percentage
A. Inputs				
Chicken	kg	51.5	531.96	0.28
Human Labor	h	65.27	127.93	0.07

Machinery	kg	3.54	196.06	0.10
Diesel fuel	l	2314.49	11,0632.79	59.20
Feed	kg	5501.49	59,311.40	31.74
Electricity	kWh	4468.26	16,058.73	8.61
B. Output **Broiler**	kg	2601.82	26,876.78	97.87
Manure	kg	1948.11	584.43	2.13

The study concluded that diesel fuel covered the largest share of heating demand, about 59.2%. An average of 2314 liters of diesel is consumed to heat 1000 birds in a poultry farm which was less economic and high investment factor. The shares of each energy input in broiler production are shown in Table 1.
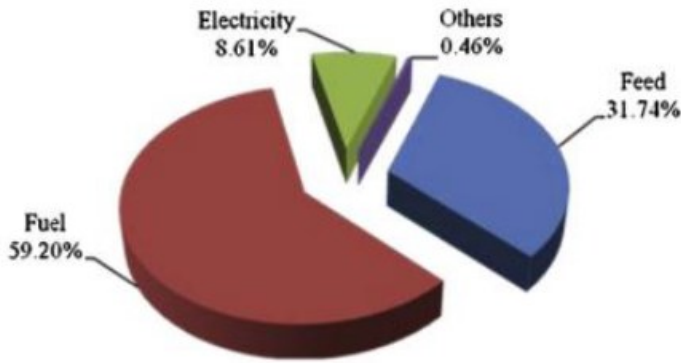
Figure 1-1 The shares of energy inputs in broiler production [7]

In research conducted by Mohamad et al. [8], it was found that Syrian chicken farms consume 173 x 10^3 tons of coal annually which results in an energy demand of 1196 GWh. This significant amount of coal consumption contributes to global warming by emitting 4 x 10^{10} MWh of heat and 3 x 10^{10} tons of CO_2. The study focused on a 500 m^2 chicken farm in Syria to estimate the demand for heating and cooling and compared different heating/cooling systems. The results revealed that the ground source heat pump (GSHP) outperformed all other techniques.

Table 2 demonstrates the COP of the heat pump with different heat sources, coal heater and diesel heater.

Table 2 Comparative analysis of a typical chicken farm for heating and cooling in Syria [8]

	Energy Cost (MSP)				
	Energy demand (GWh/year)	GSHP (3.5 SPkWh^{-1})	ASHP (3.5 SPkWh^{-1})	Coal heater (8141 kWh/kg, 13 SP/kg)	Diesel heater (101 kWh^{-1}, 25 SP^{-1})
Heating	1196	675 (COP=6.2)	1047 (COP=4)	2247 (n=0.85)	3479 (N= 0.85)
Cooling	176	60 (COP=10)	138 (COP=4.3)	138 (COP=4.3)	138 (COP=4.3)
Total	1366	735	1185	2385	3617
	Energy Cost (SPkWh^{-1})	0.54	0.87	1.75	2.65

1.2.3   Heating based on heat pump

Choi et al. [9] studied the use of ground source heat pumps to meet the heating demand of broiler chickens and concluded that the use of a heat pump decreased the mortality rate of chicken significantly due to improved air quality. In this experimental study, 34000 one day old broilers straight-run broiler chickens were assigned to 2 broiler houses with five replicates in every 35 days. This was performed in winter when the outdoor temperature was 10.8 ℃. The conventional (power heater, Samsung, Seol Korea) and ground source heat pump with three oil heaters study is done inside the building, and result has proven that the ground source heat pump has lowest harmful gaseous concentration than other measures as shown in Table 3. Along with ground source heat pump, three oil heaters with same capacity were used, and heaters were only operated at the initial stage to maintain the suitable brooding temperature since the installation of the ground source heat pump (without 3 oil heaters) could not meet the brooding range at an early stage.

Table 3 Gas concentration in the farm due to the heating system [9]

Week	O₂ content (%)		CO₂ content(ppm)		NH₃ content(ppm)	
	GSHP system	Conventional system	GSHP system	Conventional system	GSHP system	Conventional system
1	20.6	20.0	4500	6500	1	3
2	20.7	20.4	3281	4304	4	14
3	20.6	20.8	2803	3967	10	25
4	20.5	20.6	3299	4945	11	20
5	20.4	20.6	3967	3866	15	21
Mean, SD	20.6±0.11	20.6±0.15	3.5±165	4716±108	8.2±5.63	16.6±8.56

During the period of 35 days, the fuel consumption during operation with ground source heat pump together with 3 oil heaters is 160 liters whereas conventional fuel (stand only) used 2813 liters. 92% of the energy is saved by using the ground source heat pump compared to conventional heating systems. Table 4 shows the fuel consumption, electricity consumption and total energy costs for heating in 35 days. It shows that 2147 dollar is a saving obtained by substituting conventional system (fuel heater) with ground source heat pump.

Table 4 Total energy consumption and costs of heating the broiler houses during the experimental period (1-35d) [9]

Item	GSHP System	Conventional system	P-value (Probability)
Fuel consumption (l)	160	2813	0.012
Electricity consumption (kWh)	1905	292	0.000
Total energy cost for heating(won)^2	222,363	2,711,217	0.012
One US dollar = 1,159.87 won (as of January 2010), diesel price = 960 won/L, and electricity price = 36.1 won/kWh (as of January 2010)			

Kwak et al. [10] and performed a thermos-economic analysis on ground source heat pump, and found that unit cost of heat delivered to a poultry farm was calculated to be $0.063 per kWh, for input of electricity with a unit cost of $0.140 per kWh for a ground source heat pump with COP 3.27. They also believed that better result is expected from other heat pump system and stated the unit cost of heat is inversely proportional to COP and directly proportional to electricity input. The greatest losses occur in geothermal heat exchanger whereas the mass of brine flows pipes and in fan coil with complex configuration of pipes in the air passages respectively. Heat pump can control the relative humidity within poultry shed and proves that technology has huge impact to improve birds welfare and generating reliable and low energy cost by saving energy bills from 30-70% than conventional heating LPG or oil**.**

A six 14 kW air source heat pump was installed in Gloucestershire in an area of 1620 m^2 into a poultry shed which was delivered to be poultry shed in England to use such system. With an LPG heater, poultry sheds energy consumption was approximately 3.75 kWh per bird to maintain specific humidity and carbon dioxide level. But it was believed that it would drop below 1 kWh per bird after installation of the heat pump. As expected, operational cost turned out to be about £400 for heat pumps for one cycle of insertion, which would cost £3500 with LPG heaters. This gave the savings of £18000 in a year, proving that heat pumps accounts for less payback period [11].

Alongside, Bokker et al. [12] performed field study in 25 farms to study on the effects of heat exchangers on broiler performance, energy use, and calculated carbon dioxide emission at commercial broiler farms. The study was performed for 25 farms based in different location. Among them,21 farm was in Netherlands, 3 farms in Belgium and 1 in Germany. Each farm had heat exchanger and data were collected from 251 production cycles (with or without a heat exchanger) using Natural gas / Heat exchangers for heating. Gas and electricity were analysed to obtain energy use and CO_2 emission. The surface area of the farm ranges from 885 to 2000 m^2 with maximum air flow capacity of the heat exchanger was 0.35 m^3/h. It was concluded that gas use in the farm was reduced by 38% ($P<0.01$) after the heat exchanger installation whereas three farms were exception. The use of heat exchangers had an increase in the daily weight gain of broilers.

1.2.4　Drying based heat pump

This deals with the mass and energy balance for drying surface/food to obtain designing ideas, working mechanisms for drying system (tunnel drying) along with the description using a psychometric chart, selection of refrigerant for drying system. The drying rate curve is drawn to make the process clearer. The drying process is illustrated in Figure 1-2. It shows A-B is initial adjustment, B-C is the constant rate period of drying, C-D is first falling period, D-E is the second falling rate. When water is evaporates the surface and water is freely available throughout the surface of the product for drying is known as the constant period. When water is still available at the surface, only some part of product has got water film outside. Insufficient water inside product transfers to the outer part from the inner surface and forms a film. At this condition, drying time is regarded as a falling period.
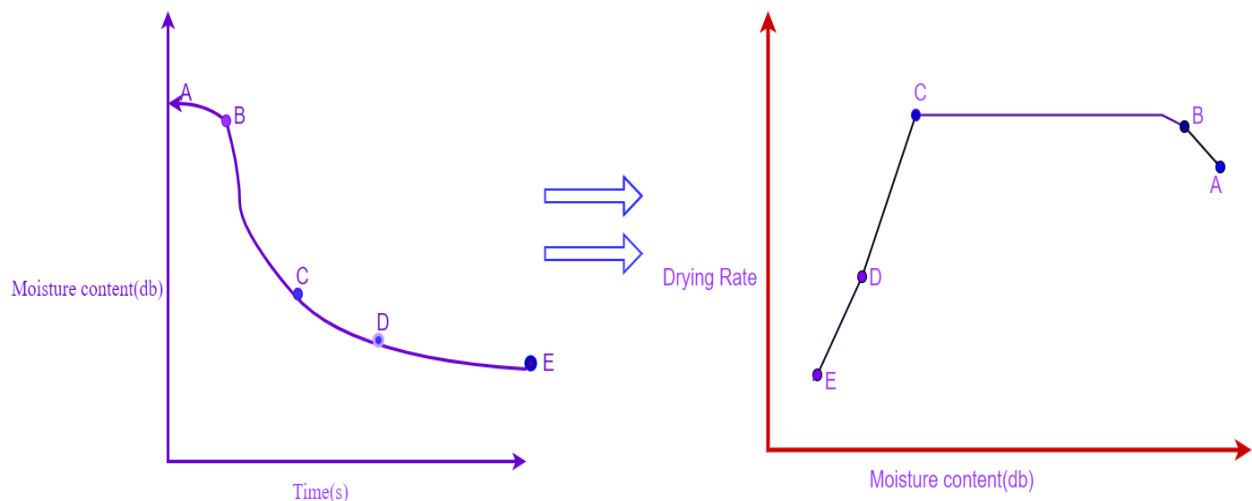
Figure 1-2　Drying rate curve

Various types of drying systems can be introduced depending on the necessity. Some drying systems are tunnel, fluidized bed, and spray drying systems. In a fluidized bed dryer system, the drying air flows through a powder bed, and the product remains in the air with maximum heat transfer when it reaches minimum fluidization velocity. This type of dryers is used in industrial applications like chemical reactors, agglomeration, combustion, and drying. In spray dryers, the feed from liquid condition is sprayed into a warm drying agent. In this phenomenon, the operation takes place in one stage with a continuous liquid feed. Spraying dryers are mostly used to dry the product in powder form [13].

A tunnel drying system can be used for drying the surface, product etc. The behaviour of the tunnel drying system is shown in Figure 1-3. The ambient air is heated to a higher temperature, and relative humidity is decreased significantly. Heated air is supplied through the product containing moisture, so that hot air absorbs the water and is carried towards the exhaust (Point B). The exhaust air can be reused at the inlet to reduce the energy consumption during drying. This phenomenon is explained in the psychometric chart in Figure 1-3.
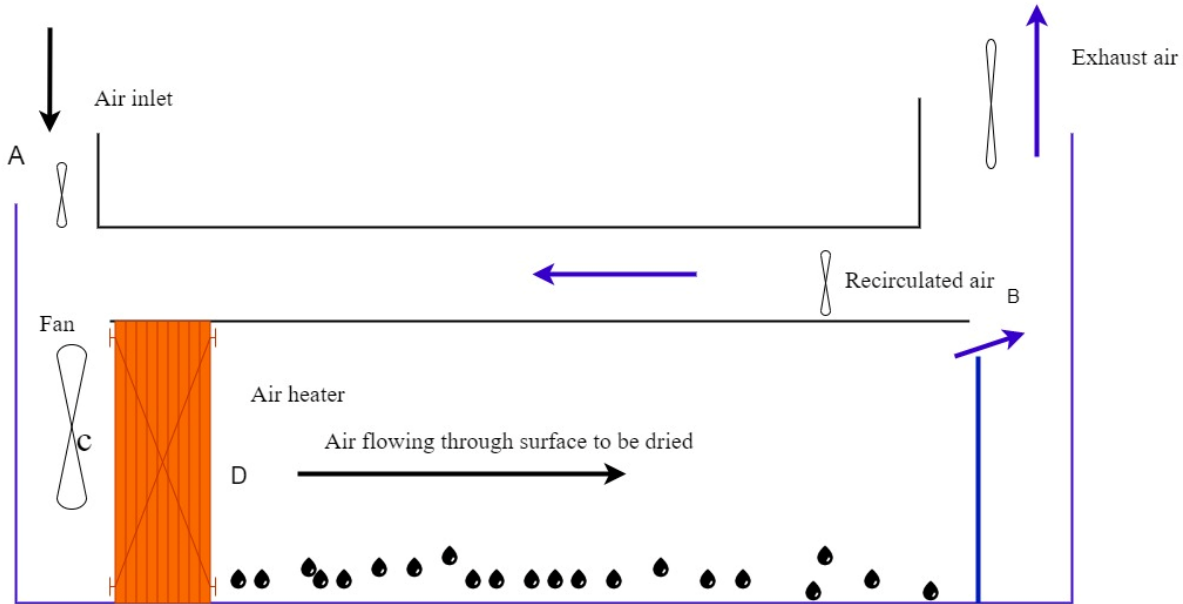
Figure 1-3 Tunnel drying system

In Figure 1-4, ambient fresh air (Point A) is to be heated up to certain condition and blown over the product or surface to be dried. Heating the ambient air reduces relative humidity. It reaches Point B (dry air) before entering the drying tunnel and absorbs the moisture from the surface to be dried (product). Hence, relative humidity increases in the air from Point B to C. The temperature is drops with an increase in humidity because energy to evaporate the water is taken from the air. The air at Point C is recirculated or send to exhaust.

If the air at Point C is recirculated to a drying tunnel or building, the Point C is moved slightly down due to mixing with the ambient source. This reduces Δh will reduce at the same time as ΔX. Hence $\Delta h/\Delta X$ is reduced which gives less energy per kg of water removed, but the drying process take longer.

A heat pump is typically operated in a subcritical zone for drying purposes. However, SINTEF/NTNU has developed the transcritical operation of heat pump for CO_2 as a working fluid has the potential for SMER to increase by 20-30% when the inlet air is 30 to 50 °C [14].
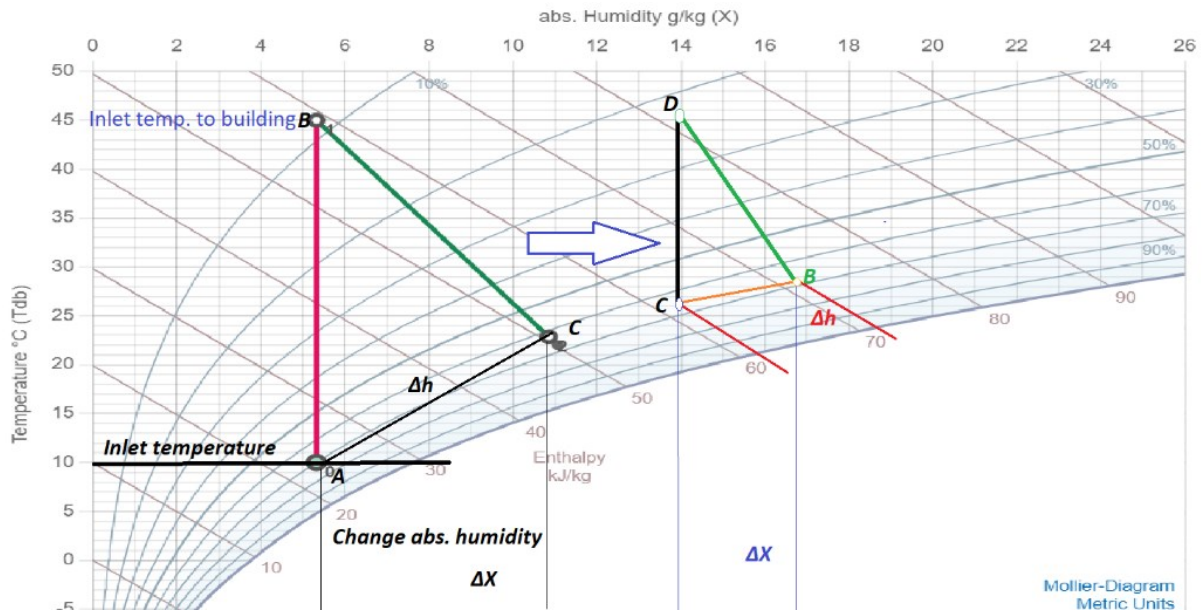
Figure 1-4 Psychometric chart for drying tunnel

The carbon dioxide has a gliding temperature operating at transcritical mode. Hence, it is possible to get desired output for inlet air inside drying chamber at different operating condition. SMER is also a function of inlet air in the drying chamber for different working fluids. The higher the inlet air temperature more will be moisture extraction. SMER of R744 operational under transcritical mode has higher values than other working fluids in subcritical region as illustrated in Figure 1-5.
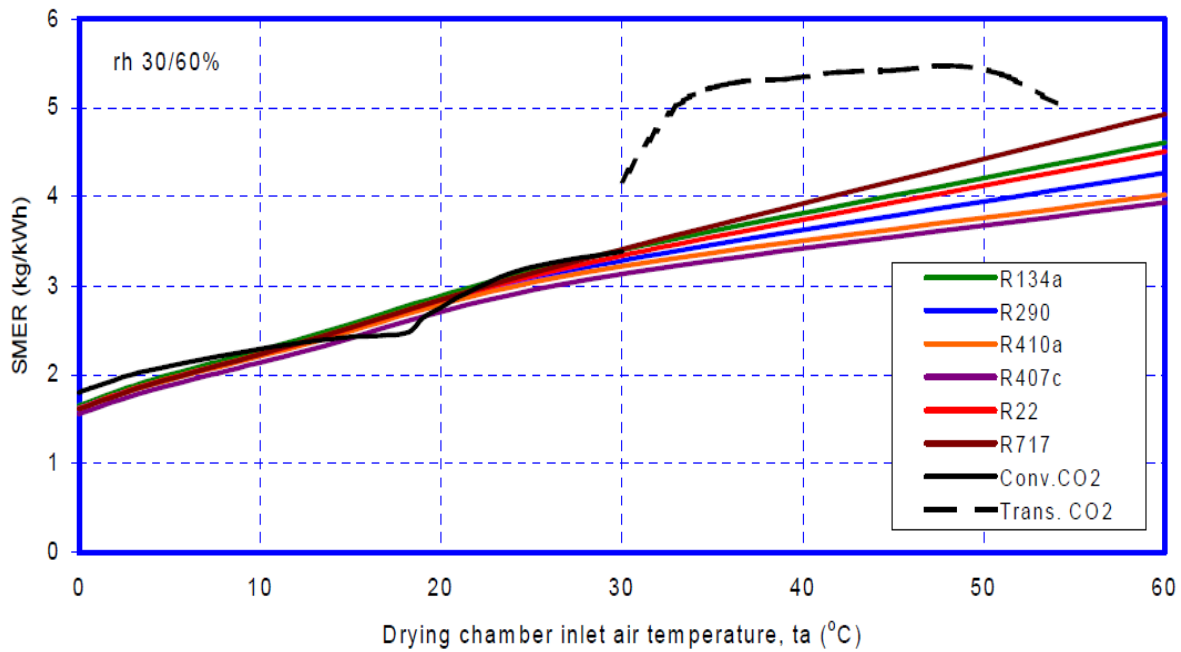
Figure 1-5 Comparison between SMER and inlet air temperature for different refrigerants [14]

1.2.5 Integration of Heat Pumps with Photovoltaic Panels

Hartmann et al. [15] compared solar thermal and solar electric cooling systems for a typical building in two different European locations (Freiburg and Madrid) using TRNSYS. The primary energy savings with a solar PV system is 40% for Freiburg and 60% for Madrid respectively. The investigation shows that a PV system is more reliable for an energy-friendly market. Alessandro et al. [16] analyzed a typical small house of 160 m^2 and a volume of 450 m^3 equipped with a GSHP, assisted by a PV plant of nominal power 3.7 kW and 3.8 kW, respectively. The data analyzed after operating throughout the year gave that energy consumed by GSHP and the energy produced by PV arrays was similar. However, household appliance also receive energy from PV generators due to which electricity is taken from the grid. Hence it is difficult to achieve self-consumption mode (building produces electricity by its own for operation). Elena et al. [17] analyzed the ASHP with a PV system and found that heat pump coupled across different locations in Europe varies on factor like temperature, radiation, and type of system. Heat pump efficiency, thermal losses, and PV

12

efficiency act as a function of temperature. There is no even distribution of solar radiation and heating/cooling demand across Europe. The self-produced energy yearly needs a storage system to use it throughout the year so that the consumer can use it later. The PV system is equipped with a battery (12.5 kWh) to increase the self-consumption rate of electricity produced. In cities like Athens, Palermo and Rome, the solar energy system with batteries could cover 90% of yearly energy use whereas this is 20% in Helsinki even if the building performance is high. Figure 1-6 is the hydronic and control system layout aligned with the electric fluxes.
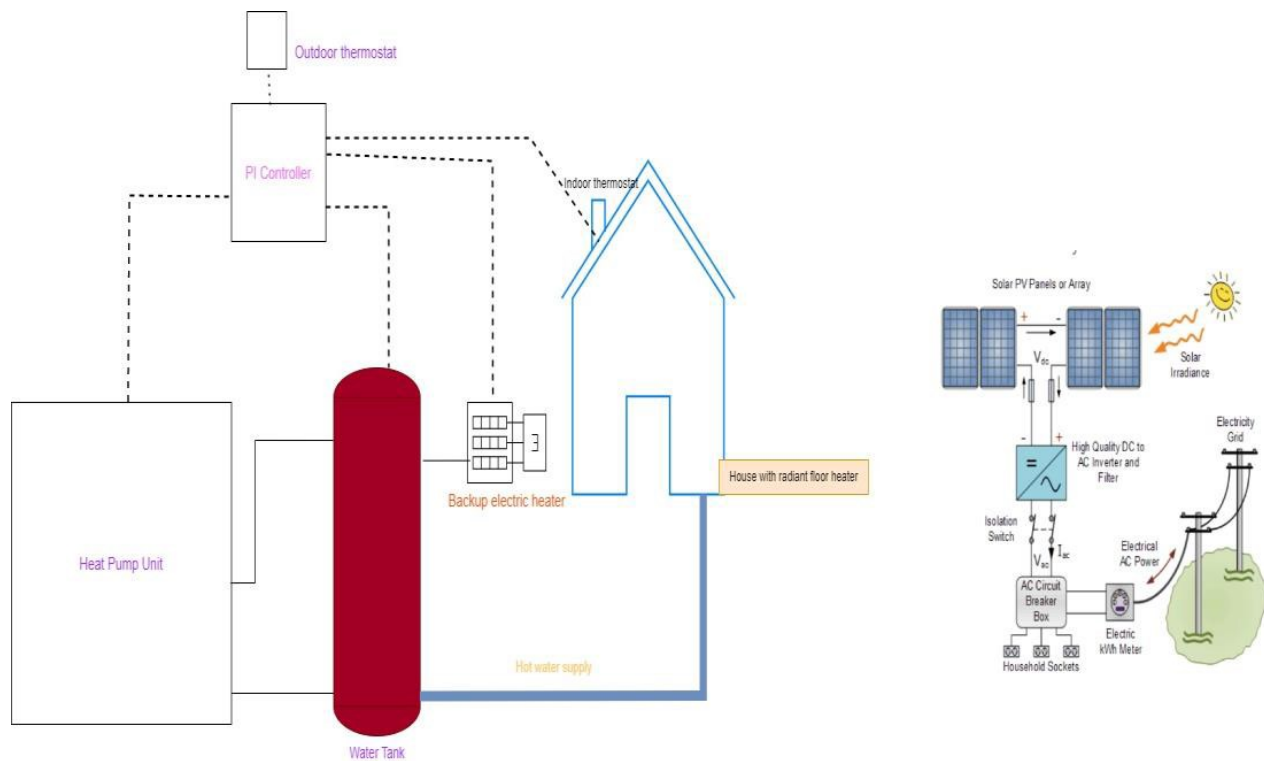
Figure 1-6 Hydronic and control system layout (left) and electricity fluxes(right) [17]

Bakker et al. [18] performed an analysis combining photovoltaic/ thermal panels to generate both heat and electricity simultaneously. The performed analysis was based on Dutch reference model to heat a dwelling of 8.9 GJ for space heating and 10.5 GJ for tap water heating. This Dutch dwelling consists of total area of 132 m^2 of which only 88 m^2 needs to be heated. Floor heating, mechanical ventilation and installation of hot water storage vessel takes place that meets the daily consumption of 170 liters of water. The integrated system layout with heat pump used in the analysis is illustrated in Figure 1-7. PVT panels had a surface area of 25 m^2 that have been modeled

based on the thermal efficiency curve and found that electrical efficiency as Equation 1 and Equation 2.

$$\eta = 0.0968 - 0.00045\,(T_{pv} - 25)$$

Also, thermal efficiency of the PVT panels is expressed as:

$$\eta_{th} = \eta_o - \alpha_1 \frac{T_g - T_a}{I}$$

Where, η is the electrical efficiency, T_{pv} is temperature of photovoltaic cell, T_a is the ambient temperature, T_g is the inlet temperature in PV, α_1 is the heat transfer coefficient, I is the irradiance, η_o is the original/ theoretical efficiency and η_{th} is the thermal efficiency.
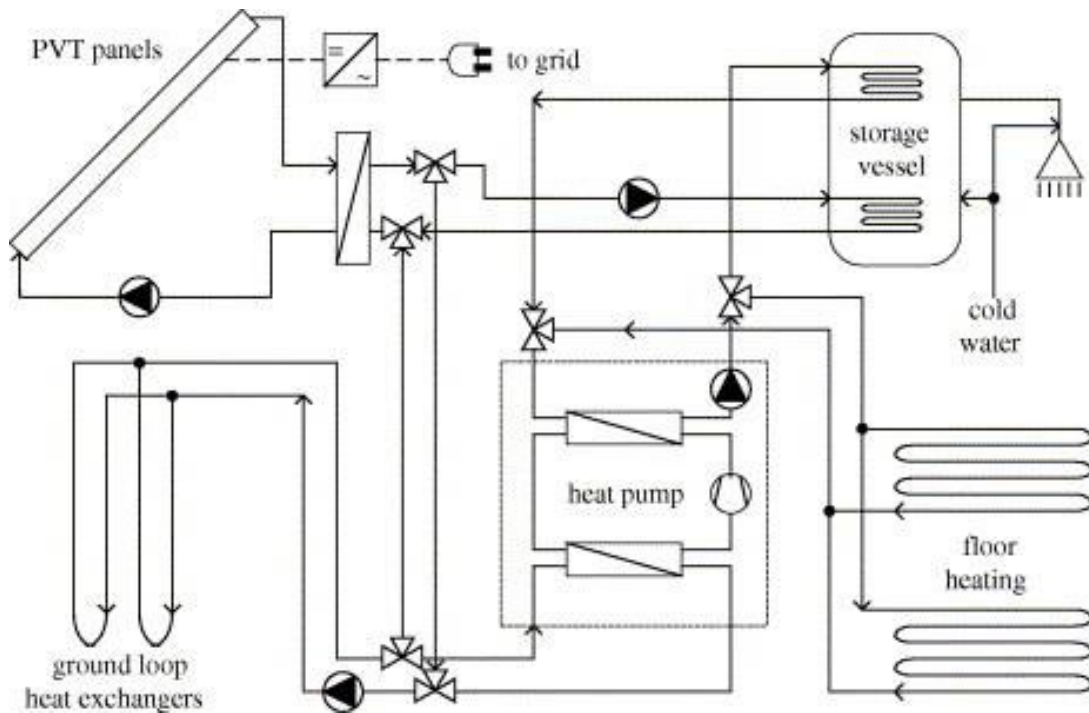
Figure 1-7 Photovoltaic / Thermal (PVT) system with Ground source heat pump [18]

E. Wang et al. [19] designed the dual source solar assisted heat pump which uses two evaporators. The first evaporator is placed in a storage tank loop, and the second evaporator is at outdoor of the heat pump. Hence, the heat pump used either collected solar energy or the air at ambient as a source that ultimately helps to get the highest COP system the highest temperature source. The air source evaporator could be turned off if the storage tank loop evaporator side can cover the whole heating demand of the building as shown in Figure 1-8.
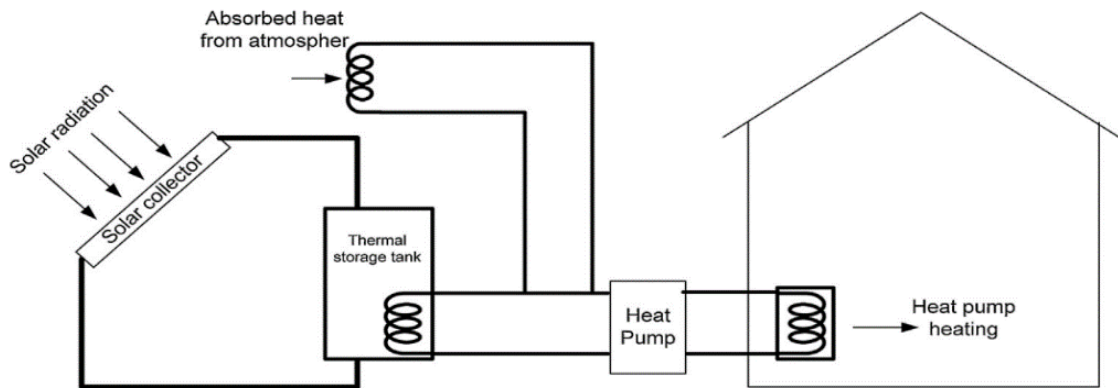
Figure 1-8 Dual source solar assisted heat pump configuration

The comparative analysis was performed by Freeman et al. [20] using three styles of IDX-SAHP systems (series, parallel and dual) for a single house. The results of these systems were compared to the results from conventional heat pump and solar system together. The heat pump systems were utilized for domestic hot water heating. Simulation for these configurations (Figure 1-9, Figure 1-10 and Figure 1-11) was done using TRNSYS and tested for different climatic locations like: Madison, Wisconsin and Albuquerque, New Mexico. The series configuration uses solar storage as a source, parallel configuration used ambient air as a source whereas dual configuration used both air and solar storage, depending on the best performance. With those configurations, dependency of solar combined heat pump on the collector area, number of glazing, main storage volume and collector area ratio were analyzed. The result concluded that parallel combined configuration was the most practical solar heat pump configuration. Thermal performance at a given collector area for series and dual systems were similar.
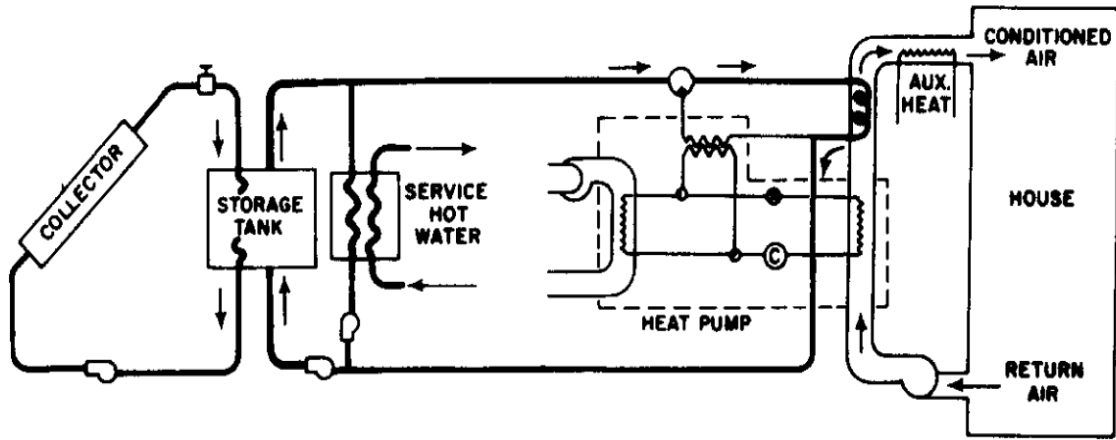
Figure 1-9 Dual source solar combined heat pump
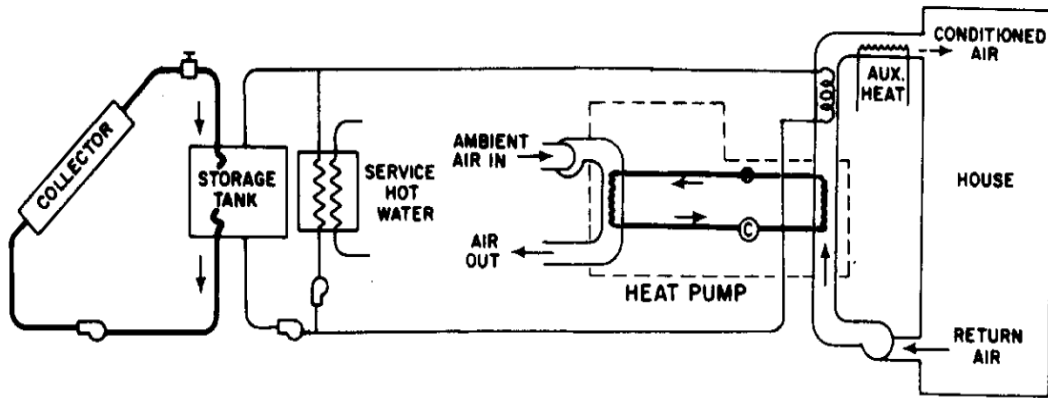
Figure 1-10 Parallel solar assisted heat pump configuration
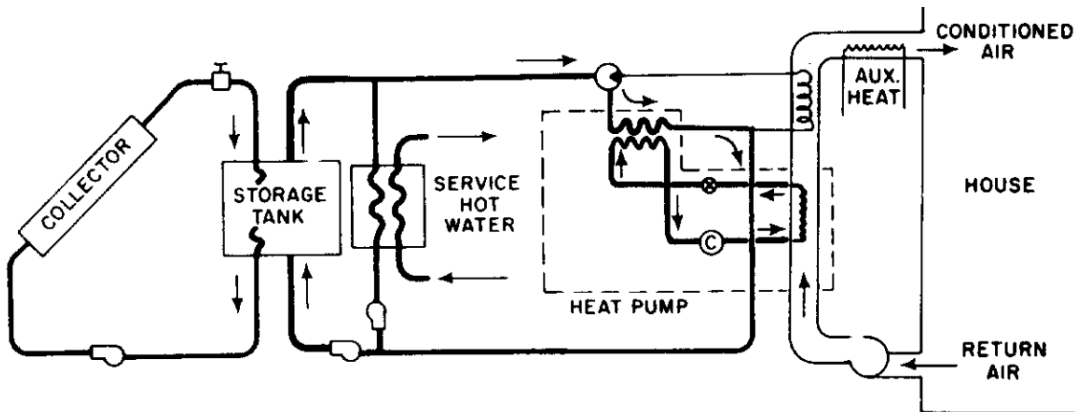
Figure 1-11 Series solar assisted heat pump configuration

1.3 Scope definition

This master's thesis aims to study the effective heating, cooling, and drying process followed by the design procedure of a system for a Norwegian poultry farm. The main objective of this thesis is divided into different sub-goals as follows:

- Review of literature

- Describing current forms of heating for barns standards that must be followed, heat pumping systems that use environmentally correct working media, and thermal energy storage.

- Develop and describe the possible heating concepts for barns based on heat pumps.

- Describe and develop the subsystems for energy distribution and thermal storage.

- Describe and document the energy measurement equipment installed in the demo barn.

- Perform simulation for energy flows.

- Analysis and discussion of the simulated system alternatives and comparison to measured values.

- Describe the possible implementation of the drying technology concept along with heating using a heat pump.

- Master report including first comparisons, discussion, and summary chapter.

- Proposals for further work

- Draft Scientific article

<u>Thesis continuation:</u>

This master thesis will further investigate the proposed heat pump system in an Inderøy poultry farm owned by Norsk kylling. The sensors are fitted to measure thermal energy consumption of

farms. Hence, the uncertainty of energy consumption has been calculated. The possibility of replacing the existing system with a heat pump has been studied. Likewise, comparison of heat pump system best suitable for farm is examined and proposed two system COP is compared. A theoretical calculation is performed to determine drying time of a poultry farm after cleaning.

Hence, the literature survey, theory and other chapters from the project work are relevant to this master thesis work. With the agreement with the supervisors, Armin Hafner and Håkon Selvnes, the most applicable chapters from the project are utilized. This made me convenient to analyze a broader spectrum of existing systems and propose a new sustainable heat pump system. Simulation models are developed using Dymola for two proposed systems. Likewise, ANSYS Fluent is used to see evaporation of the concrete floor on the farm. A layout has been made with the integration of ducted dehumidifier attaching the heat pump system. In addition, a Helioscope has been used to calculate photovoltaic energy production in the farm location.

Report Structure:

This thesis consists of different parts which are explained below:

Chapter 1: Introduction

This chapter gives background information and motivation for the thesis work. The problem statement is briefed and benefits of implementing sustainable solution (heat pump system).

Chapter 2: Literature review

This deals with study of poultry farm heating using heat pump system, assistance of heat pump with solar, and comparison between the conventional heating systems and heat pumps.

Chapter 3: General theory

This chapter gives basic information about the heat pump cycle, thermal storage, and integration of heat pump with PV. Different stages of the heat pump cycle are mentioned in brief, along with the comparison of different working fluids.

Chapter 4: Methodology

In this chapter, methods of the calculation of heat production from chicken, suitable ventilation rate, estimation of drying time with heat pump is analyzed. The software used to analyze is described in short to make familiar during explanation of results.

Chapter 5: Results

This chapter includes the results followed by methodology. First, a description of the newly proposed system is provided along with the details of the main components. The new proposed system is simulated using the software Dymola to find out about efficiency of system and provide high temperature. A theoretical analysis for drying the surface after cleaning is given using a new proposed system. Results from the ANSYS Fluent and integration of heat pump with ducted dehumidifier are analyzed. Alongside, the energy production installing PV panels on the roof of farm is calculated.

Chapter 6: Discussion

The chapter on results elucidates all critical discoveries in a comprehensive and articulate manner. It delivers a summary, focusing on the main insights derived from the study. The technical assessment of these results is delivered with a broader scope, augmenting the depth of understanding provided by literature review in the context of this research work.

Chapter 7: Conclusion

This chapter is the summary of the simulation result, COP of the proposed heat pump system, drying time, and mass transfer coefficient. Detailed information on the energy requirement for each process is analyzed.

Chapter 8: Further work

Despite the thoroughness of the thesis work, there is still potential for expansion and enhancement. Techniques not covered in this work will be elaborated upon in subsequent studies. This ongoing research will serve as a valuable reference for other investigators delving into this field of study.

Appendix

The relevant calculations for ventilation rate at each stage in farm is included, helioscope generated report is attached. Lastly, the scientific article drafting is included at the last as an attachment.

2   General Theory

This chapter gives basic information about the heat pump cycle. Different stages of the heat pump cycle are mentioned in brief, along with the comparison of different working fluids.

2.1   Heat Pump and the refrigeration principle

The fundamental concept of refrigeration revolves around absorbing heat at a low pressure, releasing it at high pressure, and exerting some mechanical work on the system. This cycle utilizes working fluids such as NH_3, CO_2, R-134a, R-600a, R-290 etc. These refrigerants take in heat from various environmental sources such as air, water, or the ground.

The process begins when a refrigerant absorbs heat from its surroundings. Next, this heated refrigerant is compressed using a compressor. The heat absorbed earlier is then expelled into the surrounding environment from the high-pressure side. This part of the system, where heat is discharged, is known as the condenser.

After passing through the condenser, the refrigerant undergoes expansion, resulting in reduced pressure and leading to evaporation. The entire refrigeration cycle, proceeding from state point 1 to 4, as illustrated in Figure 2-1.
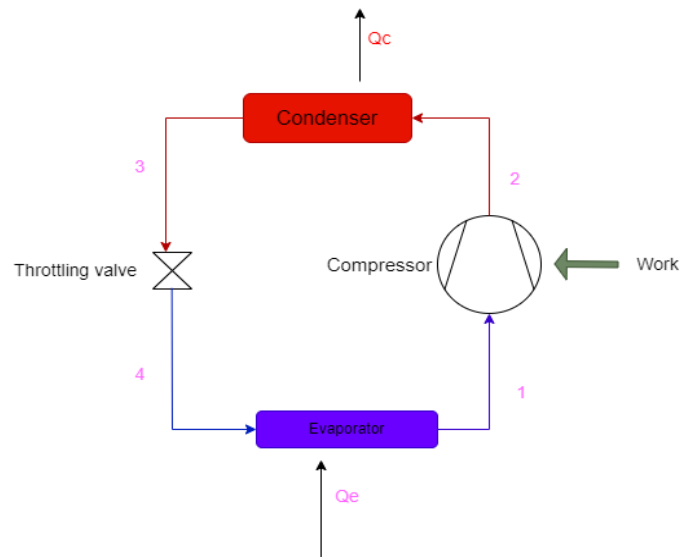
Figure 2-1 A simple refrigeration cycle

A thermodynamic process involved in different state points is as follows:

State 1-2: The compression of the refrigerant takes place isentropically, where work with certain displacement to obtain the desired pressure at the high-pressure side. The isentropic work done by compressor and efficiency is given in Equation 3.

$$W_{is} = m_r(h_{2s} - h_1)$$ Equation 3

State 2-3: State point 2-3 indicates the heat rejection process that takes place with constant pressure (isobaric rejection). The condenser heat rejected equals the sum of the heat input at the source and work done on the compressor.

$$\eta_{is} = {W_{is}}/{W}$$ Equation 4

$$Q_c = m_r(h_2 - h_3)$$ Equation 5

State 3-4: At this point, temperature and pressure are reduced by throttling valves with constant enthalpy.

i.e., $h_3 = h_4$.

State 4-1: At this point, a heat source adds the heat to the refrigerant at constant pressure. Mathematically denoted by

$$Q_e = m_r(h_1 - h_4)$$ Equation 6
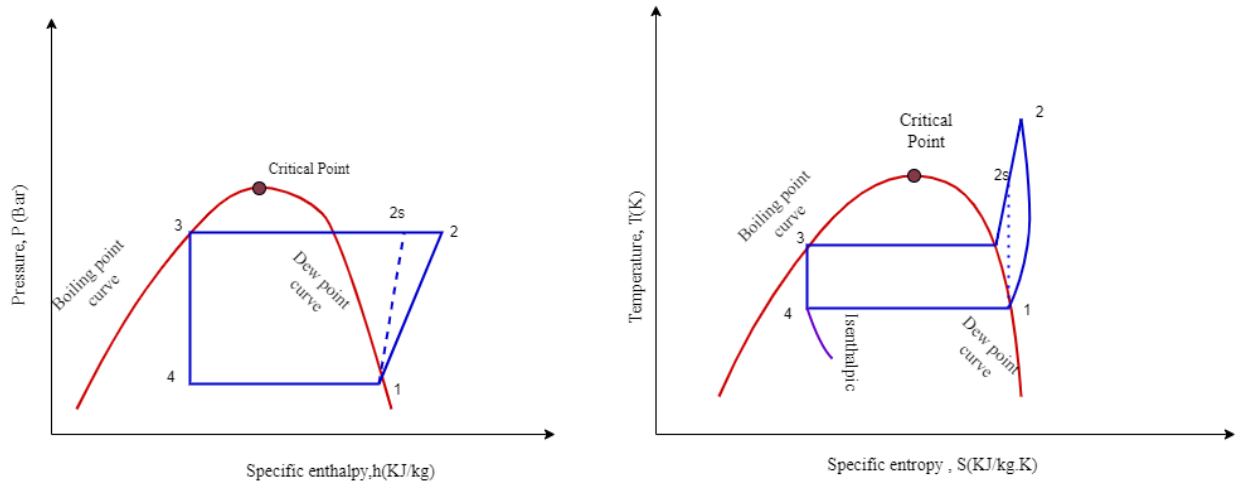
Figure 2-2 p-h and T-S diagram of the refrigeration cycle

The performance of this refrigeration cycle is given by dimensionless number. It is defined as the ratio of output to input power.

$$COP_h = \frac{Q_c}{W}$$

Equation 7

$$COP_r = \frac{Q_e}{W}$$

Equation 8

Equation 7 represents the COP of the heat pump, whereas Equation 8 demonstrates the COP of

the refrigeration capacity.

2.2 Sources of heat pump

Various types of heat sources can be used in refrigeration systems and heat pumps. Designing the heat pump, also depends on various factors like the selection of heat source, classification of system design, etc. The heat sources are used based on different operating criteria. The parameters that heat sources are dependent on are as follows:

- Temperature conditions
- System design

- Operational experiences

- Dimensioning

- Practical challenges

However, the different sources that can be used in heat pumps are as follows:

- Ambient air

- Bedrock

- Soil/ground

- Salt water-sea water

- Freshwater- groundwater, lakes, rivers

- Ventilation air

- Sewage (black water)

- Grey water (wastewater)

- Cooling water(industry)

However, a heat pump's most used heat sources are air, water, and ground source based. Those sources are described in short as follows:

Ambient air is also known as air to-water source heat pump, which transfers heat from the outside air to water via underfloor heating. The air source can be used to heat water, store and provides hot taps, water, showers, etc. In this heat pump, the heat from the air is absorbed into a refrigerant. This refrigerant is further compressed in a compressor to raise the temperature, finally heating the water. The heating capacity decreases with the decreasing air temperature. High LMTD for the evaporator and a larger flow rate is needed. Energy demands of the fans cause more energy demand which is typically higher than pumps. It is very important to have low-noise fans. If the surface temperature in the evaporator drops below 0 °C. The design outdoor temperature for Trondheim, Norway is -19 °C, whereas the average ambient temperature of the air is 4.9 °C.

Water source heat pumps are those where water is used to heat the refrigerant on a low-pressure side. This type of heat pump operation is mostly quieter and more efficient. In an air-source heat pump system, the air is mounted to an evaporator where forced convection takes place. Typically heat transfer coefficient ranges from 25 to 250 W/m^2K, whereas the forced water has a heat transfer coefficient ranging from 50 to 20,000 W/m^2K [21]. The flow rate, temperature, water quality from

groundwater, lake water, sewage water, grey water and river water can also affect the heat transfer coefficient. For seawater as a source, it has a high temperature level due to the gulf stream. The freezing point lower than that of fresh water (for reference -2.5 °C at 30% salinity). The main challenge to using sea water is it is highly corrosive than fresh water. It can cause fouling, clogging, and corrosion. This process takes place mostly in suction pipelines, pressure pipelines, and return pipelines. Normally when sea water is pumped to evaporators, the return line is cooled by 2 to 4 K and discharged to the sea. The pipelines are made of by plastic (polyethylene high density). These pipes are chemically inert, flexible, strong, and float in water.

Ground source heat pump typically depends on the extraction of heat from bedrock and ground water. The energy extracted from the ground is further compressed into higher temperatures. Ground source heat pumps are the most efficient heat pump solution than air or water. The ground is used to extract heat during winter and dump heat from buildings during summer. It is necessary to design a ground source heat pump in such a way that change in ground temperature change minimum throughout the year. Ground acts as storage for summer and winter conditions. Norway uses around 3 TWh/yr of energy from the ground and has an installed capacity of 1.2 GW. However, Norway has the potential to produce 33 TWh/yr energy [22].

2.3   Refrigerants

Refrigerants are the working fluids that transfer heat from the low-temperature side to the high-temperature side in the refrigeration system. R-610 (ethyl-ether) was used as the first refrigerant by Jacob Perkins in 1834 in the refrigeration system. It was restricted shortly due to safety concerns and the arrival of new refrigerants like ammonia(R-717), carbon dioxide (R-744), Sulphur dioxide (R-764), air (R-729), etc. Chlorofluorocarbons (CFCs) and hydrofluorocarbons (HCFCs) were introduced in the 1930 and 1950s, respectively. Due to environmental impact and better operating conditions, these refrigerants are phased out since many accidents have taken place. Montreal Protocol was signed in 1987 by 26 other countries to reduce the chemicals that deplete the ozone layer. CFCs were phased out in 1996, and HCFCs are soon going to be phased out until 2030 in developed countries to minimize the greenhouse effect. EU F-gas regulation in 2015 and the Kigali

amendment 2016 came into effect by January 2019. Kigali amendment sets a goal to cut 80% in HCFC consumption by 2047 [23].

Natural refrigerants like carbon dioxide, ammonia, and hydrocarbons are used for their inherent environmental benefits. Natural refrigerants have zero ozone depletion potential and very low global warming potential, which is substituting synthetic refrigerants. Natural refrigerants are less toxic, with various flammability properties. Out of the different natural refrigerants, the best refrigerants must be chosen according to the application in different sectors. Table 5 gives an overview of choosing the best refrigerant for their uses.

Table 5 Properties of natural refrigerants

Name	Ref. number	Evaporation Temp. range	Main application	ODP/GWP	Flammable	Toxic
Ammonia	R717	-20°- 15°C	Industrial	0/0	Yes	Yes
Carbon dioxide	R744	-5° - +5°C	Industrial/Commercial	0/1	No	No
Nitrous oxide	R744a	-70° - +5°C	Not yet	30-300	No	No
Propane	R290	-40° - +20°C 2stg. -55°C	Commercial	0/3 to 20	Yes	No
Propene	R1270	-40° - +20°C 2stg. -55°C	Commercial/ Industrial	0/3 to 20	Yes	No
Ethane	R170	-90° - +50°C	Low temp. cascade	0/3 to 20	Yes	No

R744 is non-flammable and non-toxic, with the lowest ODP value and a wide range of applications at industrial and commercial levels. Besides these characteristics, R744 has many other reasons for a wide range of applications, proving it is very efficient. Some of the other reasons for choosing R744 as a working fluid is as follows:

- Low-pressure ratio
- Low-temperature losses

- Small compression volume due to extremely high density

- Dimensioning of the equipment is done according to the CO_2 system.

- 20-40% lower weight of the pipeline despite the thickness

- Smaller pipe diameter

Also, less compressor volume is preferred for different types of refrigerants. The comparative bar chart between different types of refrigerants is illustrated in Figure 2-3.
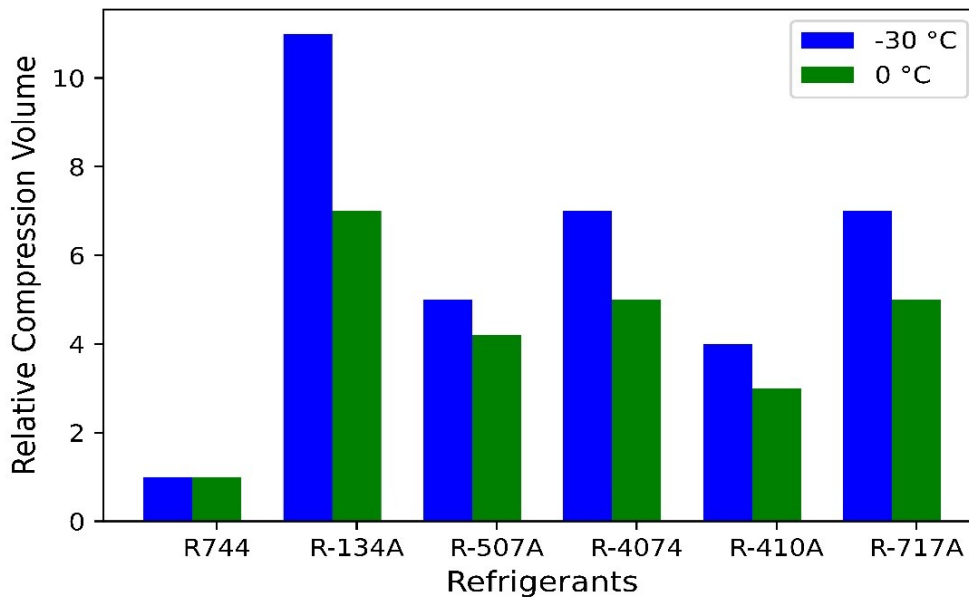
Figure 2-3 Relative compression volume for refrigerants

All refrigerants should be used according to the situation. Classification and refrigerant charge are important for safety analysis. The safety group indicates which refrigerants can be used in a different type of building. The restrictions for the working fluids charges are applied with respect to class and type of occupancy. The maximum allowable charge for R744 is relatively more than other working fluids because of low global warming potential. The comparison between GWP and the safety group is stated in Table 6.

Table 6 Characteristics of refrigerants

Working fluid	NBP(t°C)	T$_{cr}$ (°C)	P$_{cr}$(°C)	Safety Group
R717	-33.1	132.3	113.5	B2
R290	-42	96.7	3	A3
R404A	-46.5	72.1	37.5	A1
R744	-78.4	31.1	73.8	A1
R600a	-12	135.9	36.8	A3
R134a	-26.1	101.1	40.7	A1
R407c	-36.7	86.7	1650	A1

Alongside this, the refrigerant used in the heat pump must be sustainable, eco-friendly, and cost-effective. The Norwegian government charges high taxation to the industries for importing HFCs and PFCs. The tax rate of these hydrofluorocarbons and perfluorocarbons is according to the amount they produce or import. The rate for 2022 is NOK 0.766 per kilo, which is multiplied by the GWP value of each taxable gas. The prices and tax for the working fluids in refrigeration or heat pump are shown in Table 7.

Table 7 Price of Refrigerants in Norway [24]

Gas	GWP	Purchase Price (NOK)	Plus, tax (NOK)
HFC-32	675	69	52
HFC-134a	1430	75	110
R-410a	2088	92	160

2.4 Thermal Energy Storage

TES is the system that stores energy for later use, and this storage can be integrated with a heating and cooling system. This refers to saving energy during low demand and low prices and use of it in peak hours when a high price is applicable. Thermal energy storage is done by changing the internal energy of a material by means of sensible heat, latent heat, and thermo-chemical heat. In TES, we charge energy during low-cost hours and discharge during high-cost hours. The two basic processes involved with TES are as follows: Charging, discharging, and storing. Storage system design and choice of medium are important factors that determine size, and capacity. The use of PCM, storage tank, and any other system is determined according to necessity. Heat transfer in storage system can be done by following steps:

- Exchanging heat by exchanging storage medium
- Exchanging heat on large surface within storage
- Exchange heat at the surface

The first two phenomenon are used for storage in industrial application due to high heat transfer rate.

2.4.1   Sensible heat

Sensible heat is dependent upon the change in temperature of a certain material, whether solid or liquid that utilizes the heat storage capacity of a material. The amount of energy stored by a material is given by:

$$Q = \int_{T_i}^{T_f} mC_p dT = \frac{\rho.V.Cp.\Delta T}{3600} \text{ [kWh]} \qquad\qquad \text{Equation 9}$$

Where T_f and T_i are the final and initial temperature respectively, m is the mass of material, C_p is the specific heat capacity and dT is the change in temperature.

As illustrated in Equation 9, energy stored is dependent on specific heat capacity. That is why water is used as an energy storage medium. It is also cheap and can be found in most places. Water storage tanks are made of a variety of materials like steel, concrete, and fiber glass, which is

insulated with glass cool, mineral wool, and PUR. The insulation thickness mostly ranges from 10 to 20 cm in storage tank. Water can be stored at 100 °C at atmospheric pressure and is possible to store at slightly concrete higher than 100 °C using pressurized tanks. It can be used as a heat transfer medium as well as storage medium which reduces the number of heat exchangers during the transfer of heat. In sensible heat storage system, liquids like water, oils, and inorganic molten salts play a vital role whereas solids used to store heat are rocks, pebbles, and refractory. In the case of solids, materials are normally available porous form, and the heat is extracted by the flow of a gas or liquids through voids [25]. The choice of material or substance largely depends on application. Sensible heat storage tanks into consideration of various materials. The heat input and outputs while charging ad discharging for a packed bed volume is given in Equation 10.

$$V = \frac{Q_s}{\rho c (1 - \text{€}) \Delta T}$$

Equation 10

Where, V is the volume of storage, € is the porosity of packed bed and c is the specific heat capacity and Q_s is the heat stored in a medium.

Heat transfer oils have a storage capacity from 100 to 300 °C. Oil like downtherm and therminol provides better stability [26]. The problem with using heat transfer fluids is that they degrade with time. However, the problem is not that serious if the temperature is below the limit. The use of oils can cause safety problems and should be used always below the flash point.

2.4.2 Latent TES

Latent heat storage uses a phase charging material (PCM) as storage medium. PCM breaks up as a phase change occurs. This can be described as an endothermic process absorbing heat. When the phase change temperature of a material is reached, the material starts to melt, and the temperature is kept constant until the melting process is completed. The heat stored during the process is called latent heat. The amount of heat storage is given by:

$$Q = m a_m \, \Delta h_m + \int_{T_i}^{T_m} m C_p dT + \int_{T_m}^{T_f} m C_p dT$$

Equation 11

In Equation 11, Δh_m is the phase enthalpy for the given substance. A common example is the use of water, or ice. It has a phase change temperature of 0 °C and a phase change enthalpy of 333 kJ/kg. The storage volume is reduced if latent storage is used over sensible heat [27].

2.4.3 Design of Hot water storage Tank for heating building

The various considerations for designing the hot water storage tank are as follows:

- Uniform deep-water container
- Very less dead water volume zone
- Minimize the surface area
- The temperature difference between each zone of the tank should not be more than 5 K
- Low-velocity water distribution from bottom
- Insulation

Water is usually stored at more than 60°C to supply hot water to the building for any other heating purpose like ventilation and snow melting. The design of a hot water storage tank for commercial application Figure 2-4.

- Charging Process

  Heat pump is ON when the temperature in buffer tank (tank c and tank d) reaches to a certain temperature. Cold water is extracted from bottom of the tank and pumped to gas cooler. Heated water is reinjected at the top of the last tank (tank d). When storage is fully charged and the stratified tanks have a high and uniform temperature in the buffer, the heat pump is turned OFF. Likewise, the surface interface between hot and cold water is moving towards the bottom of the tank. Hence, water is moved to the next cold tank. It means during charging the hot water moves from right to left of the tanks (tank a to tank d), and finally to buffer tank.

- Discharging process

  In this process, cold city water will be injected to the bottom of the buffer tank. Hot water is slowly moving towards the top of a tank and moved to the next hotter tank. Hot water is extracted from top of last tank to hot water supply line of building as shown in

- Charging of Reheat Tank

  The backup reheater is after all tanks shown in Figure 2-4. The hot water from the tank is pumped throughout the heat exchanger, and then returned to other tank in series. This

reheating tank takes place to reheat water in the building return line when heat pump is OFF. The reheat tank needs to be charged to prevent a temperature drop in the recirculating supply line.
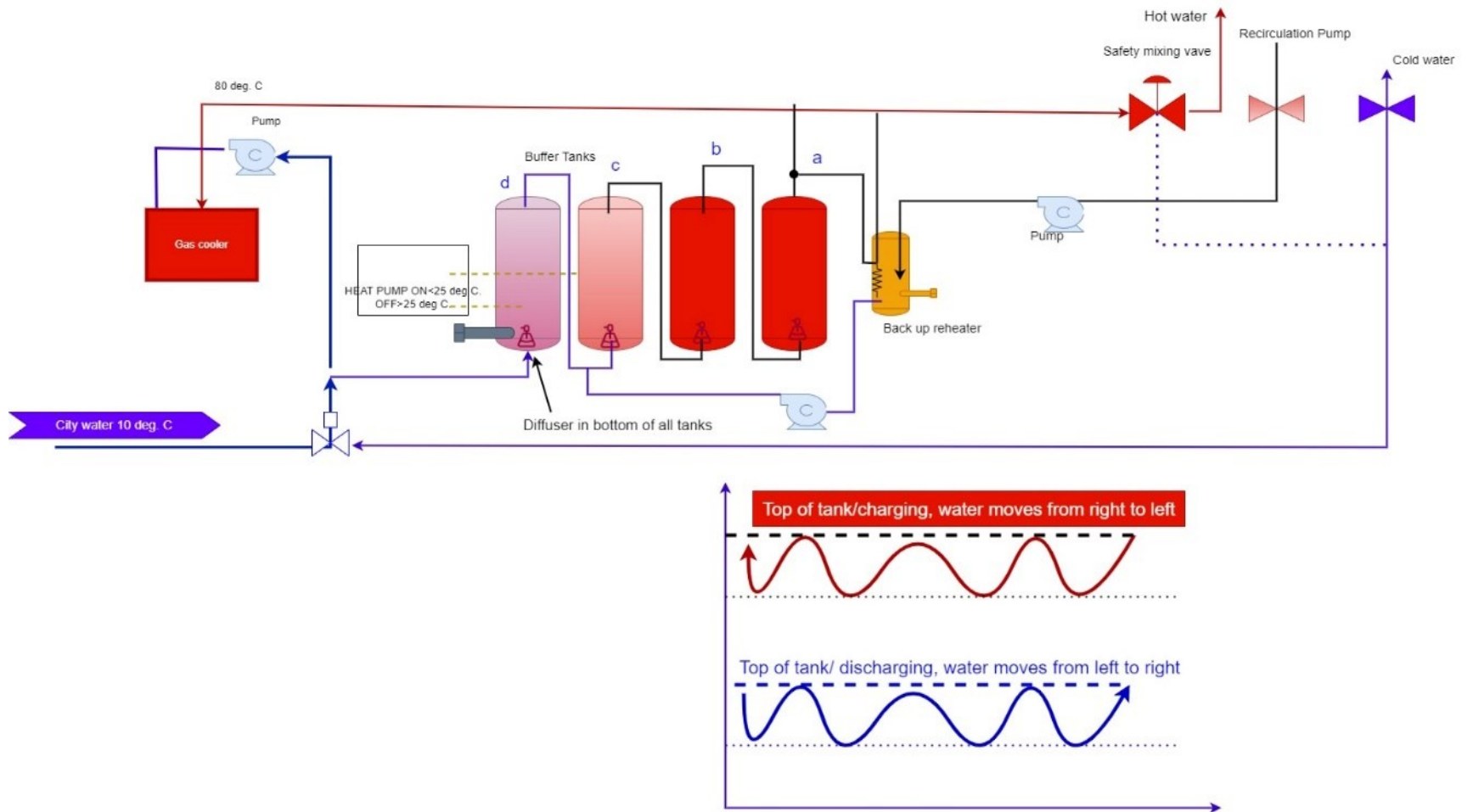
Figure 2-4 Configuration of hot water Storage Tank

2.5 Uncertainty Analysis

Measurement typically involves quantifying a physical attribute numerically. Key considerations of this process include the physical quantity being measured, the method of measurement, the most suitable device or measurement, the desired level of precision, and the procedures for processing the data. Given that nearly all measurements carry some degree of error and uncertainty, it's crucial to set realistic expectations for the accuracy of the results that align with what can realistically be achieved.

- Gross Errors: These mistakes are associated with incorrect readings due to issues such as number transposition, misplaced commas etc. It's essential to prevent these types of errors.
- Systematic errors: These errors arise from factors such as the use of non-calibrated equipment, measurements conducted incorrectly, meter hysteresis or friction, or applying inappropriate function contexts.
- Random errors: This category includes poor resolution in analog or digital meters, inadequate measurement dynamics, or external, nonsystematic interference. While these errors cannot be eliminated, they can be minimized.

Estimation of uncertainty level during the measurements [28]:

The estimation can be done using the following levels:

- **Simple measurement**
  For the simple measurements,
  Mean value

$$\bar{x} = \sum {x}/{n}$$ Equation 12

The level of uncertainty in individual measurements can be determined based on the number of measurements taken (represented by 'n'), each individual measurement value (denoted by 'x') and mean of these measurement (also represented by '$\bar{x}$'). This uncertainty is typically communicated via the standard deviation represented by symbol 's'.

$$S = \sqrt{\frac{\sum(x - \bar{x})^2}{n - 1}}$$

The uncertainty of an average value is given by:

Random error:

$$S = \pm \frac{S}{\sqrt{n}}$$

Hence Total error can be given by

$$U_R = \pm \sqrt{U_T^2 + U_S^2}$$

Where, U_R is always specified by the manufacturer of the meter.

Compound measurements

Most physical measurements are complex, implying that the result is dependent on the measurement of multiple variables that are then incorporated into a mathematical equation. As a result, the uncertainty associated with the final measurement result is influenced by multiple distinct factors. When directly measured quantities are denoted as u, N is a resultant value from the compounded measurements, each u is measured with an associated degree of uncertainty, denoted as Δu.

$$N \pm \Delta N = f(u_1 + u_2 + \cdots, u_n \pm \Delta u_n)$$

Assuming that the uncertainty of the individual measurement is independent. For example, not measured with the same meter or method the resultant error can be estimated as follows.

Replacing ΔN by U_R.

$$U_R = \pm \sqrt{\left(\frac{\partial f}{\partial u_1} . \Delta u_1\right)^2 + \cdots + \left(\frac{\partial f}{\partial u_n} . \Delta u_n\right)^2}$$

Linearly independent variables

If N is comprised of an independent variable such that N = u_1+u_2+……. +u_n, then $\frac{\partial f}{\partial u}$ = 1, then the equation is simplified into:

$$U_R = \pm \sqrt{(\Delta u_1)^2 + (\Delta u_2)^2 \ldots + (\Delta u_n)^2}$$

The Equation 18 indicates that priority must be given to reducing the errors in the elements that are most important. It is not always necessary to strive for the greatest possible accuracy in all elements.

Dependent variables

If it cannot be assumed that the errors in the individual measurements are independent of one another, the following model must be used.

$$U_R = \pm \sqrt{\left(\frac{\partial f}{\partial u_1} . \Delta u_1\right)^2 + \cdots + \left(\frac{\partial f}{\partial u_n} . \Delta u_n\right)^2}$$

3   Methodology

In this chapter, the calculation of heat production from chicken, suitable ventilation rate, estimation of drying time with heat pump is analyzed. The software used to analyze is described in short to make familiar during explanation of results.

3.1   Calculation of heat production from chicken

All mammals are homothermic and must be kept at a reasonable temperature for growth and development. Mammals also emit heat from their body. Likewise, chickens also dissipate heat partly, and heat dissipation mainly depends on body mass, activity level, and energy concentration in the feed. Chicken reared in the poultry farm also produces two types of heat which are sensible and latent heat. Sensible heat loss is the heat dissipated by chickens through heat transfer to surrounding air resulting increase in temperature inside farm whereas latent heat loss from birds during the respiratory system which results increase in humidity [29]. In, the block diagram shows that sensible heat and latent heat both has the simultaneous relation with ambient temperature. The total heat production depends on many other factors such as humidity and body weight of chicken. Hence, it is difficult but important to calculate the heat production from chicken at different stage.
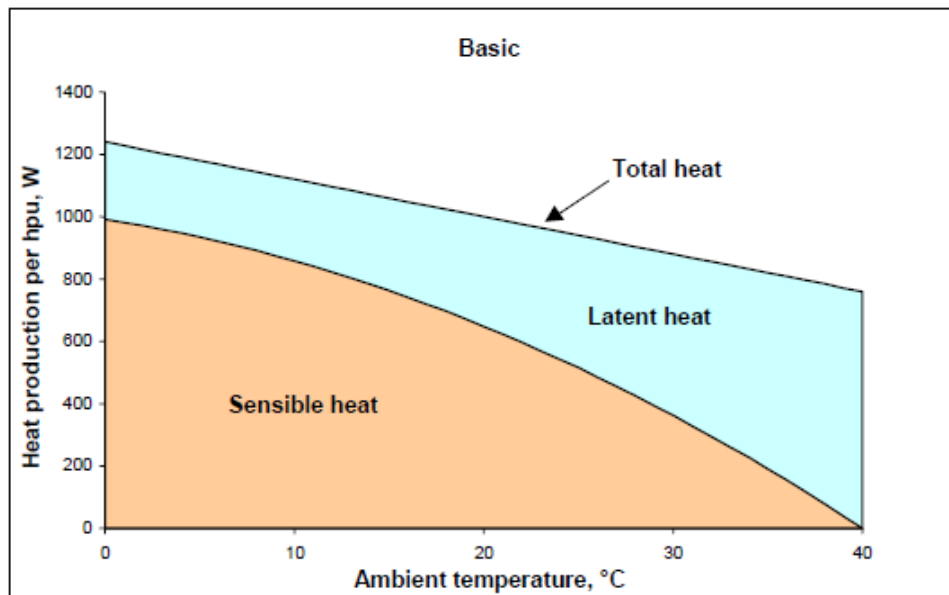
Figure 3-1 Basic relation to latent and sensible heat for specific species [30]

In 1978, Stroem et al. [31] , reviewed the literature on poultry farms, and developed predictive equations for calculating sensible and total heat production. The literature published by Stroem was further reviewed in 2002 and 1984 by a CIGR working group which gives equation for the different livestock comprising cattle, pigs, poultry, horses etc. CIGR equations were mainly based on heat and moisture production in climatic chamber. The water vapor is released from water spill, feed, and manure inside the chamber. The evaporation of water vapor takes place by the heat taken from the animal's sensible heat production. Hence, measured sensible heat is always less than that in climatic sensible zone. Therefore, a provisional correction factor is provided while calculation of latent heat and sensible heat in the equation. In the aspect, high indoor relative humidity also effects the evaporation of water that brings possible changes in latent heat production from chicken.

 The heat production from broiler varies according to its growth. Also, the expected growth depends on the indoor air quality, feed ad thermoneutral science. Table 8 states the comparative model of heat production of poultry at themos neutral conditions (20 °C) during periods of the past five decades.

Table 8 Total heat production from different poultry species

Poultry Species	Year(s)	Φ_t (W/bird)
Broilers	1968	$8.55M^{0.74}$
	1982-2000	$10.62M^{0.75}$
Pullets & Laying Hens	1953-1990	$6.47M^{0.77}$
Turkeys	1974-1977	$7.54M^{0.53}$
	1992-1998	$9.86M^{0.77}$

In the CIGR report [30] it is highlighted that the total heat production per bird can be calculated using the following equations:

$$\Phi_t = 10M^{0.75}$$ Equation 20

Here, Φ_t represents the total heat generated by a chicken in Watts, while M denotes the chicken's weight in kilogram.

Furthermore, the distribution of sensible and latent heat is influenced by various factors, including the dryness of the skin and feathers, age, body surface area, and the ability to sweat. Consequently, Stroem et al. [31] proposed a set of fundamental equations to compute sensible heat and a correction factor, as shown from Equation 21 to Equation 22:

$$\Phi_s = F\Phi_t(0.8 - (1.85 * 10^{-7})(T_i + 10)^4)) \qquad\qquad \text{Equation 21}$$

$$F = 4 * 10^{-5} * (20 - T_i)^3 + 1 \qquad\qquad \text{Equation 22}$$

$$\Phi_l = F\Phi_t - \Phi_s \qquad\qquad \text{Equation 23}$$

Gates et al. [32] further revealed an equation to get more accurate sensible and latent heat production from chicken. For Sensible heat production (SHP) the following regression were obtained (x= bird age, days, SE = standard error of regression). Units for these equations are BTU/(lbh) if K=1, and W/kg if K= 0.64631.

For all brooding temperatures:

$$SHP = k\exp(-6.5194 + 2.9186x - 0.24162x^2) \qquad\qquad \text{Equation 24}$$

SE =0.284K: $\qquad\qquad\qquad\qquad\qquad\qquad\qquad$ $3 \leq x \leq 5$

$$SHP = k\exp(1.8662 + 0.0542123x - 0.00161x^2) \qquad\qquad \text{Equation 25}$$

SE = 0.0129K: $\qquad\qquad\qquad\qquad\qquad\qquad\qquad$ $6 \leq x \leq 19$

For temperature t= 15.6°C:

$$SHP = k(38.612 - 2.6224x + 0.072047x^2 - 0.00066x^3) \qquad\qquad \text{Equation 26}$$

SE= 0.045: $\qquad\qquad\qquad\qquad\qquad\qquad\qquad$ $20 \leq x \leq 41$

SHP = 6.717K: $\qquad\qquad\qquad\qquad\qquad\qquad\qquad$ $42 \leq x \leq 48$

For temperature t= 21.1°C:

$$SHP = k(36.070 - 2.3107x + 0.058862x^2 - 0.00051x^3) \qquad \text{Equation 27}$$

SE = 0.110K: $\qquad\qquad 20 \leq x \leq 39$

SHP = 5.220K: $\qquad\qquad 40 \leq x \leq 48$

For temperature t= 26.7°C:

$$SHP = k \exp(5.3611 - 0.16177x) \qquad \text{Equation 28}$$

SE = 0.052: $\qquad\qquad 20 \leq x \leq 23$

SHP = 5K: $\qquad\qquad 24 \leq x \leq 48$

For latent heat production LHP, the regression is independent of temperature for the first 19 days.

$$LHP = k(-42.961 + 27.415x - 2.84344x^2) \qquad \text{Equation 29}$$

SE = -0.296K: $\qquad\qquad 2 \leq x \leq 5$

$$LHP = k(36.424 - 2.8998x + 0.08676x^2) \qquad \text{Equation 30}$$

SE = 0.029K: $\qquad\qquad 6 \leq x \leq 15$

$$LHP = -k(15.812 - 0.22611x) \qquad \text{Equation 31}$$

SE = -0.031K: $\qquad\qquad 16 \leq x \leq 19$

For temperature, t = 15.6°C:

$$LHP = k(22.285 - 0.78279x + 0.011503x^2 - 0.000038x^3) \qquad \text{Equation 32}$$

SE = 0.192K: $\qquad\qquad 20 \leq x \leq 43$

LHP = 6.87K: $\qquad\qquad 44 \leq x \leq 48$

For temperature, t = 21.1°C:

$$LHP = k(11.221 + 0.40495x - 0.02727x^2 + 0.000353x^3) \qquad \text{Equation 33}$$

SE = 0.069K: $\qquad\qquad 20 \leq x \leq 43$

LHP = 6.278K: $\qquad\qquad 44 \leq x \leq 48$

For temperature, t = 26.7°C:

$$SHP = -k(20.094 - 0.70318x + 0.015182x^2 - 0.000108x^3) \qquad \text{Equation 34}$$

SE = -0.022K: $\qquad\qquad 20 \leq x \leq 42$

LHP = -9.340K: 43≤x≤48

For temperatures of 15.6 and 21.1°C during grow out the latent heat production is nearly identical, a pooled regression yielded.

$$LHP = -k \exp (20.874 - 0.61708x + 0006528x^2)$$ Equation 35

SE = 0.034K: 20≤x≤41

It is essential to consider that the chicken's weight changes over time inside the farm, and consequently, heat production varies.

3.2 Estimation on Ventilation rate for a Poultry farm

Several types of ventilation can be implemented for poultry farm based on requirement of farm, the local temperature, humidity, the type of birds bring raised. Some examples of ventilation system used in poultry farm are as follows:

- Natural ventilation: this system relies on natural air flows through the vents, windows, or opening in the walls or roof. Wind and temperature differences between the inside and outside of the building drive air movement. Natural ventilation can be cost effective, but it is not effective to control the internal temperature and humidity required for the farm.
- Mechanical ventilation: this type of system uses a fan and air inlets to control air exchange per hour and maintain optimum temperature, humidity, and air quality. Mechanical ventilation systems can be further categorized into the following types:
  i. Negative pressure ventilation (Exhaust ventilation): This system uses exhaust fans to remove stale air from the poultry house, creating a negative pressure inside. Fresh air enters the building through air inlets, which can be adjusted to control the airflow and distribution. Negative pressure ventilation is commonly used in modern poultry farms, as it provides precise control over the indoor environment.
  ii. Positive pressure ventilation (Supply ventilation): This system uses fans to push fresh air into the poultry house, creating a positive pressure inside. Stale air is forced out of the building through vents or openings. Positive pressure ventilation

is less common in poultry farming, as it can be more challenging to control air flow and air distribution.

iii.   Cross ventilation: this system uses fans and air inlets arranged on oppositive sides of the poultry house, creating a horizontal airflow across the building. Cross ventilation is effective in maintaining a uniform temperature and air quality but may be less suitable for very long or wide poultry houses.

iv.   Tunnel ventilation: This system uses fans at one end of the poultry house and air inlets at the other end, creating high velocity, longitudinal air flow along the length of the building. Tunnel ventilation is highly effective in cooling the poultry house during hot weather and is commonly used in large, modern broiler farms.

v.   Mixed-mode ventilation: This system combines natural and mechanical ventilation, utilizing the advantages of both systems. Mixed-mode ventilation can help to reduce energy costs and improve the indoor environment under a range of weather condition.

Hence, the choice of ventilation system depends on factors such as the size and design of poultry house, type of birds being raised local climate conditions.

The ventilation must be designed in such a way that the birds get enough oxy gen for growth and should be regulated according to carbon dioxide and ammonia concentration inside the building is within acceptable range. Therefore, the factors affecting ventilation rate are bird age, number of birds, weight of bird, ambient temperature, and relative humidity. Figure 3-2 illustrates that leakage occurs through infiltration and exfiltration within the poultry farm building. Heat generation inside the building arises from various sources, such as lighting (5 W/m^2) and the metabolic heat produced by chickens, which depends on their activity level and feed intake. The air inlet and exhaust systems are driven by highly efficient EC motors. A heat exchanger is strategically placed at the inlet of the supply air and the exhaust of hot air and water, allowing for the recovery of heat exiting the building. This design contributes to the building's energy efficiency by reducing heating demands through various mechanisms.

Optimal internal parameters must be maintained to ensure the healthy growth of chickens. The ideal relative humidity for chickens of all ages is approximately 55%, while the temperature requirements fluctuate throughout their growth, from the time they are introduced to the farm until

the end of the production cycle. Ventilation plays a crucial role in the well-being of chickens; excessive ventilation can create a wind-chill effect, which may be advantageous for larger birds but can adversely affect smaller, more sensitive chickens. The perceived temperature experienced by the chickens should be prioritized over ambient room temperature [33].
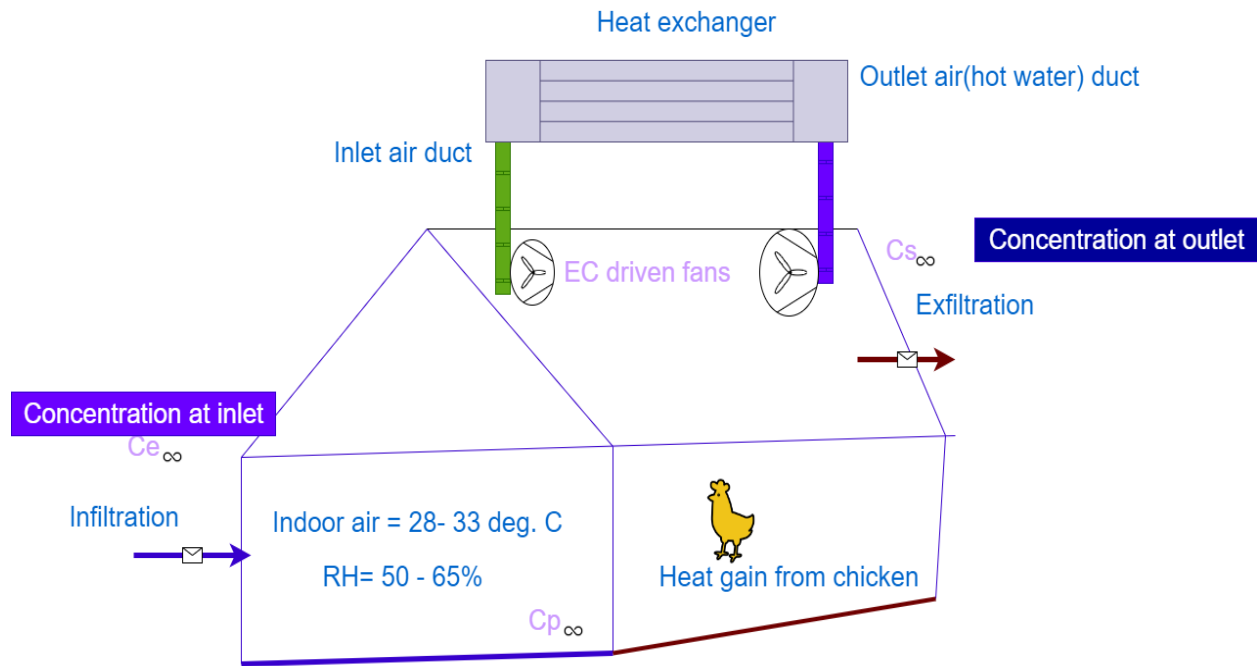
Figure 3-2 Layout of Poultry farm requirements

3.3 Requirements and rules of farm at poultry farm

The poultry farm's internal climate must be regulated according to the chicken's various developmental stage. The optimal temperature and humidity levels for the poultry farms based on the age of chickens. The data reveals that the temperature requirements are higher during the initial stages of their introduction to the farm and gradually decreases as the chickens age. An average relative humidity of approximately 55% is suitable for all developmental stages. Furthermore, the ammonia and carbon dioxide concentrations within the farm should not surpass 25 ppm and 3000 ppm, respectively. The necessary ventilation rates for poultry farms of varying sizes are documented in a APPENDIX I.

Table 9 Required temperature and humidity inside poultry farm

Age [Days]	Air temperature [°C]	Relative humidity [%]
0-3	33-31	40-60
3-7	32-30	40-65
7-14	31-29	50-65
14-21	29-27	50-67
21-28	27-24	50-67
28-35	24-22	50-70
>35	22-18	50-70

Also, the temperature must be analyzed in three different considerations:

- Actual temperature as measured by thermometer.
- Effective temperature the chickens feels that changes with the relative humidity and the air movement.
- Temperature must be measured at the head of bird. Temperature and humidity both effects the feeling of warmth. So, but must be adjusted in relation to each other.

3.4 Case study of demo poultry farm

This section focuses on general overview of concept implemented in poultry farm, uncertainty analysis of measurement equipment, fossil free heating system P& ID based on heat pumps. To design any specific system, it is necessary to study the climatic condition of that place. The poultry farm is based in Inderøy, Trondheim where temperature ranges from 20 °C to 28 °C. The climate registration center is Maere III which is located nearest from the farm as shown in Figure 3-3.
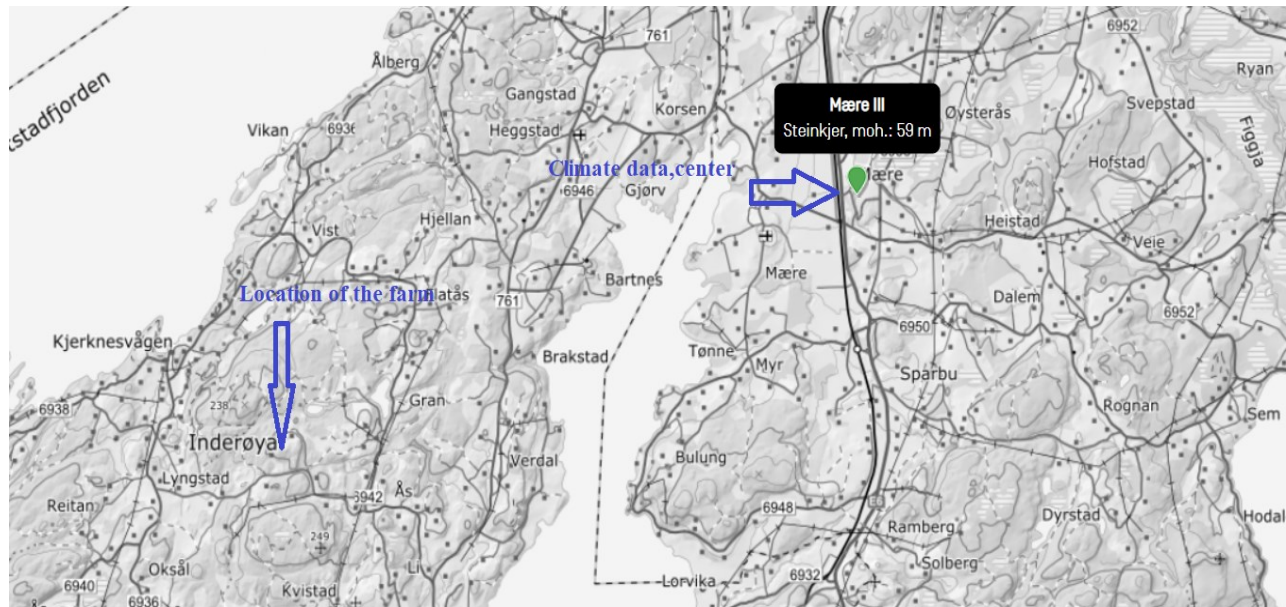
Figure 3-3 Climate centre and Poultry farm location in Trondheim

The consideration of extreme weather during the designing process is important to assure the longevity of the designed system. Air can be used as a source for fossil free heating system whose temperature is at 2.5 to 14.5 °C and mean relative humidity ranges from 72 to 86% for past 12 months. The mean relative humidity is necessary for the supply or ambient air because the adjustment to indoor air must manage accordingly. The data's are obtained from Norsk klimaservicesenter [34].
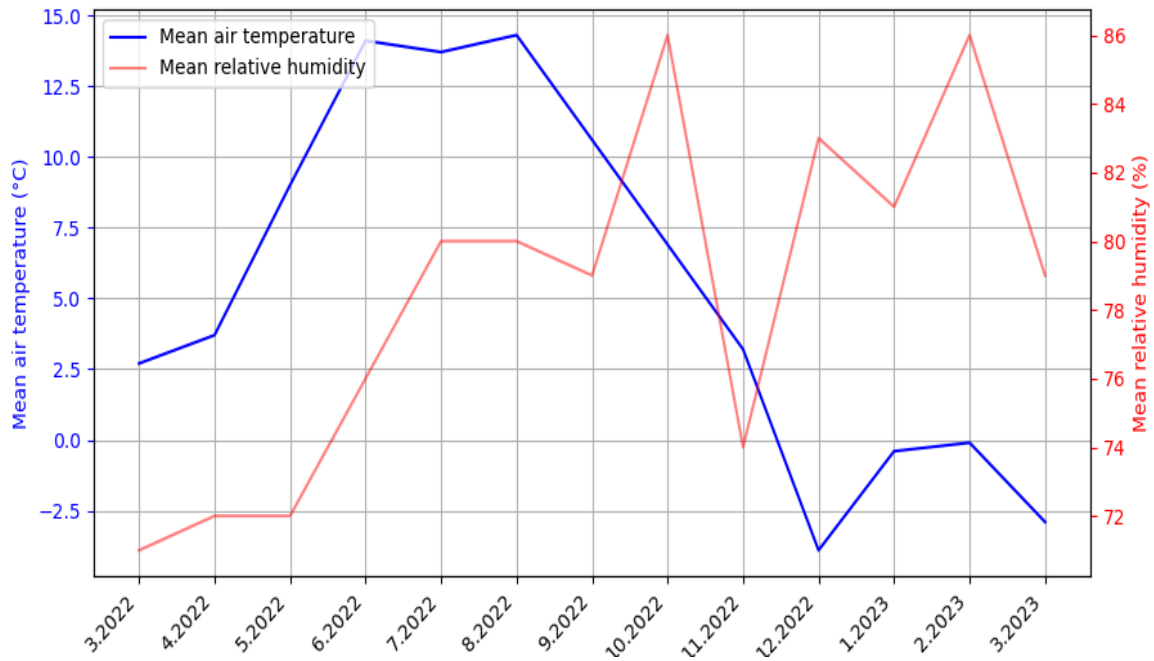
Figure 3-4 Mean air temperature and mean relative humidity

3.4.1 Characteristics of farm at Inderøy

This study is based on a poultry farm at Inderøy, Trondheim where oil boilers or pellets are used to heat the chicken farms. The purpose of this study is to study the feasibility of exiting systems and compare them with heat pumps which will find effective and efficient ways of energy saving. The case study is based on two farms with following dimensions and volume as illustrated in Table 10.

Table 10 Dimension of Poultry farm

Types of farms	Dimension(m^2)	Volume of farm(m^3)	No. of chickens
New Poultry	80x25	10890	25000
Old Poultry	64x16	5575.7	1300

The elements of construction for roof, ceiling, interior and exterior walls are provided with material properties and U-value. These values are kept from the study of existing buildings and accordance with the study of existing poultry farm model as shown in Table 11. The characteristics of the roof and floor plan are on the basis provided by the supplier.

Table 11 Characteristics of building material

Construction	Structure	U-Value
Exterior Wall	Steel Sandwich Steel plate- 0.4mm Polyurethane (PUR)- 100mm Steel plate- 0.4mm	0.22
Interior wall	Double gypsum on 95mm, 30mm light insulation	0.61
Floor Slab towards the ground	Insulation (Sprinkles, from the chickens) concrete- 300mm Floor coating= 0.35m Concrete=0.5m Heavy insulation-20mm	0.15(Equivalent) 0.2
Roof	Steel sandwich Steel plate= 0.4 mm Polyurethane (PUR)	0.22

Likewise, windows, door and infiltration having different properties for both new and old poultry farm in Table 12. Infiltration is mentioned according to TEK17 requirement for standard building of medium production industry.

Table 12 Dimension requirements door, windows, and Cold bridge

Type	Dimension	U-Value	Number/Reason
Window (3 Pane glazing)	1.3x1.3 (m^2)	1.9	26(new Poultry farm), 14 (Old Poultry)
Infiltration	1.5(ACH), wind driven		As per TEK17 requirement
Cold bridge		0.06	Corresponds to steel sandwich, wall, and 10 cm cold bridge in façade
Door	2x1.8 (m^2)	0.73	

3.4.2   Study on Existing system layout

The existing system consists of the pellet boiler. Measurement of the energy production and supply to various units are done in the following allocations. Figure 3-5 demonstrates the energy mapping to the poultry farm. The heating demand is fulfilled with the following system and opening the windows vent is done in case cooling is required. The energy flow is distributed to different units like floor heating, heat recovery unit, fan coil unit, drinking unit for chicken and old poultry farm. Different sensors are allocated in the system to study the flow (m^3/h), supply and return temperature in various units. The flow meter installed in the farm has class 2 accuracy type and the temperature sensor in the farm is pt1000 type. For class A Pt 1000 sensor, the potential error is ± 0.15°C. The data measured by the sensor are mentioned in APPENDIX I.

The sensor's location along with the major components are shown in Figure 3-5.
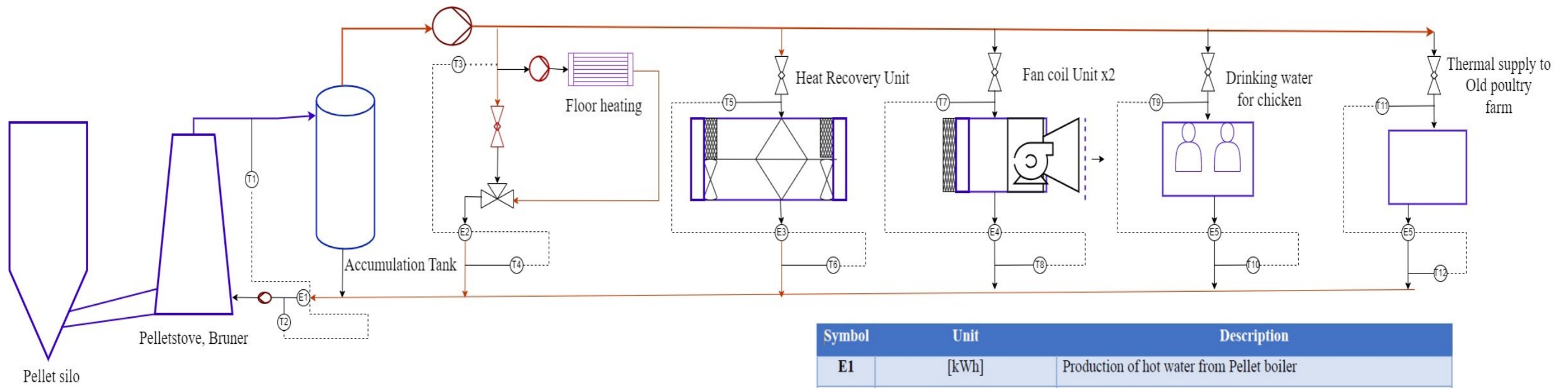
Symbol	Unit	Description
E1	[kWh]	Production of hot water from Pellet boiler
E2	[kWh]	Energy supply to Floor heating
E3	[kWh]	Energy supply to heat recovery unit
E4	[kWh]	Energy supply to Fan coil unit
E5	[kWh]	Energy supply for drinking water of chicken
E6	[kWh]	Energy supply to Old Poultry farm
T1	[°C]	Supply temperature from Pellet boiler
T2	[°C]	Return temperature to pellet boiler
T3	[°C]	Supply temperature for floor heating
T4	[°C]	Return temperature for floor heating
T5	[°C]	Supply temperature for the heat recovery unit
T6	[°C]	Return temperature of water from heat recovery unit
T7	[°C]	Supply temperature of hot water to Fan coils
T8	[°C]	Temperature of return water from Fan coils
T9	[°C]	Supply temperature of hot water to drinking water unit
T10	[°C]	Return temperature of water from drinking water unit
T11	[°C]	Supply temperature of hot water to old poultry farm
T12	[°C]	Return temperature of water from old poultry farm

Figure 3-5 Existing system at Poultry farm

The energy supply from the pellet's burner is shown in the following graph. The data in the farm is measured during the cold days in winter. It was measured from 29th October 2022 to 28th. February 2023. An average of energy consumption throughout the time frame is measured of each day. The maximum capacity produced by the Pellet broiler is 160 kW. It was just 10 days in those 89 days of measurement where the capacity of pellet stove exceeded 120 kW.

According to dimensioning of heat pump, we design the capacity from 40-70% of full capacity. rather than running it in part load throughout the year. Hence, 120 kW heat pump is designed to cover the heating and cooling demand in the building. The capacity of pellet burner with uncertainty bar is given in Figure 3-6.

The average maximum thermal power demand during coldest days was 160 kW incase no alternatives are provided to the heat pump for back up.

$$Q_{DHW} = P_a * 24\ h$$
<div align="right">Equation 36</div>
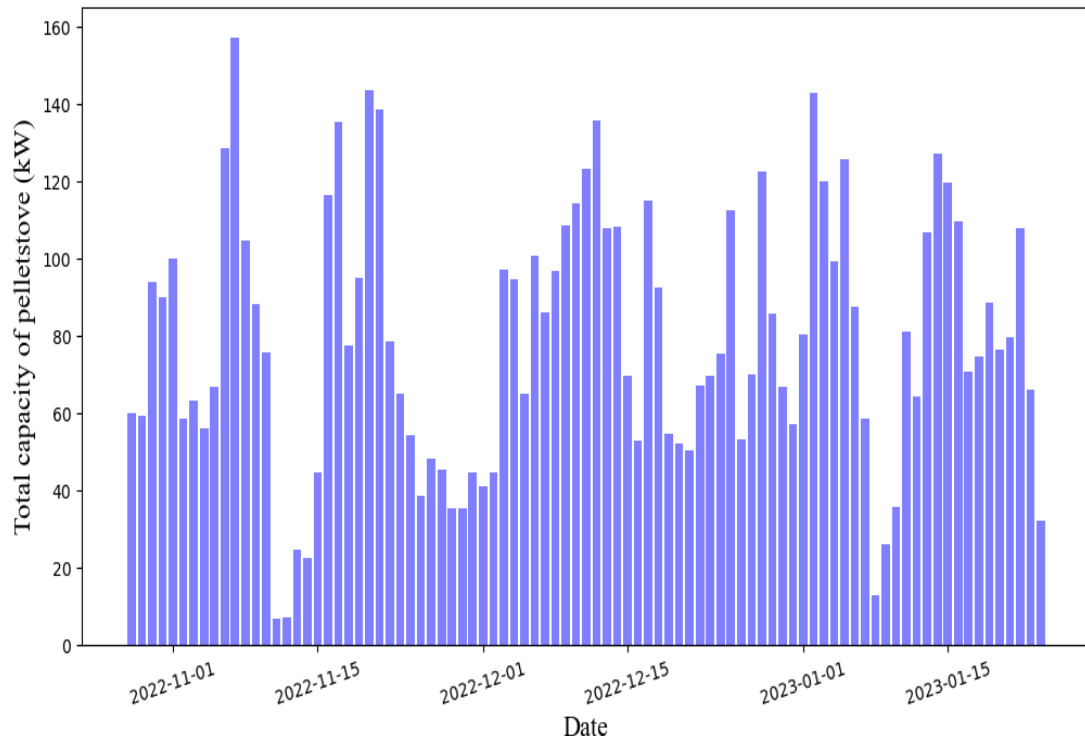
Figure 3-6 Total capacity from Pellet stove without uncertainty

3.5   Data logging process from the poultry farm

This chapter provides a detailed description of the measurement equipment used in poultry farms, focusing specifically on the Ultrasonic energy meter. The ultrasonic energy meter is designed to measure energy consumption in small pipe sizes made of different materials such as PVC, Carbon steel, Stainless steel, and copper. The Time comb Technology (TCT) is utilized by the meter for measuring the signal flight time and dropper effect, which ensures highly accurate measurements. The device is compact and portable, making it highly convenient to use. The meter also features advanced network-supporting functions such as Bluetooth and Wi-Fi, and data logging, it has acess to "Gentos iCloud" or "iCloud's own data center". The device is built to withstand various environmental conditions, making it highly robust. Additionally, the installation process of the meter is quite simple, requiring no pipe cutting or pump stopping. Instead, the meter can be directly

clamped onto the pipe section and tightened with the screw. The chapter further provides an in-depth explanation of the working principle of the meter, which involves transmitting and receiving ultrasonic signals through the moving liquid and calculating the transit difference between upstream and downstream to determine flow and velocity as shown in Figure *3-7*. Finally, the chapter concludes with an overview of the meter's technical equipment.
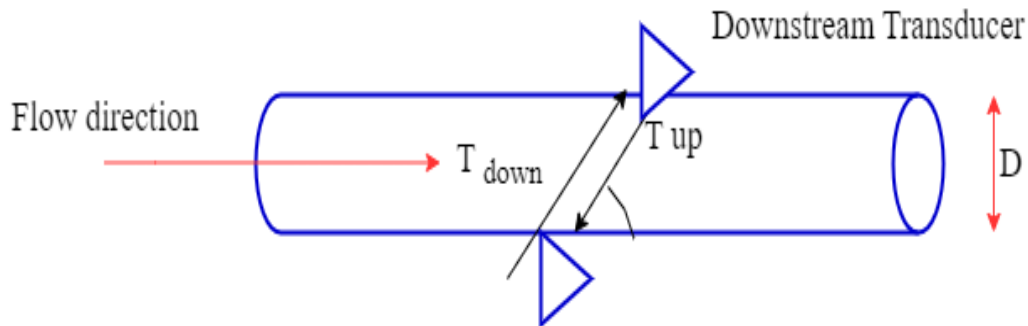
Figure 3-7 Principle of ultrasonic flow meter

The measurement equipment is fitted in the new poultry farm and machinery room to study the total energy consumption in different units like floor heating, Fan coil units and heat recovery units, drinking water for chicken as well as heat sink to old poultry farm. The specification of the ultrasonic flowmeter is given in Table 13.

Table 13 Specification of ultrasonic flowmeter used for measurement in farm

Performance Specification	
Flow range	0.03m/s-5m/s
Accuracy	Class 2
Pipe size	DN20, DN25, DN32, DN40, DN50, DN65, DN80
Fluid	Water
Pipe material	PVC, carbon steel, Stainless steel, Cooper

Functional Specification	
Outputs	Analog Output: 4-20mA, max load 750Ω
Power Supply	10-36VDC/500 mA
Temperature	Transducer measurement medium: 0°C-60°C Transmitter: -10 to 50°C
Humidity	0-99%, Relative humidity

The temperature sensor and the associated transmitter and transducer are used in a poultry farm. The Pt 1000 sensors are platinum resistance temperature sensors that have a resistance of 1000 ohms at 0 °C. These sensors are capable of measuring temperature ranging from 0 °C to 100 °C. The transmitter and transducer, on the other hand, are devices to convert one form to another. Specifically, they are used to measure flow velocity by sensing the movement of liquid passing through the primary device. The flow rate is typically recorded in m^3/h. The transducer is equipped with a 2-meter cable length, and the transmitter enclosure has an IP54 rating and made of PC/ABS material. Overall, these components play a crucial role in monitoring the temperature and flow of liquids in poultry farms, which is critical for maintaining optimal conditions for the birds.

Figure 3-8 Ultrasonic flowmeter

3.5.1 Calculate uncertainty of equipment in farm

The uncertainty analysis investigates the changes in the output that is because of the variability of input. The analysis is often investigated by using mean, median, standard deviation, and population quantiles. This estimation depends on uncertainty analysis propagation techniques. The uncertainty calculation can be done using different techniques. There are two errors to calculate the uncertainty. They are random and fixed errors. The random error can be calculated by using the following steps:

- The mean value of a set of N observations of each measurement.
- The precision index of the mean δx and the estimation of the standard deviation of the number of the set of N observations. This gives random error.
- The bias limit of each measurement has fixed δx has a fixed error. The fixed error depends on the accuracy of the measuring index which is normally estimated at 95% of confidence intervals.

The precision index of a measurement gives a random error and can be estimated from the measured values by the sensor. Precision is usually determined by standard deviation and shows how measurement differs from each other. If the standard deviation is high, the precision is low. The uncertainty deals with the description for each result which is as follows:

- The overall fixed error is the root sum square of all residuals fixed in the present experiment.
- The overall random error is from the data.
- The overall uncertainty is calculated as the root sum square of the fixed error and the random error.
  Mathematically, it is represented as follows:

$$\delta x = \sqrt{(fixed\ error)^2 + (random\ error)^2} \qquad \text{Equation 37}$$

There are different sensors used in the poultry farm. The data are recorded with an ultrasonic flowmeter manufactured by p-flow. The different pipes size is used as listed in the specification with the record of flow measured in m³/h. This sensor records the supply

54

and return temperature used for heating the poultry farm. The energy consumption is denoted by Equation 38:

$$E = mass\ flow\ rate\ \times C_p\ \times \Delta T \qquad\qquad \text{Equation 38}$$

According to OIML R49 for class 2 flow meter, the maximum permissible error (MPE) is ±2% of the measured value. According to IEC 60751 standard for pt 1000 sensors has tolerances from ±0.10°C to ±0.6 °C based on classes. The uncertainty for the specific heat capacity of the fluid is assumed to be negligible.

The uncertainty propagation in the energy production is given as:

$$\frac{\Delta Q}{Q} = sqrt\left(\left(\frac{\Delta m_{dot}}{m_{dot}}\right)^2 + \left(\frac{\Delta C_p}{C_p}\right)^2 + \left(\frac{\Delta(\Delta T)}{\Delta T}\right)^2\right) \qquad \text{Equation 39}$$

Now, since C_p is constant, the Equation 39 becomes Equation 40.

$$\frac{\Delta Q}{Q} = sqrt\left(\left(\frac{\Delta m_{dot}}{m_{dot}}\right)^2 + \left(\frac{\Delta(\Delta T)}{\Delta T}\right)^2\right) \qquad \text{Equation 40}$$

3.5.2 Calculation to estimate drying system

- Properties of air are obtained at a temperature of 50 °C, using the air properties from Table A.4 [35]. These properties, which include air density, specific heat capacity, and thermal conductivity, are critical subsequent calculations in the methodology.
- Properties of Saturated water vapor

  The properties of saturated water vapor were determined from Table A.6. [35] at a given temperature. The parameters like specific volume, heat of vaporization, thermal conductivity etc. are obtained.
- Reynold number was calculated using the standard formula as follows:

$$RE_N = \frac{uL}{\vartheta}$$

<div align="right">Equation 41</div>

Where,

RE_N = Reynold number

u= velocity of air

L =length of the surface to dry

ϑ= kinematic viscosity

- Determine Schmidt number: The Schmidt number, which is a dimensionless number describing the ratio of momentum diffusivity (kinematic viscosity) to mass diffusivity, was calculated.

$$Sc = \frac{\vartheta}{D_{AB}}$$

<div align="right">Equation 42</div>

Where,

Sc= Schmidt number

D_{AB} = diffusion coefficient

Afterwards, heat and mass transfer analogy are utilized to find the Sherwood number.

$$Sh_l = \frac{h_m L}{D_{AB}} = (0.037 Re^{\frac{4}{5}} - 871)Sc^{1/3}$$

<div align="right">Equation 43</div>

Where,

Sh_l = Sherwood number

h_m = average convective mass transfer coefficient

Equation 43 gives the average convective mass transfer coefficient.

Likewise mass rate of water evaporation per unit plate is calculated using the following equation.

$$n_A = h_m L(\rho_{AS} - \emptyset \rho_{A\infty}) \qquad \text{Equation 44}$$

This gives an evaporation rate per unit length for different velocity.

Afterwards, humidity added in air after hot air supply to the air, and humidity leaving the surface is calculated accordingly from the psychometric chart.

The drying time is calculated based on the following expression obtained after mass balance of control volume about water.

$$-n_A = m_{Ast} = \frac{d}{dt}(\rho_f.V) \qquad \text{Equation 45}$$

$$\frac{dz}{dt} = -h_m \frac{\rho_{Ast}}{\rho_f}(1 - \emptyset_c) \qquad \text{Equation 46}$$

Integrating Equation 46,

$$\int_z^0 dz = h_m \frac{\rho_{Ast}}{\rho_f}(1 - \emptyset_c)\int_0^t dt \qquad \text{Equation 47}$$

We get,

$$t = \frac{z.\rho_f}{h_m.\rho_{Ast}(1 - \emptyset_c)} \qquad \text{Equation 48}$$

3.6 Selection of dehumidification Unit (For HVAC duct integrated with dehumidifier)

To perform dehumidifier selection, we first determine the HVAC load. The HVAC load can be determined based on Manual J calculation [36].

The HVAC load determination formula is given by:

HVAC load= [(house surface in square feet) x (height of the ceiling)] + (Number of occupants) x100 BTU +(Number of exterior doors) x 1000 BTU+ (Number of windows) x1000 BTU

HVAC load = 412577 BTU, approx. 410000= 410000/12000 = 34.1 ton = 120 kW (approx.)

Therefore, the theoretical HVAC load of the farm volume is around 120 kW which is close to the capacity of the actual system.

Based on the HVAC load of the farm volume, we determine the specification for the dehumidifier system. The specification of the dehumidifier includes:

- Maximum capacity required to humidify the farm when the least temperature is 15°C and the humidity of the concrete is 90%. We set the desired humidity of 30%.
- From the calculation on various circumstances from [37], the maximum capacity required for the dehumidifier is 2000LPD (liters per day)

Air flow requirement for the dehumidifier is based on the air change per hour. The ACH value is set at 2 during the calculation. The airflow requirement for the selection of the dehumidifier unit is 20,000 m^3/h.

Based on all these parameters, the following dehumidifier is suitable to install in the farm, which allows the floor to get dry in 1 day if 2000 liters of water is present in the concrete.

Company	Model	Type	Capacity (m^3/h)
Bry-Air	BrySmart Series (BBS)	Dessicant	2000 - 25000
Ensoltec	EST 2000	Dessicant	20000
Munters	HCE Series Stand-Alone Dehumidifier	Dessicant	15000 - 40000
Condair	DA 19000SP, DA 27000SP	Dessicant	19000- 27900
Industrial Drying Solutions	DH 15000	Dessicant	25000

Among all these models, the models of dehumidifiers from condair DA19000SP and DA27000SP model are the two dehumidifiers that fit best in the requirement for this designed layout and poultry farm.

3.7 Softwares

This provides information about the simulation methodology, simulation of different alternatives and explanation of the system how it works.

3.7.1 Dymola

The simulation for heating system is done using modelica, an open source, object-oriented language designed for modeling large, complex, and diverse physical systems. To facilitate these simulations, several other tools are employed:

- Dymola serves as the platform and interface that converts Modelica code into C using a C compiler. It employs an object-oriented modeling approach and equation -based methodology (Dymola,2022).

- TIL is a modelica library created for steady-state and transient thermodynamic system simulations. TIL media, its interface library, offers fluid and solid properties from multiple property databases for various applications (TLK-Thermo,2022)

- State viewer is a visualization tool that generates graphical representations of transient thermodynamic measurements or simulation data. This allows for easier interpretation of modelica simulation results (TLK-Thermo, 2020).

- TIL File reader enables to read the temperature of source or the load that is supplied as source in the layout.

3.7.2 ANSYS Fluent

Ansys Fluent is a comprehensive computational Fluid dynamics (CFD) application designed for simulation of a range of processing including fluid flow, heat transfer, mass transfer, and chemical reactions. The user interface is designed for simplicity, facilitating the CFD workflow from the initial and final stages. Fluent is noted for its high-quality physics modeling capabilities which encompasses a range of phenomena like turbulence modeling, single and multiphase flows, combustion, fluid structure interaction, and battery modeling. Its high-performance computing (HPC) scalability makes it ideal for complex computations, capable of managing large models across multiple CPU and GPU cores. The software offers an array of solver options from pressure-based and density-based CPU solvers covering low speed to hypersonic flows, to a pressure-based GPU solver. The analysis was carried out using ANSYS Fluent 2022 R1 software. The geometry of the model is created using SOLIDWORKS 2021.

Methodologies for numerical simulation and analysis include:

- Pre-processing: The few steps are used during this pre-processing phase, these include, Geometry creation, meshing, material and fluid properties, boundary conditions, initial conditions, and solver settings. The type of model used commonly are, Continuity equation, momentum equation and energy equations like Navier strokes equation.

Likewise in addition to different equations, turbulence models describe the effects of turbulence in the flow. The turbulence model includes the k-epsilon model, the omega model, and the Reynolds stress model. In ANSYS Fluent, solver setting acts as the computational powerhouse that resolves the equations related to fluid flow, heat transfer, and other relevant

physical occurrences in the system under examination. It applies the finite volume method to breakdown these governing equations into manageable parts and solve them numerically.

Pressure-based solver, density-based solver, transient solver (including algorithms are: Implicit and explicit method, Runge -kutta method or the fractional method), multiphase solver, turbulence models are used to perform different analysis. In addition, discretizing the governing equations such as the first-order upwind scheme, the second -order central difference scheme and the third order MUSCL scheme.

In essence, the selection of a solver and numerical scheme hinges on the specific problem, relevant physical phenomenon, and the desired precision and efficiency of the simulation. The ANSYS Fluent solver is an effective instrument for simulating an extensive variety of fluid flow issues in numerous sectors and research contexts.

- Post-Processing: It involves examining, visualizing, and interpreting the simulation data. This includes creating contour plots, which display changes in variables like temperature and pressure across a domain. Vector plots are used for visualizing velocity vectors, while streamlines help illustrate the flow patterns. XY plots show the variation of a particular variable along a line or plane. Integral calculations, both surface and volume, are performed for determining actors like total mass flow rate or overall energy within a domain. ANSYS Fluent also enables the creation of animations to illustrate the temporal behavior of the flow.

During this analysis, the mathematical model used in the analysis is K-epsilon (2 equation) because of the following reasons, like: it causes balance between accuracy and computational cost, applicability to turbulent flows, sensitivity in flow and geometry changes, compatibility with multiphase flows.

 For the boundary condition, the mass flow rate is given at 9 kg/s. The inlet to the building is given at two places through the Fan coil units. The temperature of the hot air at inlet 50 °C. The material on the floor is concrete with 1cm thickness, which is uniformly distributed throughout the surface of the poultry farm.

The inlet and outlet of the hot air is provided by a fan that can be in line with the duct [38] .The specification of the fan provided at two inlet and one outlet are as follows:

Performance Characteristics:

- Maximum airflow: The fan's maximum airflow is 10689 m^3/h that signifies passing air through the duct system.
- The fan can handle air temperature up to 60 ℃.
- Mounting Orientation: The fan can be mounted either horizontally or vertically, providing versatility in its placement.

Physical Characteristics:

- Duct Diameter: The fan is designed to fit a duct with a diameter of 0.51 m.
- Power consumption: 2443 Watt
- Overall height: 0.69 m
- Overall diameter: 0.67 m
- Voltage: 230/460 volts AC, 3-phase
- Enclosure Rating: IP54

3.7.3   Helioscope

Folsom Labs created a Helioscope for an advanced solar PV design and sales tool [39]. Helioscope helps to design the photovoltaic design (PV) and sales instrument simplifies the process of creating and marketing solar projects by integrating user friendly layout tools with dependable performance modeling. It is a web-based tool, that includes Solar panel layout, shading analysis, single line diagram expert, 45000 component library, quick design revision etc.

In Helioscope, the following process is included:

- Create a Project- This includes creating a profile and project overview.
- Create a Design- This includes a design making a physical layout of solar array, design of module layout, roof shape, and surrounding obstructions which also includes electrical design, including wires and inverter.
- Draw the Mechanical Layout- A mechanical layout involves filling the field segments in the defined areas. The keep outs define areas to be excluded and generate shade from its obstruction.

- Define the Electrical settings - This involves choosing your inverter, assigning inverter quality or target DC/AC ratio, string range (set automatically according to ASHRAE) data.
- View a report.

3.7.4 Solid Works

Solid works is a versatile computer-aid design (CAD) and computer aided engineering (CAE) tool primarily used for solid-modeling. It employs a parametric feature-based approach to create models and assemblies. Starting with a 2D drawing, solid works facilitate the conversion into a precise 3D model. It offers a range of tools to enhance the construction and development of the model, enabling a comprehensive design process.

3.7.5 Jupyter

JupyterLab is the most recent online interactive platform for notebooks, coding, and data manipulation. It provides a versatile interface that enables users to organize and adapt their workflows in data science, scientific computation, computational journalism, and machine learning. During data analysis, Jupyter Notebook (Anaconda 3) was used for processing the available measured data and simulated data [40].

4 Results

In this chapter, it includes the result obtained by using the literature survey formula and data measured in the poultry farm. The sensible and latent heat produced by chicken barns are calculated based on data measured by installed sensors in farm. The sensible and latent heat is calculated in the section 4.1 using formula by Gates et al. [32]. Ventilation rate in section 4.2 includes minimum ventilation rate requirement, required to grow chicken for the period of 46 days. At this section 4.1 and 4.2, age and weight of chicken are measured from demo farm and other heat production and ventilation rate are calculated based on formula given in literature aforementioned.

Here ventilation rate according to arbor management guidebook and Norsk regulation are compared. The remaining section gives insights of proposed new heat pump that could be implemented in farm, discussion about different alternatives, mechanism of drying with heat pump, evaporation of water in concrete floor, energy production from PV panels from roof of farm.

4.1 Heat Production from chicken

According to the literature from Gates et al. [32] and data provided by Norsk Kylling [41], the expected weight of a chicken increases to 2.5 kg of live weight within 46-48 days. The growth pattern of chickens with respect to age is illustrated in Figure 4-1 . It should be noted that although chickens are introduced to the farm simultaneously, their weight is not uniform due to factors such as feed, activity level, and internal body factors, which contribute to the development of their physical structure.
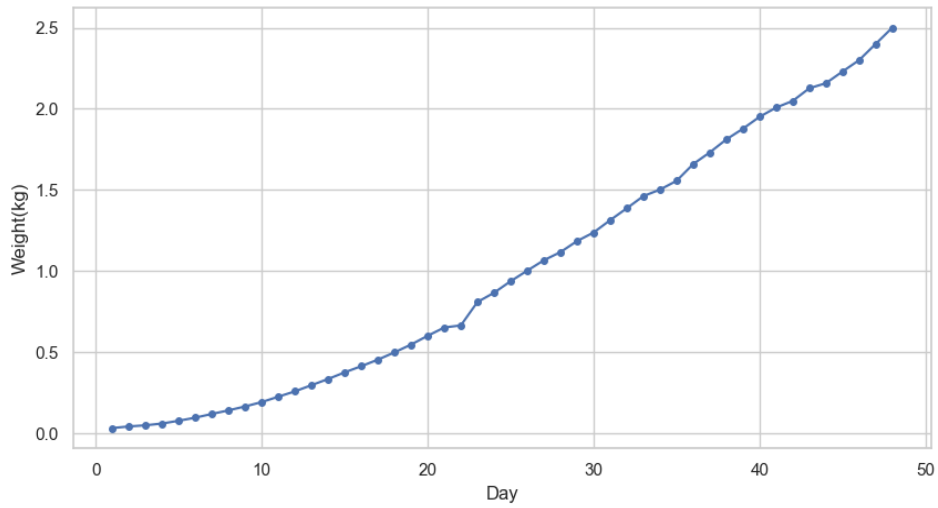
Figure 4-1 Age of chicken Vs Weight gain

Gates et al. [32] equations had potential to calculate the sensible heat and latent heat as the weight of chicken increases. The sensible and latent heat depend on many factors, but both shows the increasing trend along with age and weight. Figure 4-2 demonstrates the sensible and latent heat with respect to weight of chicken.
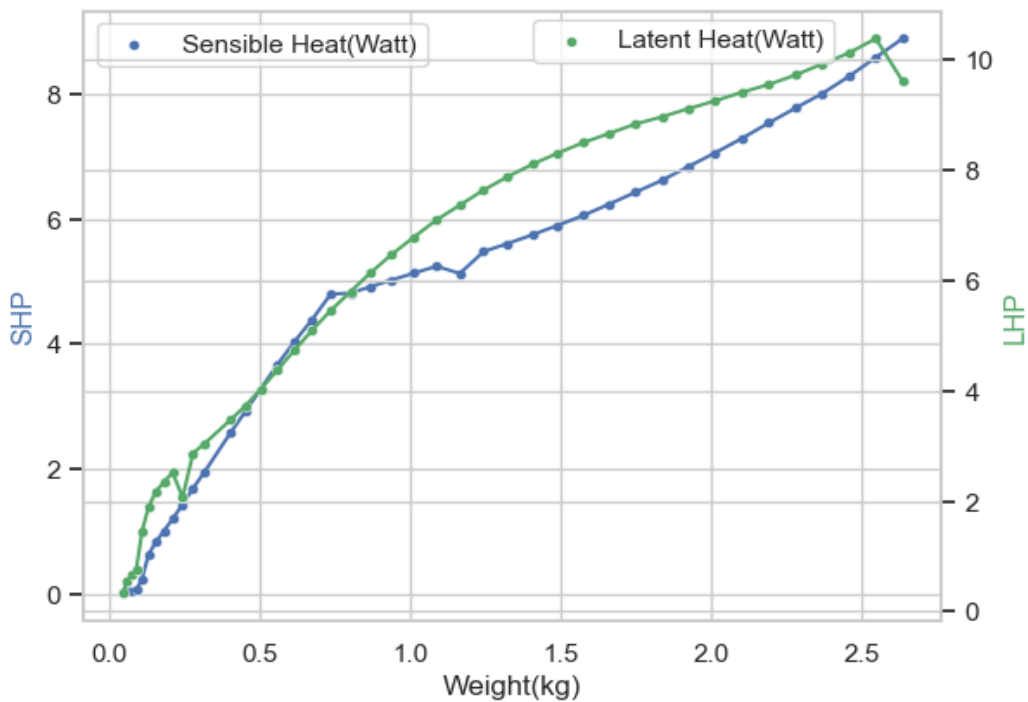
Figure 4-2 Sensible and latent heat with respect to chicken weight
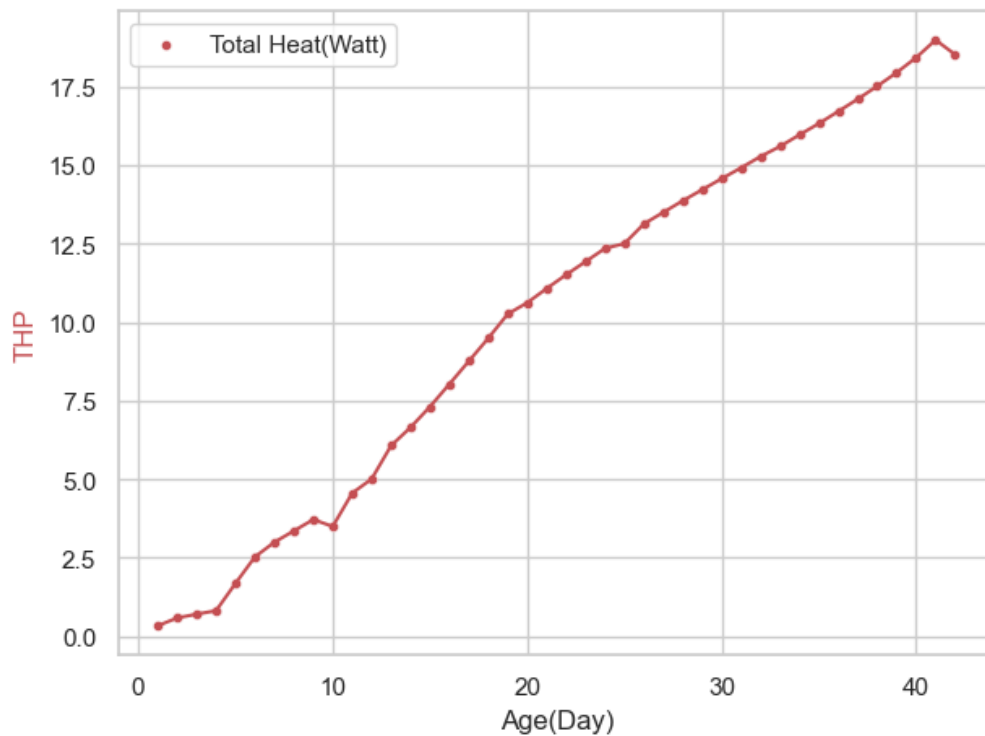
Figure 4-3 Total heat supplement from chicken with respect to weight of chicken

4.2   Ventilation Requirement in Poultry farm

The ventilation requirements for poultry farms in Norway are assumed to adhere to a standard of 4 m^3/h per kg of live weight. This implies that the demand for ventilation increases concurrently with the growth and age of chickens. However, this value is anticipated to represent the maximum ventilation demand for each kg of live chicken weight. In contrast, the Arbor Acres Management Guide [42] offers alternative recommendations for appropriate ventilation rates to promote the healthy growth of chickens. The relationship between the ventilation rate and chicken mortality within the building is substantial, as these factors are proportional to one another. The data's calculated is found in APPENDIX I.
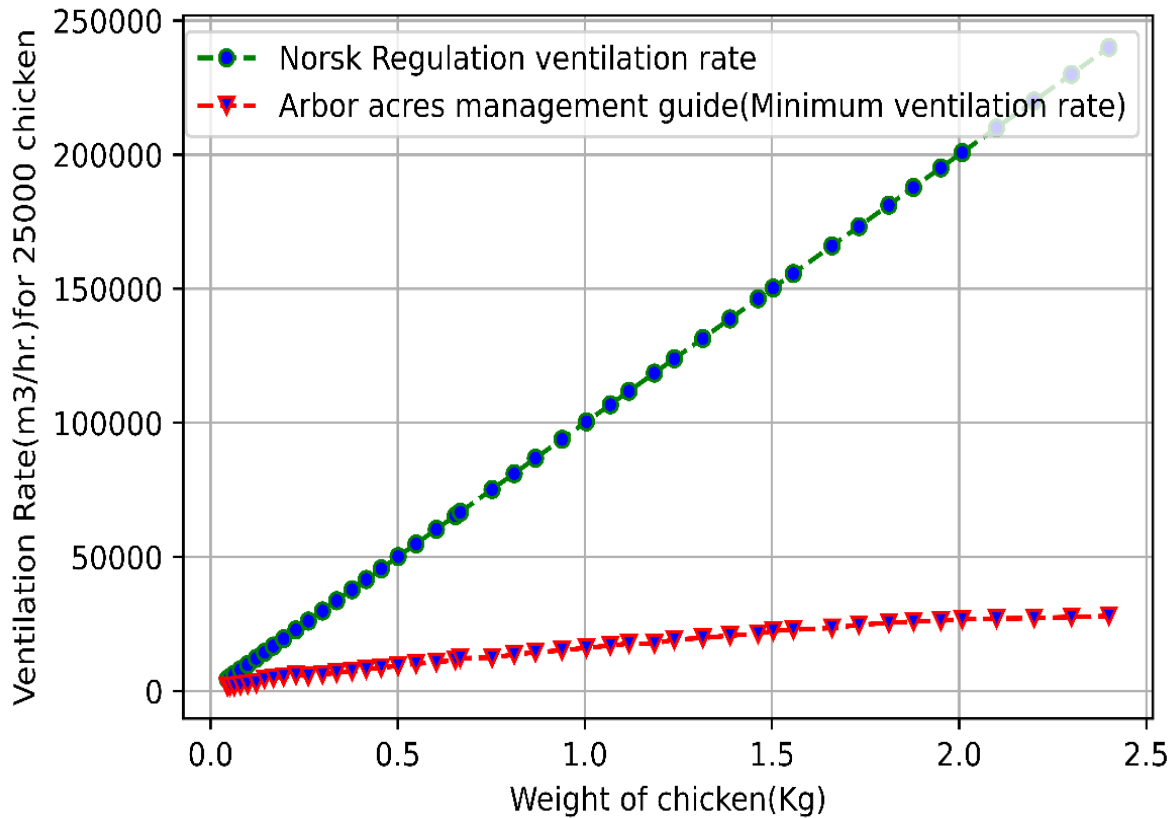
Figure 4-4 Requirement of ventilation rate for healthy chickens

4.3 Suggested (Proposed) layout that could be implemented in demo farm

This chapter demonstrates the heat pump system that could be implemented for heating and cooling the poultry farm. This option I and option II, both are proposed heating system for this demo farm. The layout provides a comprehensive demonstration of the working mechanisms for each alternative, in addition to outlining the methodology for calculating the component values. As mentioned in the earlier discussion, the proposed system incorporates a heat pump design for a capacity of 120 kW. The author proposes these P& ID diagram and believes these systems could serve as an effective and sustainable solution to the heating needs of poultry farm.

4.3.1 Option I for installation in farm

Option I demonstrate the use of exhaust humid air as a source, mounted at the heat recovery unit. Likewise, the parallel evaporators both can work as a source. In case no cooling demand is in poultry house, the refrigerant flow to 2nd evaporator could be closed. Turning on/off suction valve before two evaporators is possible. The attached layout also has a pellet boiler as a back-up solution during emergency need when heat pump is not working. The option I is multifunctional that can provide heating and cooling solutions, drinking water for domestic purpose, drinking water for chickens. The study mostly focuses on new poultry farms with 2000 m^2 since the energy is supplied from this farm to provide heating to other ones with less area. At the end, it is just shown that energy is supplied to old farms for heating since machine room is present in new poultry house.
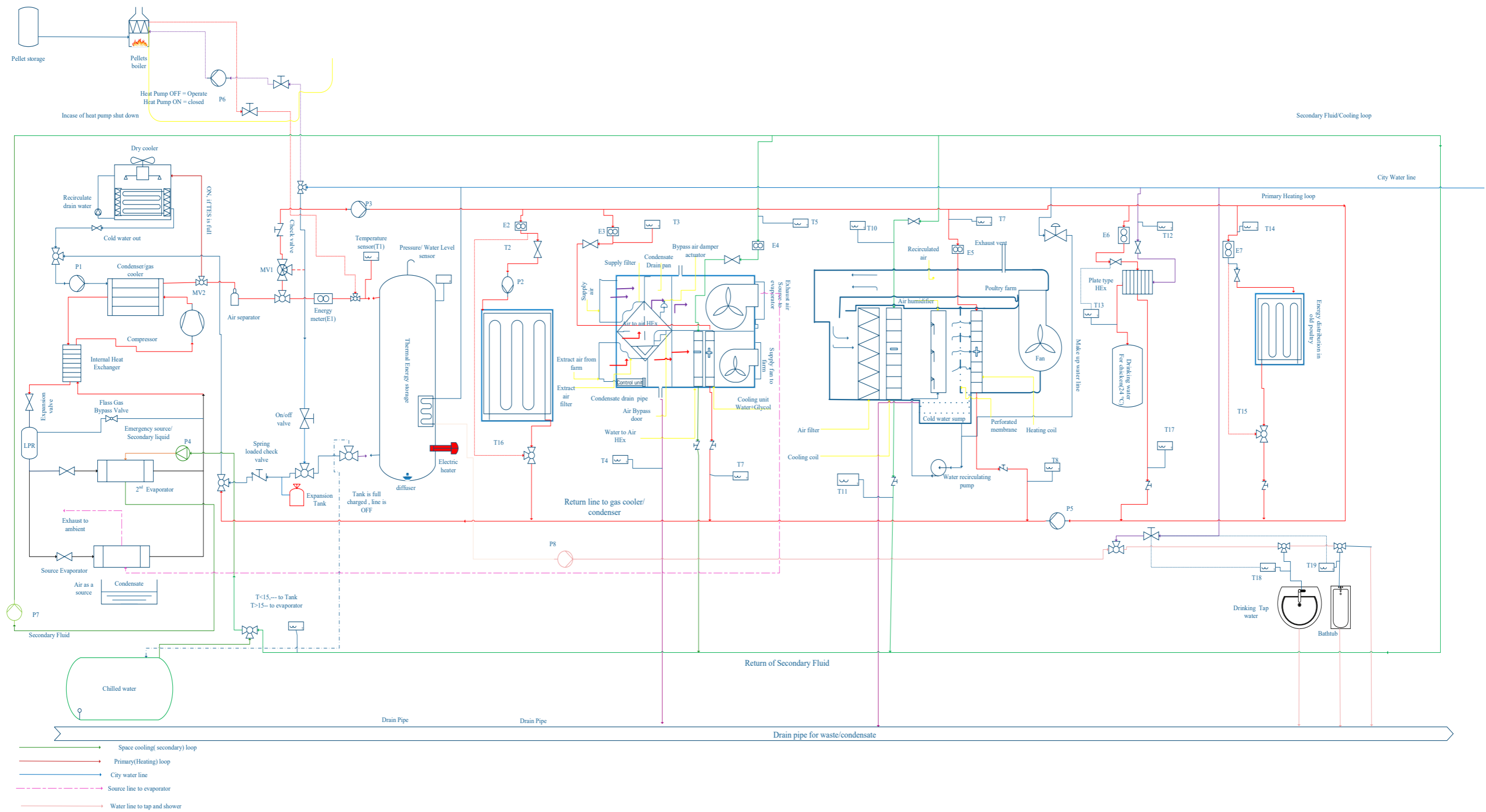
Figure 4-5 P & ID for schematic layout suitable to install in demo farm (zoom it for clear resolution and high quality)
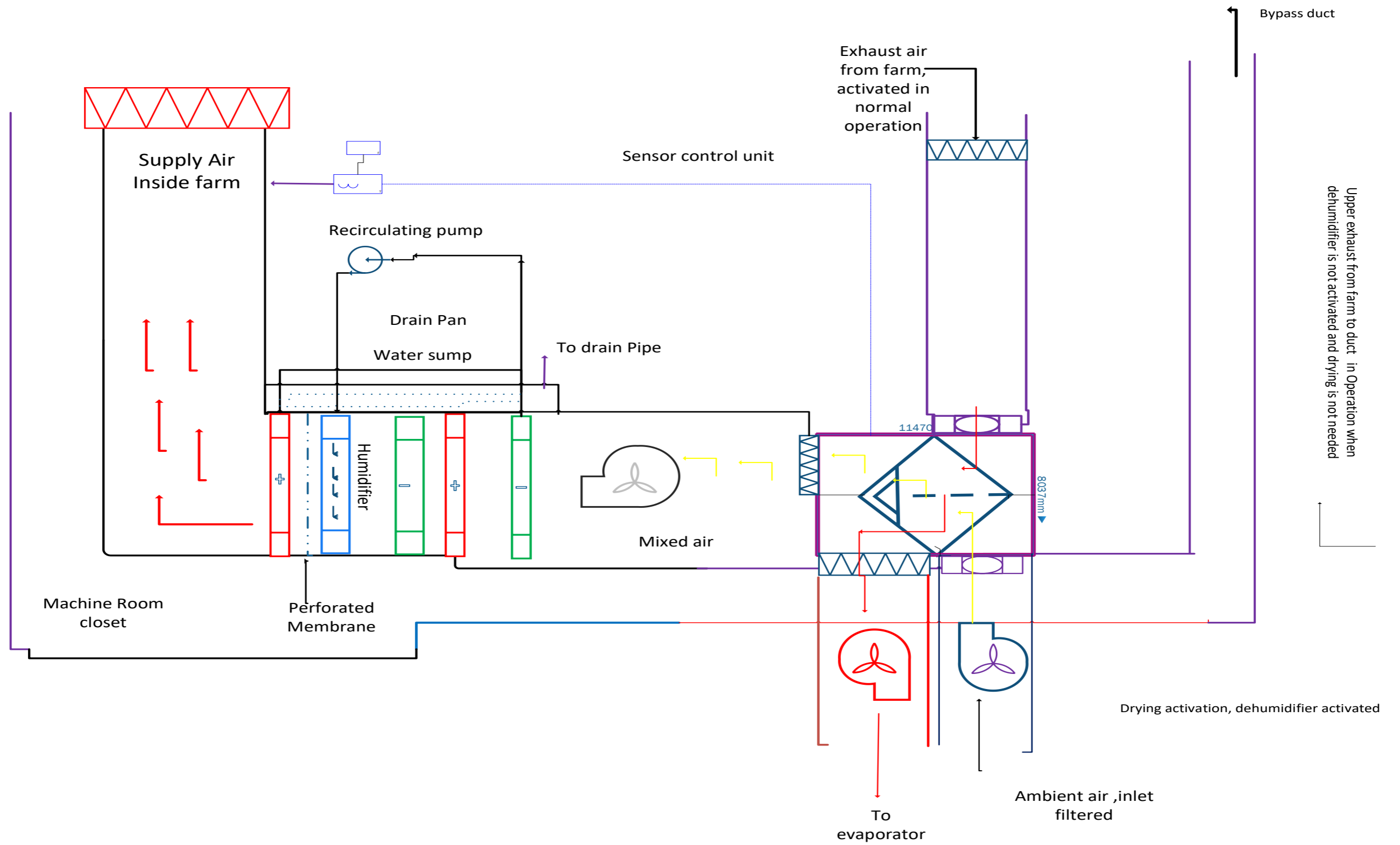
Figure 4-6 Integration of Heat Recovery Unit and Fan coil unit

Symbol (Unit)	Description
P_1	Pump to gas cooler
MV_2	Three-way valve
MV1	Shunt regulation valve
P_3	Pump for supplying hot water to different units
P_2	Pump for floor heating
T_1 (°C)	Supply temperature to thermal storage tank
E_1 (kWh)	Energy supplied to thermal storage
E_2, E_3, E_4, E_5, E_6, E_7 (kWh)	Energy supplied to different unit like floor heating, heat recovery unit, fan coil unit, drinking water for chicken, energy supplied to old farm respectively.
P_4	Pump to 2nd evaporator of cold water or chilling
P_7	Pump to supply cooling load to different units
P_8	Pump for domestic use in bathtub and drinking water tap
T_4, T_7, T_{11}, T_{16}, T_{15}, T_{17} (°C)	Return temperature line sensor from different units
T_2, T_3, T_5, T_{10}, T_7, T_{12}, T_{13}, T_{14}, T_{18}, T_{19} (°C)	Supply temperature line sensor from different units
	Space cooling (secondary) loop
	Primary (Heating) loop
	City water line
	Source line to evaporator
	Water line to tap and shower
	Three-way valve
Number of Fan coil unit for new poultry farm	2

<u>Working Mechanism (Winter condition):</u>

The heat pump cycle designed for a poultry farm incorporates two evaporators, a flash gas bypass valve, an internal heat exchanger, a compressor, a gas cooler, pressure regulating valves, a modification unit, dehumidification unit and storage tank. In this layout, the first evaporator takes air as a source, while the second evaporator exchanges heat between the secondary loop (water) and the refrigerant. The flash bypass valve bypasses vapor refrigerant from the low-pressure receiver (LPR). Both the lower temperature refrigerant (suction to the compressor) and the higher temperature refrigerant (return line from the gas cooler) pass through the internal heat exchanger unit.

The compressor compresses the refrigerant, which then passes through a gas cooler, delivering high temperature and pressure refrigerant in the transcritical mode. After the gas cooler, the return line of the refrigerant passes through the internal heat exchanger and an expansion valve, which reduces its pressure and temperature. Pressure regulating valves are added on the suction sides of both evaporators, connected in parallel. The humid air from the heat recovery unit (HRU) is used as a source in this layout, producing condensate when used as a source in the evaporator. This condensate is collected in a drainpipe.

City water is supplied to the gas cooler via a three-way valve and is then pumped into the gas cooler. The gas cooler produces hot water at temperatures ranging from 75-85 °C. An air separator is placed at the outlet to remove the air pockets. The primary heating loop supplies hot water to floor heating tubes, the HRU, Fan coil units (FCUs), and the farms drinking water system. A detailed explanation of the HRU and FCU can be found in the chapter.

The FCU and HRU include humidifiers, heating coils, and cooing coils. When heating demand is low, the hot water from the gas cooler is stored in a stratified tank. The drinking water temperature for chickens is maintained at 24 °C by exchanging heat between primary heating line and the city water using a plate heat exchanger. The return line from all units is supplied back to the gas cooler for further heating.

Heating and cooling are controlled according to the requirements inside the farm. When hot air with less humidity than requirement is present, the air is further humidified with the help of a humidifier connected to the city water line. The condensate produced is collected in a sump and

recirculated with the help of a pump. This comprehensive heat pump cycle design ensures optimal temperature and humidity conditions for the poultry farm.

Working Mechanism (Summer condition):

During summer conditions, the heat pump system adapts to provide adequate cooling and maintain optimal temperatures and humidity levels in the poultry farm. Here's the system that operates in summer conditions.

- Reduced heating demand: As the heating demand decreases during the summer, the hot water produced by the gas cooler is stored in the stratified tank for later use when needed. This storage helps balance the heating and cooling demands throughout the day or during changing weather conditions.

- Cooling via FCUs: The Fan coil unit is utilized to provide by circulating cooled water or glycol solution through the coils. The cooled air is then distributed throughout the poultry farm to maintain comfortable temperatures for the chickens. This process helps to counteract the heat generated by the chickens and any external heat entering the facility.

- Humidity control: During summer months, humidity levels can fluctuate. The humidifiers are present in the HRU and FCU system to maintain required humidity levels by adding moisture to the air when needed. The humidifier is connected to the city water line, and the condensate produced is collected in a sump and recirculated using a pump.

- Evaporative cooling: The evaporators in the system can also contribute to cooling. As the refrigerant evaporates and absorbs heat from the secondary loop (water), it helps lower temperature of the circulating fluid, which can be used for cooling purpose in the facility.

The dry cooler is integrated into a heat pump system. When a dry cooler is integrated into a pump system with a fully charged storage tank, it effectively prevents overheating and maintains efficient operation. The control system continuously monitors the storage tank temperature, the dry cooler is activated. At this point, the control system diverts the hot water flow from the gas cooler towards the dry cooler using a three-way valve (MV2). The dry cooler, consisting of a heat exchanger with a finned tubes or coils and a fan system, dissipates excess heat from the hot water to the ambient. Consequently, cooled water returns to the system, and excess heat is released to the environment. Once the storage tank temperature drops below the

predefined threshold, the control system deactivates the dry cooler, returning the hot water flow to its normal path. This ensures the heat pump system continues to operate efficiently without necessary heat loss, effectively managing excess heat with the help of the dry cooler. The FCU are 2 to provide uniform distribution throughout the area in the poultry farm. The heating and cooling loop are all in a closed loop. The pellet boiler which exists in the farm now is connected to provide emergency heating in case the heat pump shout down. Moreover, the storage tank has a coil to heat city water in bathtub and shower. In total, this is all in one solution with the best use of available components in the farm now.

4.3.2 Option II for installation in farm (Water as a source)

In option II, instead of using two parallel evaporators, the city water or from the bottom of the storage tank. Using one evaporator as a source will help to produce the chilled water to use for cooling and heating. This makes it easier to produce installation and gives low cost to install.

During analysis, we are going to compare the parallel and single evaporators as a source. Both other components in the P& ID will work on similar mechanism. These will enable us to check the COP of two different under different load conditions.

4.3.3 Components used in system

I. Evaporator

The evaporator is used for the heat source. Source implemented in these models will be moist air or water from the bottom of the thermal storage tank. A steady state the system is designed to take heat source of 99 kW. The evaporator has a heat transfer coefficient of 4000 W/m^{2}K. The heat exchange takes place between air and refrigerant in a source evaporator. Hot moist air at the exhaust of the poultry farm is given as an input source. Figure 4-7 represents the uncased source evaporator.
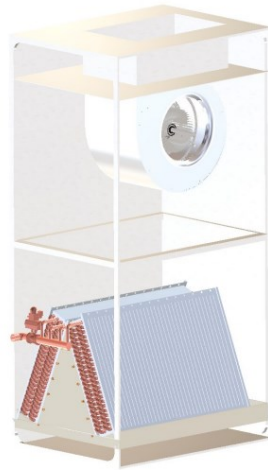
Figure 4-7 3D modelling of source heat exchanger

[Alfa Laval AC line of brazed plate heat exchanger](#)/plate and frame heat exchanger can be used for the application in this situation. The heat exchanger consists of a pack of corrugated metal plates with valves in front inlet and outlet of separate fluids. It can be used to chill water, 2nd evaporator for option I and source evaporator for option II. The capacity available is 1-1000 kW.

II.   Compressor

The compressor compresses the fluid to high temperature to cover the heating demand of the building. The pressure ratio is 2.42 while compressing the CO_2 from 39.69 bar to 96 bar. The compressor used in the system is a piston compressor. The isentropic efficiency is assumed to be 0.7 which gives the volumetric efficiency of 0.85.
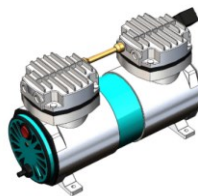
Figure 4-8 Compressor for the system

Specification of the compressor:

Compressor Type	Piston
Volume of flow inlet to the compressor	17.82 m^3/h
Enthalpy at compressor outlet	483.26 kJ/kg
Stroke volume/ displacement volume of the compressor	20.97 m^3/h
Shaft power	24,68 kW
Isentropic compressor capacity	17.27 kW

A Dorin compressor for CD series can be used in the system to fulfill the demand in the farm. The compressor operates at trans critical mode with operating pressure up to 110 bar. The displacement of these compressors ranges from 1.12 to 80 m^3/h (50 Hz, single stage). Likewise, GEA's, a German manufacturer OEM, HG CO2 T compressor could be used instead. However, this can cost more because of its upward operating pressure.

III.   Internal Heat exchanger

The internal heat exchanger helps to increase the overall efficiency. It allows hot refrigerant to transfer heat to cold refrigerant. The hot refrigerant leaving gas cooler transfers heat to refrigerant before entering compressor. It reduces the workload of the compressor, so that less liquid refrigerant enters onto it. In the steady state, the internal heat exchanger is assumed to give 5 K of superheating and subcooling respectively.

IV.   Expansion valve

A thermostatic or expansion valve can be used in the system. The valve needs to have a capacity of at least 7.4 kW. According to the necessity, the thermostatic expansion valve from Danfoss could be used.

V.   Gas cooler

The gas cooler is designed to exchange the heat between hot refrigerant and water for the aforementioned layout. Here, the gas cooler has a heat transfer coefficient of 4000 W/m²K. The outer surface is designed to cool using water jacket. The heat exchanger used in gas cooler is counter current direction. The recirculated water from the system or city is assumed to be 20 °C which is further heated to 75-85 °C using gas cooler.

VI.   Liquid receiver/Separator

The fluid line from the internal heat exchanger is expanded from 96 bar to 39.6 bar through the expansion valve. The two phases separation takes place in the tank. The gas in tank is passed from the top of tank whereas liquid line is further taken to evaporator. The evaporator ca be single or multiple depending upon the requirement and system. The liquid droplets settle in the tank using the following relationship in Equation 49.

$$F_g = \frac{M_p(\rho_l - \rho_v)g}{g_c \rho L}$$

Equation 49

Where,

F_g = gravity force

M_p = mass of droplets

g = gravitational constant

ρ_l = liquid density

ρ_v = vapor density

g_c = gravitational constant/ (gravitational force- vessel material stress²)

Hence, the vertical terminal velocity is determined by Equation 50.

$$U_T = K \sqrt{\frac{\rho_l - \rho_g}{\rho_v}}$$

Equation 50

Where,

U_T = vertical terminal velocity

K = separator k values

The refrigerant used in the system is R744, with a density of 1.98 kg/m³. The mass flow rate at steady state is 0.5 kg/s, compressor capacity of 24 kW. Assume that the separator efficiency is 0.8 and a residence time of 5 seconds. The separator mass is 2.5 kg. The separator volume needed is calculated as 1.58 m³ (1580 liters).

VII.   Thermal storage tank

A thermal storage tank is used to store hot water. Hot water can be used to heat the floor. Thermal storage tank has an electric heater which can be used during high heating demand in the building or failure of heat pump. Stored hot water can be used to heat ambient air in the heat recovery unit and fan coil unit before supplying inside building.

Figure 4-9 Thermal storage tank

The two ports are used in parallel to each other in the storage tank. The upper port is used for inlet and outlet of the hot water. The lower port is used to supply water to gas cooler or evaporator for heating and cooling respectively. The other port opposite can be used for defrosting evaporator if needed or utilized during cooling.

Specifications that can be used for thermal storage tank are:

Capacity	4000l
Diameter	1.74 m
Height	2.84
Maximum operating temperature	95 °C
Maximum operating pressure	10 bars
Insulation Thickness	0.12m (PU flexible foam with foil shell)
Material	Stainless steel
Option	Electric heating element

VIII. Expansion Tank

The purpose of an expansion tank in a hydronic system with a heat pump is to accommodate the expansion and contraction of the water in the system as it heats up and cools down. When water is heated, it expands and can cause an increase in pressure in the system. Without an expansion tank, the pressure increase could potentially damage the system.

As the water in the system heats up and expands, it pushes against the bladder or diaphragm, compressing air in the tank. This compatibility of the air allows the expansion tank to absorb the excess pressure caused by the expanding water, preventing damage to the system.

The basic equation for a bladder or diaphragm expansion tank with pre-charged air s given as in Equation 51:

$$V_t = V_s * \frac{\left[\left(\frac{v_2}{v_1}\right) - 1\right] - 3\alpha\Delta t}{\left(\frac{P_{pre}}{P_1}\right) - \left(\frac{P_{pre}}{P_2}\right)}$$
<div align="right">Equation 51</div>

Mostly the pre-charged pressure (P_{pre}) is equal to minimum pressure in the system, P_1.

This makes the Equation 51 to Equation 52.

$$V_t = V_s * \frac{\left[\left(\frac{v_2}{v_1}\right) - 1\right] - 3\alpha\Delta t}{1 - \left(\frac{P_1}{P_2}\right)}$$

<div align="right">Equation 52</div>

Where, V_t is the volume of the expansion tank, V_s is the volume of the system, v_1 is the specific volume of water at low temperature, v_2 is the specific volume of water at high temperature, α is the thermal expansion coefficient.

Here, we assume that the minimum temperature of water is 20 °C and maximum temperature is 100°C along with corresponding pressure at 1 bar and 3 bar respectively. The volume of water throughout the system is 5 m³ with a 4 m³ storage tank. The tank is made up of stainless steel whose volume is 0.25m³ but, with safety factor 1.5 it must be 0.372 m³ (372 liters).

IX. Floor heating system

The floor heating tubes are embedded inside the floor at a certain depth. It is normally 3.81 cm under the top of slab. A pump in inlet is provided before the floor heating to make enough pressure for the distribution of water in tubes.

X. Heat recovery Unit

The heat recovery unit in the system consists of an air-to-air heat exchanger, heating, and cooling coil with hot and cold water respectively. The air-to-air heat exchanger is used to exchange heat between exhaust air from building to supply ambient air. The door to exhaust in ambient will open according to necessity of fresh air since the system has to control CO_2 and NH_3 concentration.
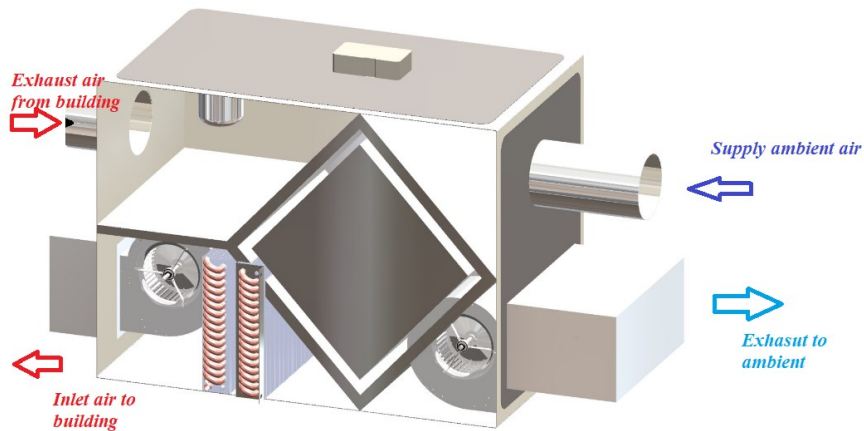
Figure 4-10 Heat recovery unit

XI. Fan coil unit

The fan coil consists of a humidifier control unit, heating, and cooling coil. The humidifier humidifies air before entering inside the building to meet the required demand. A small pump is fitted to recirculate the condensate water present in drain pan. The hot air is supplied to the farm with FCU from two different inlet points of the roof to make uniform distribution of air at every corner. There needs to be 2 FCU installed in the new poultry farm for uniform distribution of air over the entire surface.
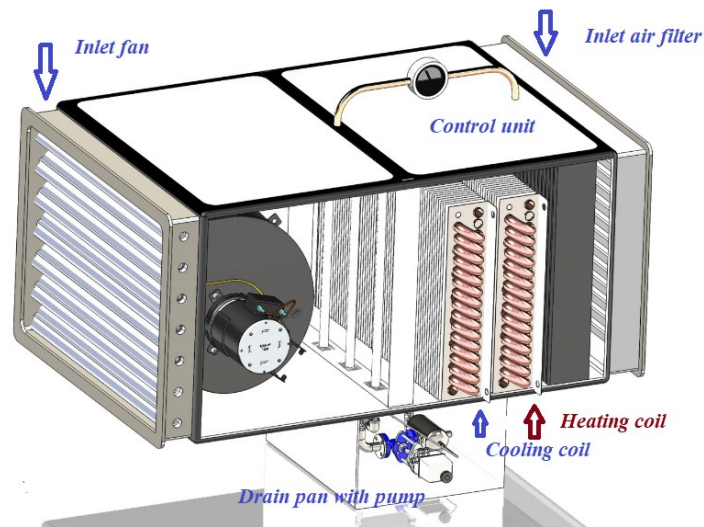
Figure 4-11 Fan Coil Unit

XII.   Arrangement for chicken to drink water

The most comfortable temperature for drinking is 10 ℃ to 20 ℃ by mature birds. A comfortable water temperature makes the chicken healthy. However, 24 ℃ reduces the mortality rate and maintains the chicken well-being. The setup is arranged to maintain 24 ℃ using heat exchanger between city water and hot water line.

XIII.   Shunt Regulation Valve

Shunt valves are employed in hydronic systems to regulate the appropriate flow and supply temperature to distribution units. Specifically designed to integrate with manifolds, these valves help create a compact, low temperature heating distribution system. Mixing shunts play a crucial role in accurately blending hot water from the heat source with cold water, ensuring optimal temperature control for individual heating zones.

By facilitating accurate temperature regulation, shunt valves significantly enhance the efficiency and performance of the hydronic heating system. These valves are integral components that contribute to the effective management of heat distribution and flow rates, allowing for a stable and energy-efficient heating environment.

Shunt valve regulation is important because of the following reasons:

- Balances the flow of hot water between different heating zones, ensuring even heat distribution and optimal comfort.
- Helps to avoid overloading or underloading the heat source, which can improve the system's overall efficiency.
- Provides better control of individual room or zone temperatures, leading to improved comfort and efficiency.
- Reduce risk of temperature fluctuations and noise in the system, which can be caused by unbalanced flow rates.

XIV.   Dry cooler

Selection of the appropriate dry cooler for a system is essential for achieving optimal performance and efficiency. To choose the right dry cooler for a system, we need to consider the following factors:

- Cooling capacity: the total heat load needed to dissipate to provide cooling in the building.

- Fluid type and temperature: the type of fluid being cooled needs to be considered since different fluids have different heat capacities and requirements.

- Air flow: The dry cooler should have sufficient airflow for effective heat dissipation. We need to consider fan type, air velocity, and the potential for air recirculation, which could reduce the cooler's performance.

In our system layout, CO_2 as a refrigerant and Air/water or water/water version can be selected according to the heat source used. The Enerblue IRRIDIUM-IRIDIUM WW product can be used for this system implementation. The available capacity ranges from 16.8 kW- 124.3 kW that can operate in the external temperature -20 °C and produce hot water up to 90 °C.

4.4 Calibration of measured data from farm

The uncertainty analysis indicates that systematic errors need to be rectified to a recognized or accurate value. This can be accomplished by adjusting the various sensors in the system. Calibration is a process that entails comparing the data obtained from different sensors in the system to a calibration benchmark of known precision. The poultry farm consists of a series of sensors to measure the thermal energy demand at different units.

The features and accuracy of different sensors in the facility to measure data in the poultry farm are as follows:

Table 14 Features and accuracy of different sensors in the facility

Sensor Type	Type	Accuracy Class	Measuring range	Accuracy
Temperature	pFlow	Class B		±(0.3+0.005T) °C
Power	Split-core current Transformer	Class 1	-20 to 55 °C	Class 1
Volumetric mass flow	pFlow	Class 2	-10°C to 60 °C	±2%
Data logger (eGauge Pro Specifications)	ANSI C12.2		-30 to 70 °C 80% humidity up to 31 °C	0.5%

The sensor gives the uncertainty for the energy consumption based on the accuracy of data logger. The data has a trial number of 2194 which is measured every 10 minutes in the poultry farm. The data are logged in from 01.0.3.2023 (Time = 01:03) to 16.03.2023 (Time = 06:23). In the measurement, thermal energy meter, flow meter and temperature sensor recorded energy consumption in kWh, volumetric flow rate is m^3/h, supply and return temperature in °C. The uncertainty of the sensors for energy consumption are listed as follows:

Energy consumption at units	Random error	System error	Overall uncertainty
District heating (Fjernvarme)	0.16	0.06	0.2
Floor heating (GulvvarmeE2)	0.01	0.00	0.01
Floor heating (Gulvvarme E2.1)	0.01	0.00	0.01
Heat recoveryE3(varmegjenvinning)	0.02	0.00	0.02
Fan coil unit	0.16	0.03	0.17

The overall uncertainty in energy consumption throughout the system is $\pm$ 0.41%.

4.5   Simulation Result

This chapter gives a result analysis obtained from the simulation of both the alternatives suggested to install on the farm.

4.5.1   Option I

This is the modelica layout for the 1ˢᵗ option using air as a source. The two parallel tubes represent the evaporators. One evaporator produces chilled water and the other one works as a source for moist air. TILMedia uses VLE fluids as a CO_2 as a refrigerant, moist air is used as a source, liquid used is water. The VLE fluid CO_2 refrigerant produces hot water. The internal heat exchanger helps to increase the COP. A PI controller controls the high- and low-pressure side to provide required heating and cooling demand. Figure 4-12 shows that PI controller controls inlet of cold-water flow rate to gas cooler in such a way that it can give outlet temperature for heating from 80-85°C. The figure also demonstrates a separator / liquid receiver which takes out the flash gas and bypasses directly to the suction line. The low-pressure side is 39 bars and high-pressure side is 96 bars. The component is given as input in modelica with the characteristics defined in chapter 4.3.3.

The gas cooler in the refrigerant transfers energy to the city water, hence it is either supplied to HVAC unit, floor heating, drinking water for heating. The hot water is supplied to the stratified storage tank in case there is no heating demand.
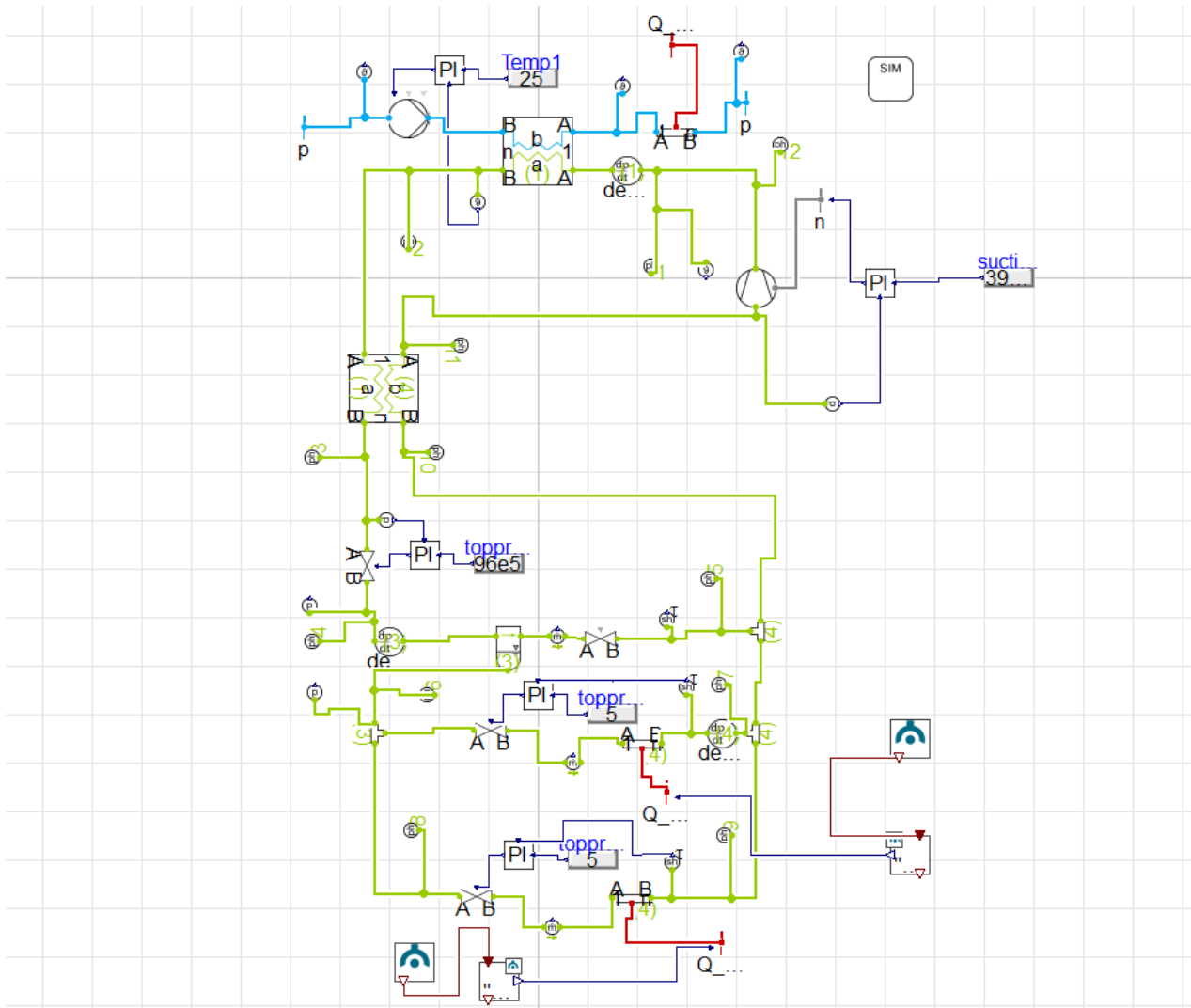
Figure 4-12 Modelica layout air as a source
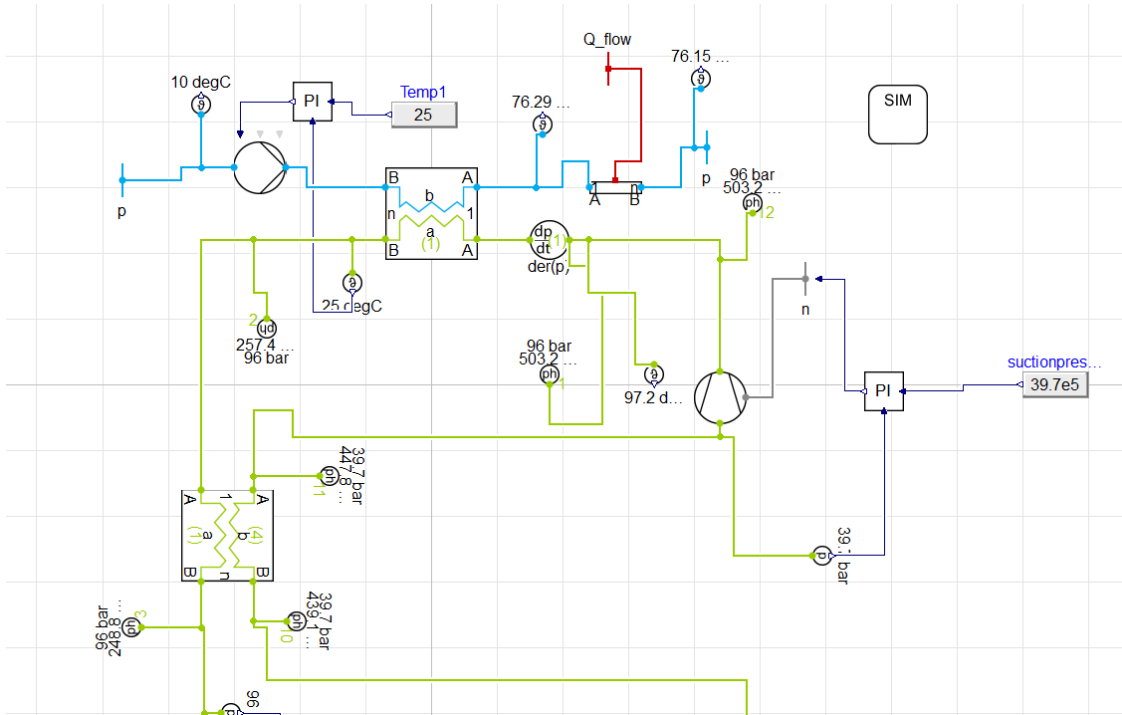
Figure 4-13 High pressure side after simulation for 100000s
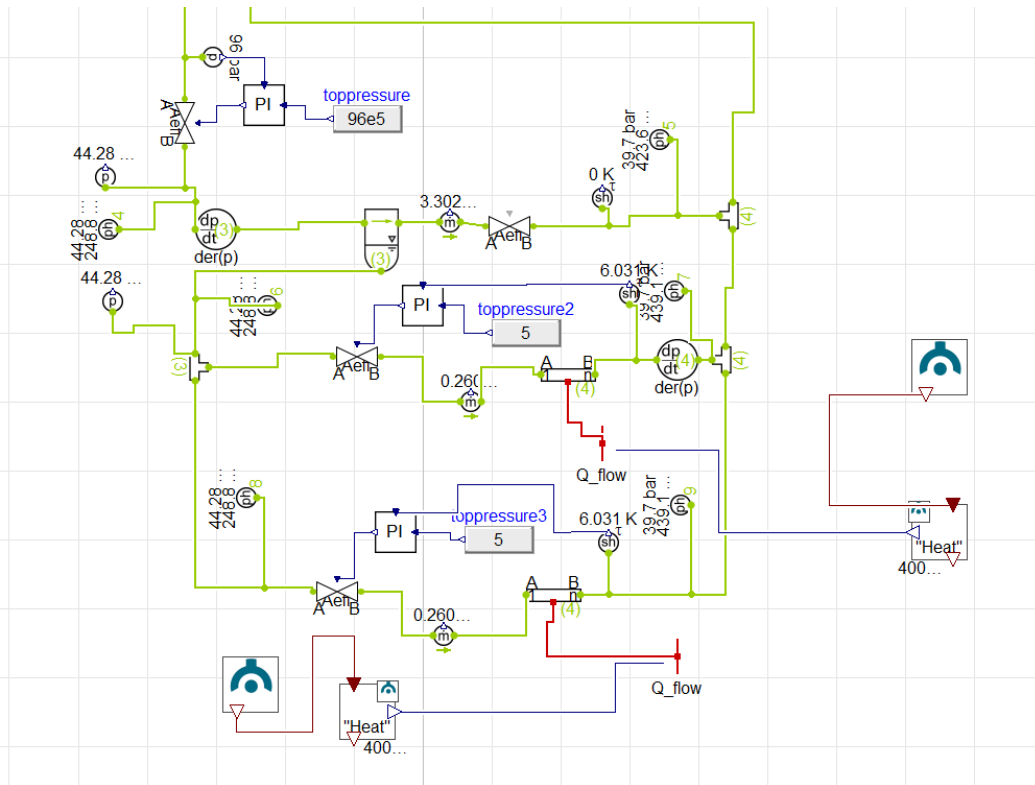
Figure 4-14 Low pressure side after simulation

In this simulation, several critical observations have been made across different stages, which are integral to understanding the process and performance of the system. At the 1st state, the pressure at the high-pressure side was recorded to be 503.2 kJ/kg.

Following this, at state 2, the gas cooler's influence on the system could be seen as the enthalpy dropped to 257.4 kJ/kg after gas cooler at 96 bars. This stage further involved a temperature transformation where cold water, initially at a temperature of 10 °C, was heated up to 76.29 °C. The heated water was then directed to a thermal storage tank, which was represented as a tube in the simulation.

At the 3rd point, the enthalpy was observed to decline marginally to 248.8 kJ/kg. Remarkably, this same enthalpy value was maintained across three different points-state points 4,6 and 8. These observations were recorded after the refrigerant was guided through the expansion valve.

Another key process involved the routing of the refrigerant pass a bypass valve to junction 4, where a mass flow rate of $3.302e^{-07}$ kg/s was noted. In this stage, two evaporators are depicted as tubes in the simulation, displaying a mass flow rate of 0.261 kg/s. These evaporators played a crucial role in producing cold water in one evaporator and other evaporators are taken as a source.

Moving to state points 5,7,9 and 10, a consistent pattern of enthalpy measurement was noted. The enthalpy remained at 447.8 kJ/kg. The conclusion of this cycle was marked by the compressor outlet's temperature, which was recorded at 97.2 °C.

P-h diagram:
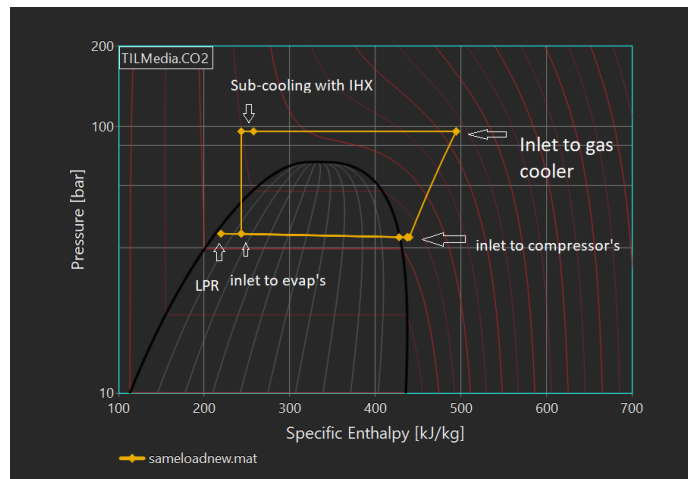
Figure 4-15 P-h diagram for air as a source

In Figure 4-15, a detailed illustration and accompanying p-h diagram, obtained from TLK Dave's, effectively demonstrate the function of a heat pump system in Modelica. The system comprises two parallel evaporators operating at the low-pressure side (LPR). The compressor comprises the refrigerant from the low-pressure side to high-pressure side, while the expansion valve operates in reverse, reducing the refrigerant's pressure and temperature.

The initial heat exchanger plays a pivotal role in the system, providing both superheating and subcooling for the refrigerant. Superheating ensures that the refrigerant vapor entering the compressor is free of any liquid droplets, preventing damage to the compressor. Simultaneously, subcooling ensures that the refrigerant remains in a liquid state before entering the expansion valve, contributing to the system's overall efficiency.

The gas(vapor) of the refrigerant bypass and is directed to the suction side of the compressor, where exits for the two parallel evaporators are provided. This design facilitates a continuous cycle of the refrigerant through the system maintaining optimal performance and efficiency in the heat pump process. The modelica-based model enables a comprehensive understanding and analysis of the system performance, efficiency, and potential improvements for real-world applications.
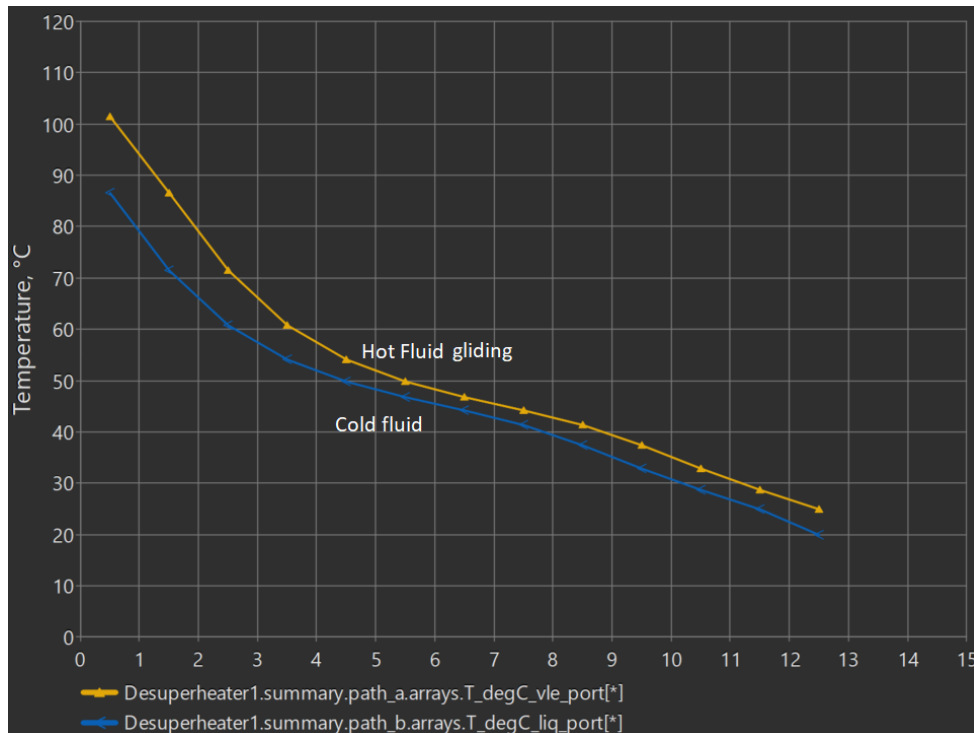
Figure 4-16 Counterflow of hot and cold fluids inside gas cooler

Figure 4-16 shows the cold-water at 20 °C being heated by the VLE fluid. The VLE fluid shows the gliding behavior inside the gas cooler. The exit at the compressor is approximately 100 °C which transfers the heat to cold water. The city water temperature rises to 85 °C when heated at the gas cooler which is further sent to different energy distribution units or thermal storage tank in case energy demand is less. The pitch point is approximately 6 K.

The system at constant steady load makes the system efficient. The COP of the system in the simulation when it became stable was 4.09. Figure 4-17 shows that PI controller effectively controls the system over time approximately around 2200s. The evaporator load was 17.5 kW for air as a source and the second evaporator cools the same load of water at the same time frame. The off-design conditions fluctuations and variations in load might get affected due to the ambient temperature of the air. At the start of simulation, the result shows an oscillation at high pressure side, resulting fluctuations on COP at initial stage. However, after 2200s, the fluctuations are damped and controlled by increasing the sensitivity of the PI controller.
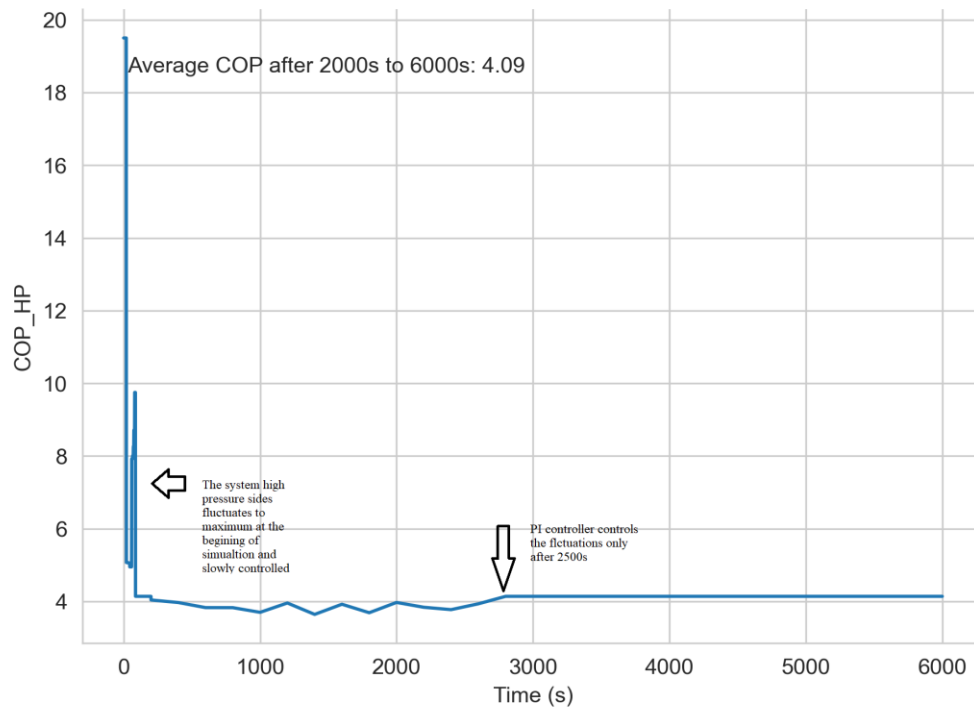
Figure 4-17 COP of heat pump over Time at steady state

In the analysis of variable load in parallel evaporators, distinct load levels were evaluated, including 8.75 kW, 17.5 kW, 20 kW, and 49.5 kW. A notable increase in COP was observed, as illustrated in Figure 4-18. In these parallel evaporators, the upper evaporator can be used to chill down water and lower to take air as a source. Each of these levels was simulated for a duration of 6000 seconds. Consequently, throughout the variable load study, the total simulation time reached 24000 seconds. This dynamic load variation exhibited a COP range between 3.74 to 4.5.
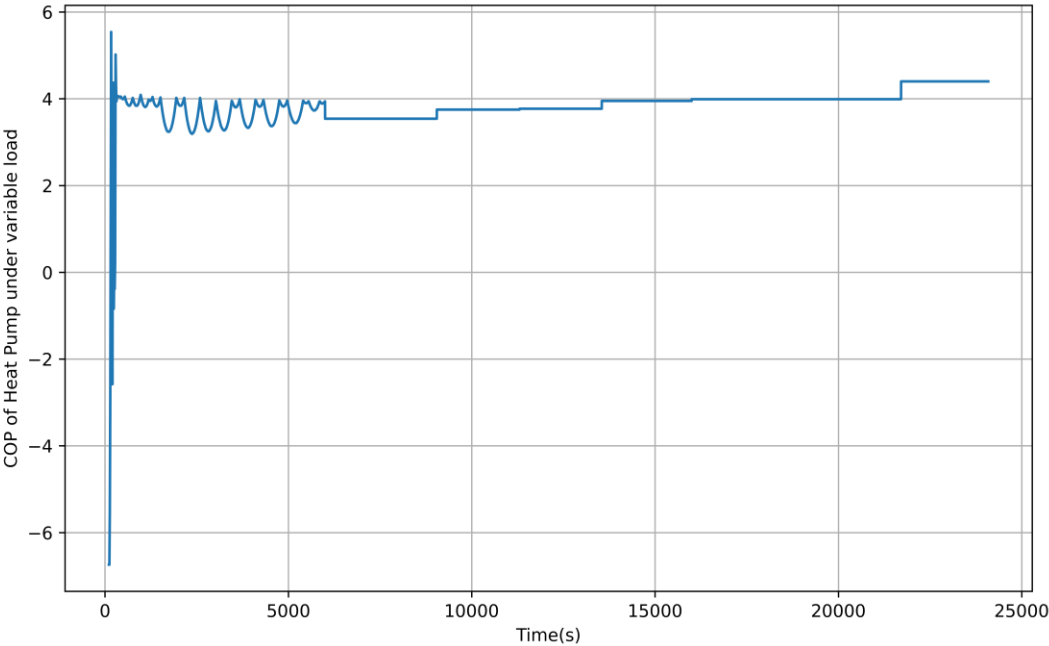
Figure 4-18 COP of heat pump under variable load

4.5.2 Model in Modelica for hot water production 2nd Option
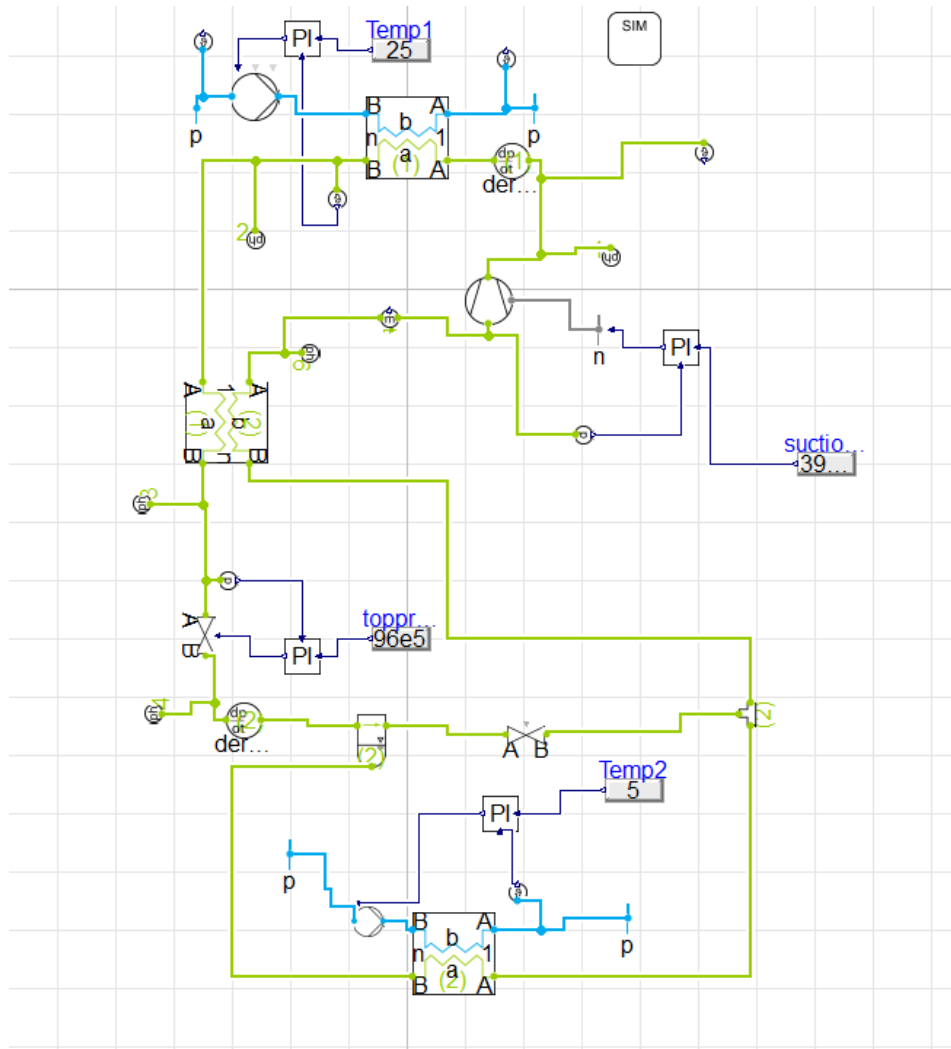
Figure 4-19 Modelica layout water as a source

 PI controller:

PI controller is one of the most widely used controllers in system simulation and practice, providing excellent control and stability in various applications. During the simulation of the refrigeration model in Dymola, it was observed that the PI controller on the high-pressure side exhibited slight fluctuations at the initial stage, causing instability in the system. To improve the performance and stability of the PI controller in Dymola, several steps can be taken, including:

- Checking the sign of the process gain to ensure correct control direction.

- Tuning the pure proportional component(P) to achieve a balance between responsiveness and stability.

- Adding the integral component(I) to eliminate steady-state errors and improve overall control.

In situations where the high pressure remains consistently too high or too low and does not change over the simulation time, the cause might be attributed to boundaries within the PI controller. In such cases, adjustments to the cross-sectional area of the valve may be necessary. Conversely, if the high-pressure side fluctuates around the setpoint, the issue could stem from the k-value or the integration time. Fine tuning these parameters can lead to improved system stability and performance.

Hence, the tuning PI controller in Dymola is an essential aspect of ensuring optimal performance and stability in a refrigeration system. By adjusting the proportional, integral, and the controller can efficiently regulate the high-pressure side, minimizing the fluctuations and maintaining overall system efficiency.

In the given P-h diagram at Figure 4-20, the high-pressure side is at 96 bar and the suction pressure (low-pressure side) is at 39.6 bar. The input of the city(recirculated) water is at 25 °C and the water passed through the gas cooler is a heater in the temperature range from 75-85 °C. The flow rate of water through the gas cooler is controlled using a control system in the pump. Refrigerant has a flow rate of 0.5 kg/s throughout the circuit. In the simulation at state point 1, the enthalpy 490 kJ/kg loses energy and becomes 257 kJ/kg after the gas cooler at state point 4. The internal heat exchanger helps to transfer heat between the high-pressure and low-pressure sides to ensure higher efficiency. Enthalpy at state point 4, 234 kJ/kg is after the throttling expansion valve. On the evaporator side, 15 °C water is passed making the water as a source, which gives out 7 °C, that can be used for drinking or other AC purpose when there is cooling demand in the farm. The compressor has the same specification as in option I of the system.
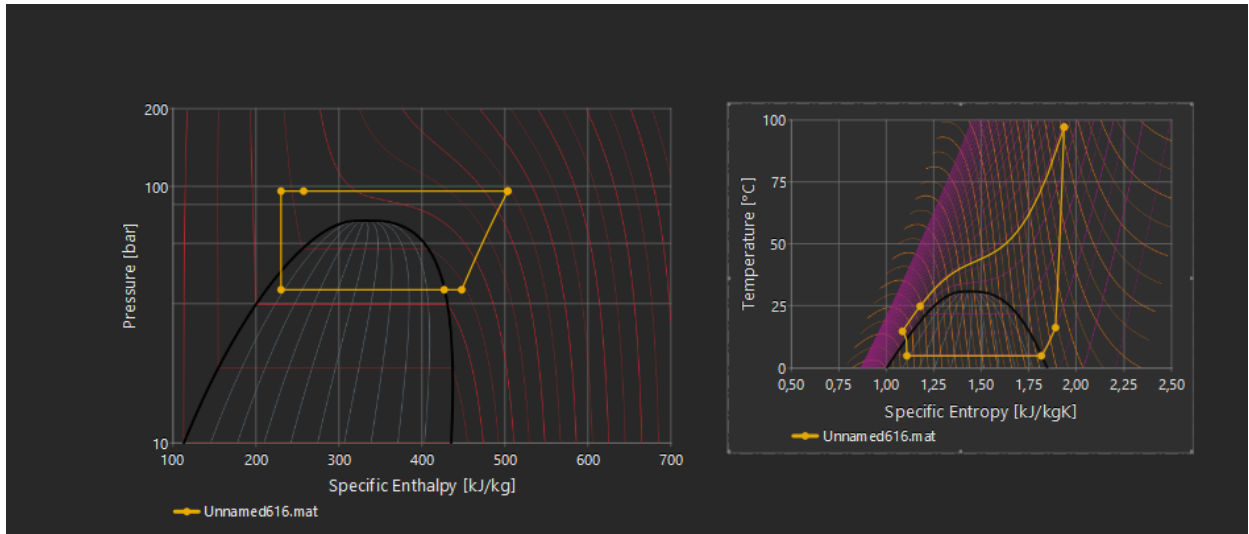
Figure 4-20 p-h and T-S diagram

In Figure 4-21, the water is heated from 25 °C to 75 °C, during a steady state when the system is operated during the simulation. Likewise, the 88 °C refrigerant after the compressor cools down to 25 °C, releasing heat to water in the gas cooler.
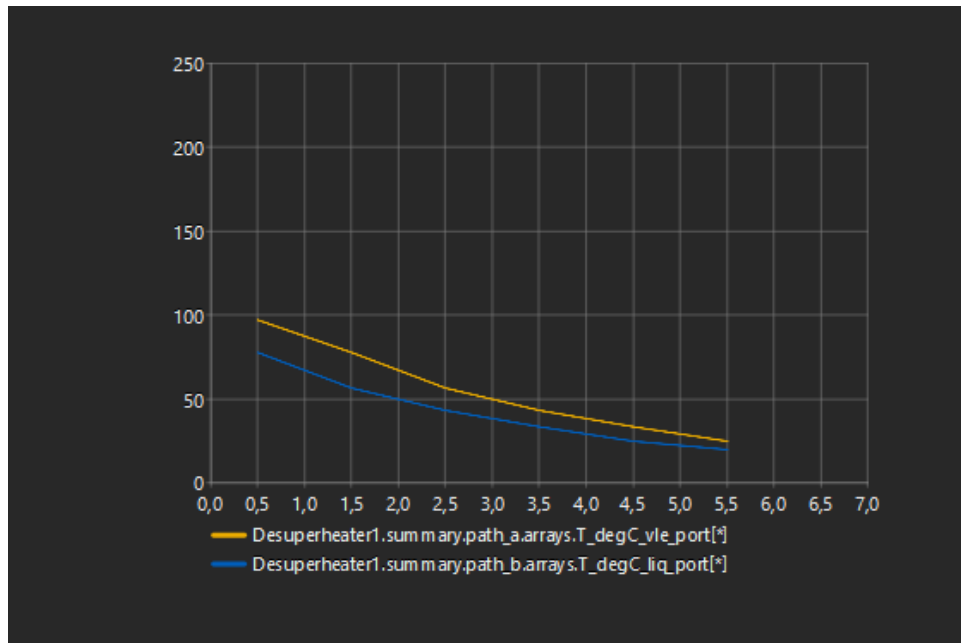
Figure 4-21 Gas cooler heat exchanger between VLE fluid and water

During the whole simulation, the COP of the system is found to be 3.6 after the simulation becomes stable. The stability of the system takes place after 700s.
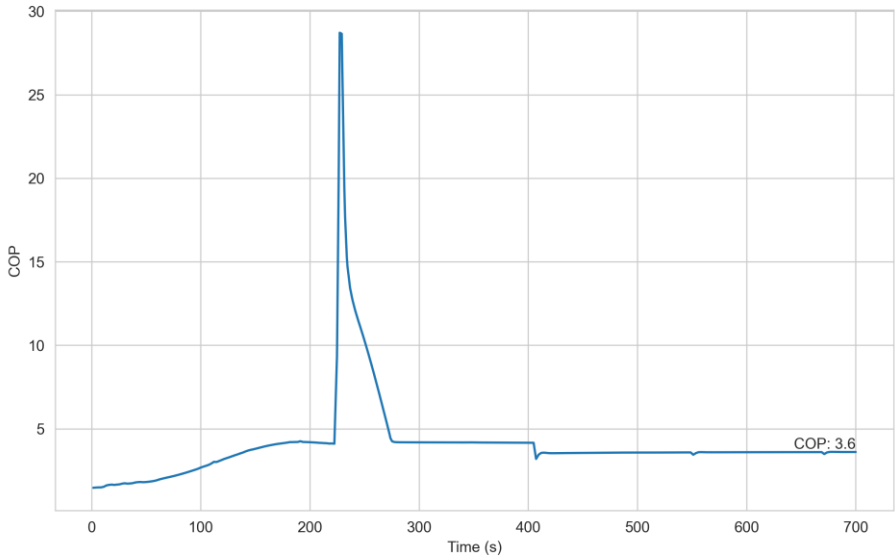
Figure 4-22 COP of the system for water as a source

4.6 Integration of HVAC duct with dehumidifier (Option II)

In a farm environment where precise humidity control is crucial, a dedicated heat recovery unit and dehumidifier are often utilized to maintain optimal conditions. When excess moisture is present, and drying is required, the dehumidifier plays a crucial role in maintaining the desired humidity levels.

The system operates as follows. Ambient air and return line from farm passes through an air-to - air heat exchanger, which heats the ambient air, providing energy savings. The exhaust from the heat recovery unit is used as a source for the evaporator after crossflow.

Once the ambient air has been heated via crossflow, it is directed through heating and cooling coil, depending on the specific needs of the farm. To adjust humidity levels, either a humidifier or dehumidifier is activated. When humidification is required, hot air in the duct is sprayed with water. This humid air then passes through the cooling coil, producing condensation that collects in a drain pan.

The water in the drain pan is recirculated by a recirculation pump, which sends it back to the humidifier for reuse. The control unit continuously monitors the operation of the HVAC system to ensure optimal functioning and maintain ideal environmental conditions for the farm.

Notable, return air to the farm during drying (illustrated Figure 4-23) just operates when drying process is going on inside the farm. Otherwise, air outlet takes place from upper part during normal heating operation. The selection of dehumidifier that can be integrated in lower part of the duct is shown in Figure 4-23.
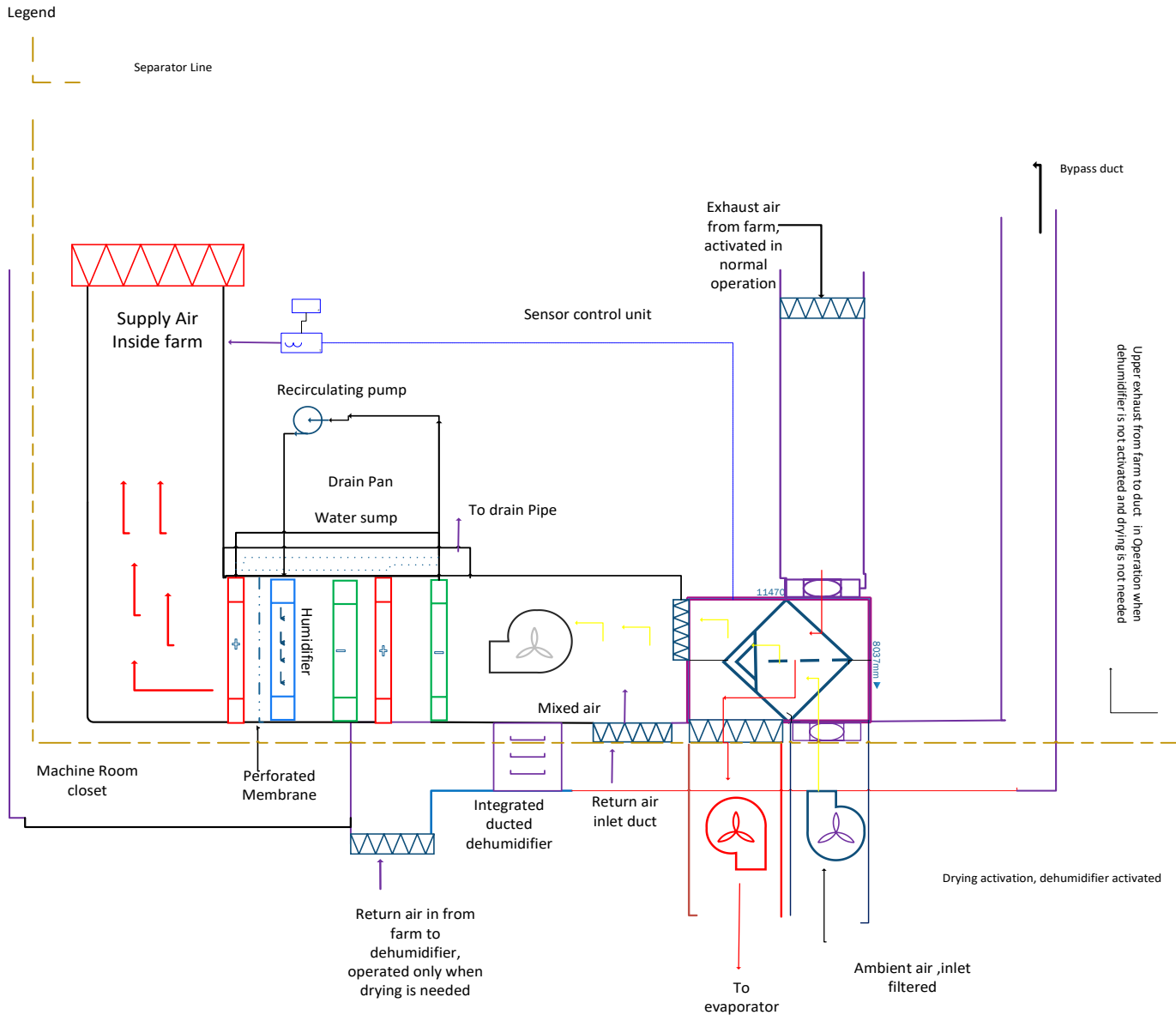
Figure 4-23 Dehumidifier combined with HVAC system.

Figure 4-24 illustrates two distinct trends related to the heat and mass transfer processes along an isothermal surface of 80 m length at a fixed temperature of 50 °C and a relative humidity of 13.1%. The thickness of water film at the floor throughout the area of 2000 m² is 2 cm.

The plot between mass transfer coefficient and between dry air velocity give that as air velocity amplifies the moisture carrying potential of the air is increased. This observation is consistent with

the theory that convective mass transfer coefficient with air velocity. With the increasing velocity of air, from 1 to 20 m/s, there is a notable increase in the mass transfer coefficient from approximately 0.0097 m/s to 0.1192 m/s. This indicates an almost 12-fold increase in the mass transfer coefficient with a 20-fold increase in the air velocity. This non-linear correlation suggests the effect of air velocity. This non-linear correlation suggests that the effect of air velocity on the mass transfer coefficient may be more complex than a straightforward linear relationship and could have been influenced by other factors like turbulence, boundary layer thickness etc.

The plot shows the increasing trend between air velocity and evaporation rate pr unit area. This trend underscores the role of air velocity in intensifying the rate of evaporation. The evaporation rate increases from 0.000867 $kgH_2O/m^2 \cdot s$ at 1m/s to 0.00892 $kgH_2O/m^2 \cdot s$ at 20m/s. Similar to the mass transfer coefficient, the evaporation rate shows an approximately tenfold increase with a 20-fold increase in air velocity.
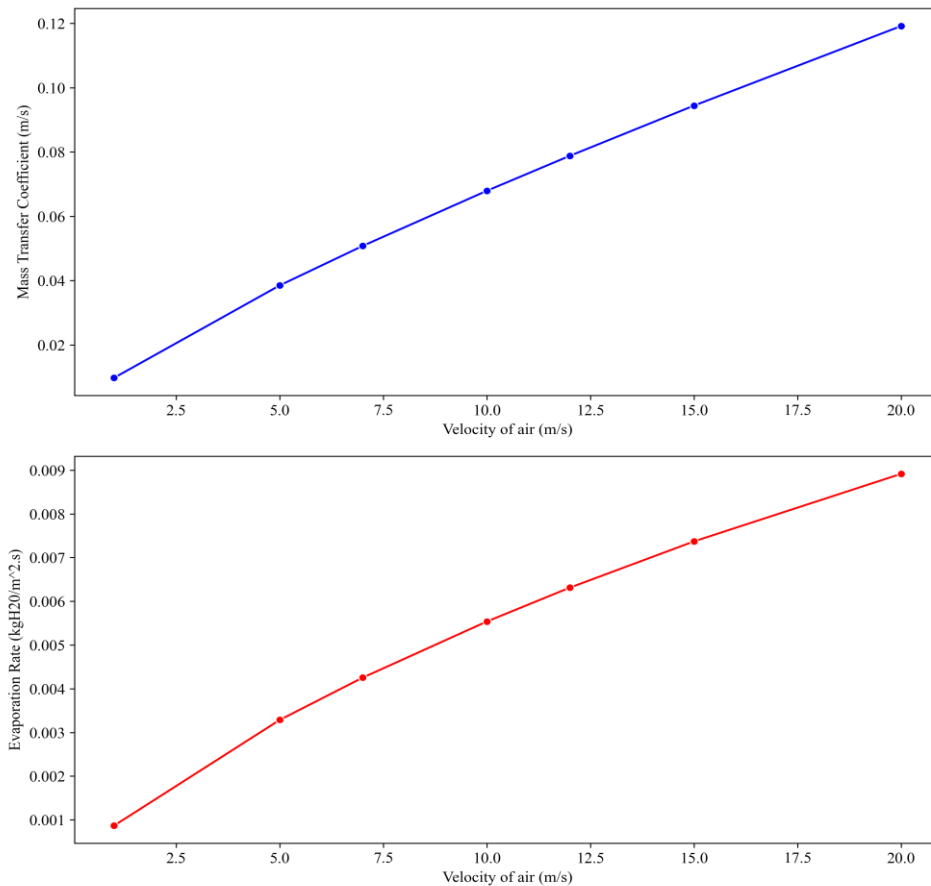
Figure 4-24 Mass transfer Coefficient, Evaporation rate with respect to velocity

Figure 4-25 presents the interdependencies of several key variables related to concrete curing processes, specifically exploring the changes in the air velocity (from 1 m/s to 20 m/s) affect these parameters.

In Figure 4-25, the mass transfer coefficient shows directly proportional relationship with velocity. After drying the absolute humidity leaving the concrete is relatively high of approximately 0.0223 kgH$_2$O/kg dry air at 1 m/s, it decreases consistently to nearly 0.0063 kgH$_2$O/kg dry air at 20 m/s. This downward trend indicates that increasing the velocity reduces the efficiency of mass transfer, possibly due to the faster-moving air having less contact time with the concrete surface for moisture absorption.

The temperature of air leaving the concrete shows a directly proportional relationship with velocity. Starting from 25 °C at 1 m/s, the temperature rises gradually to reach about 34.2 °C at 20 m/s. This suggests that a higher velocity of airflow tends to absorb and carry away ore heat from the concrete, because of less contact time with water film in the concrete surface.

The relative humidity at the point of leaving the concrete is plotted against velocity. Here we see a decreasing trend, where the relative humidity drops from 100% at 1 m/s to around humidity 48.1% at 20 m/s. The supply of hot air at less velocity gives enough time to contact and evaporate moisture from concrete floor.
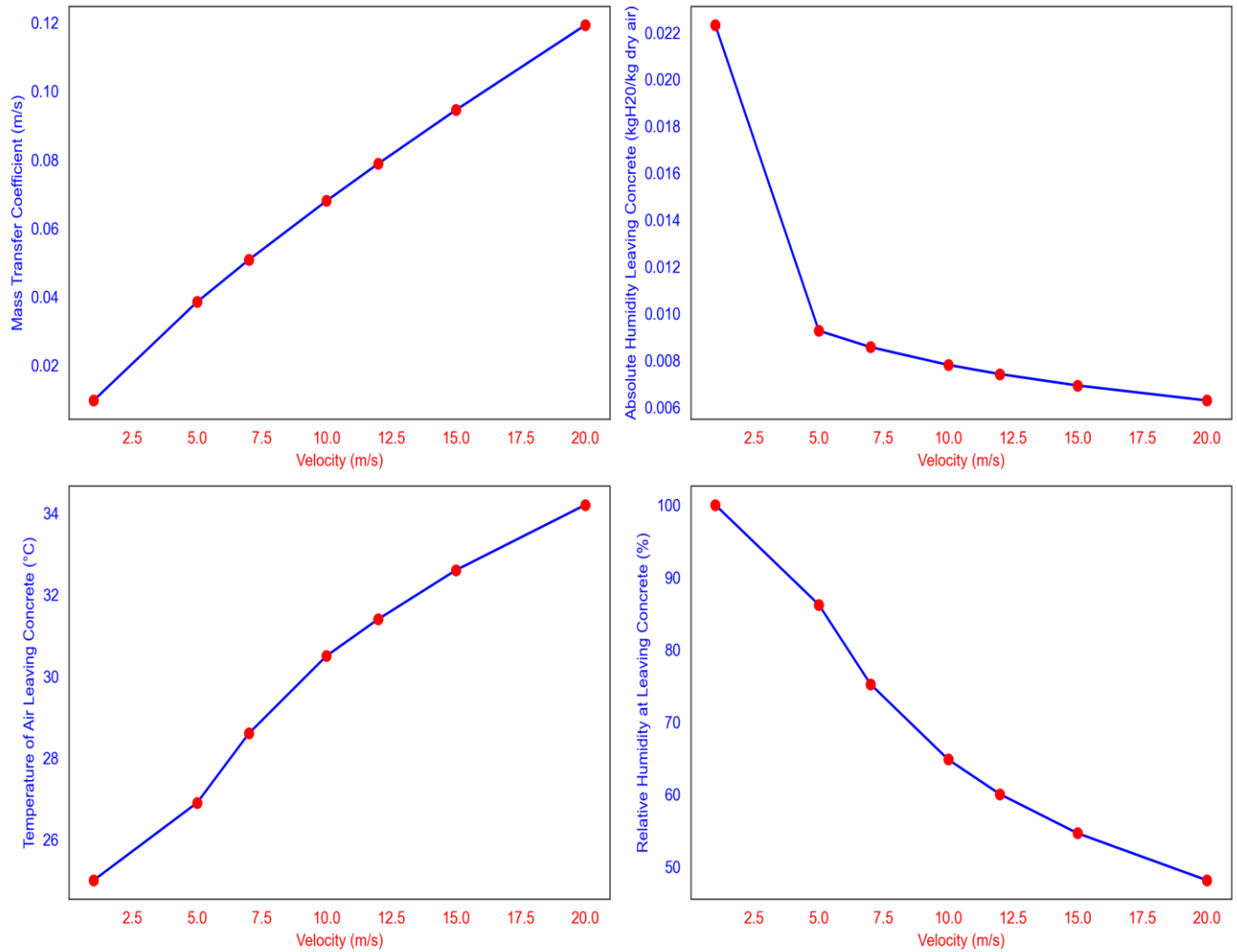
Figure 4-25 Relative humidity and temperature leaving the concrete after 323 K dry air supplied

Figure 4-26 demonstrates that the drying time with air velocity 1 m/s is 23 hours. Supplying air at 5, 7, 10, 12, 15, 20 m/s gives a drying time of 6, 4.59, 3.43, 2.96, 2.47, 1.95 hours. respectively. Likewise, the drying time decreases as the velocity of hot air increases at the inlet of the farm. It is assumed that the hot air is uniformly distributed throughout the farm. During the calculation, we have floor heating in the poultry farm and is believed that the water in the floor is heated to 50 °C during this drying process.
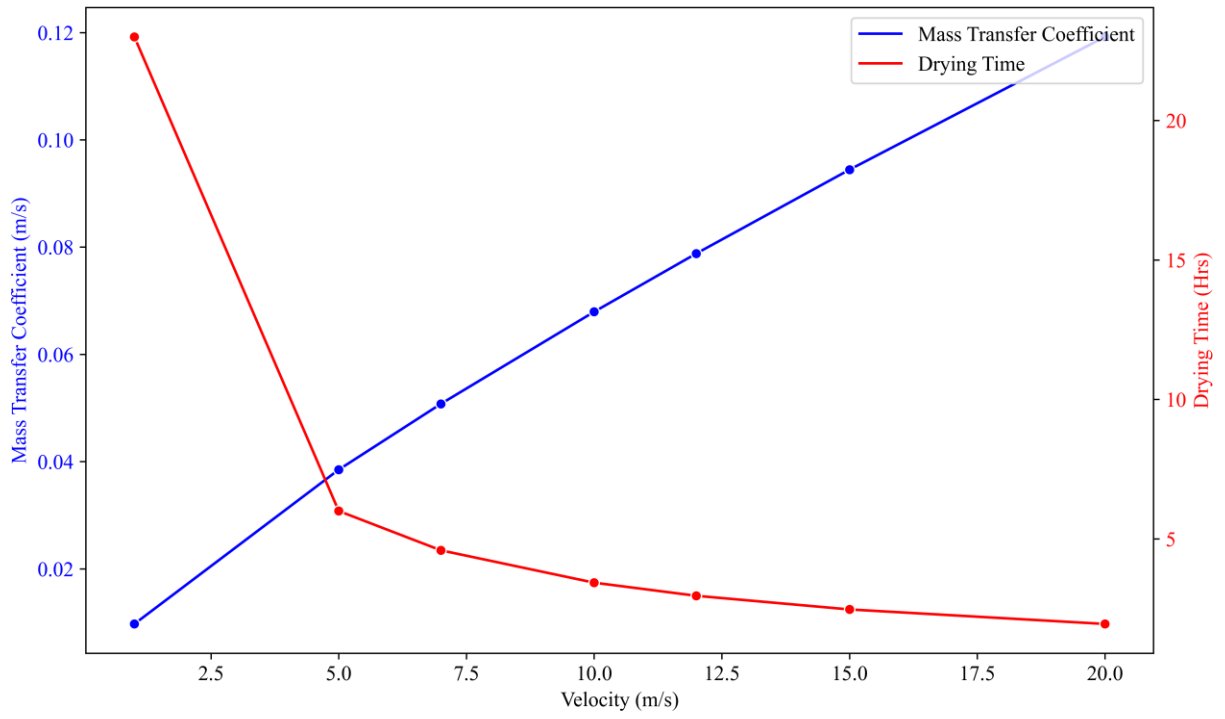
Figure 4-26 Drying Time at different velocities of air supply

4.6.1   ANSYS Fluent Result

The poultry farm had a thin water film at some concrete in 2 cm. First, the mesh generation is done based on the dimensions and complexity of the model. ANSYS mesh provides several meshing methods, including structured, unstructured, and hybrid meshing. The mesh settings, such as the element size, and meshing tolerance are defined. These settings are important to ensure the accuracy of the mesh. The mesh is visualized and checked for the quality using various tools.
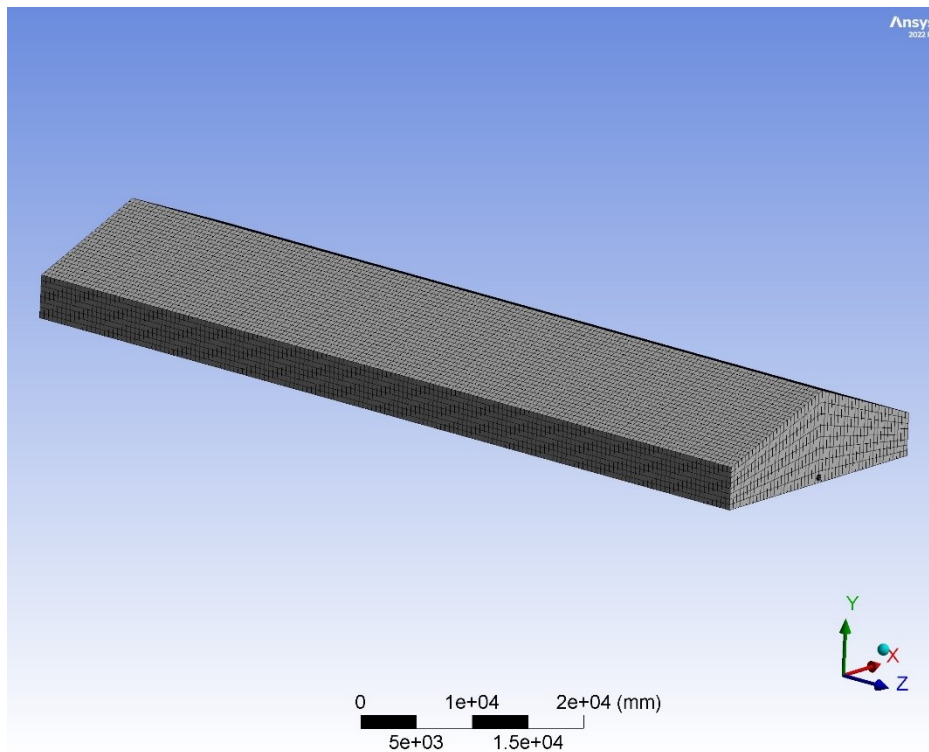
Figure 4-27 Mesh generation for ANSYS Fluent

After the mess generation, the evaporation process of the water film can be analyzed. The analysis of the evaporation after the hot air comes inside the farm at different time situation during simulation.
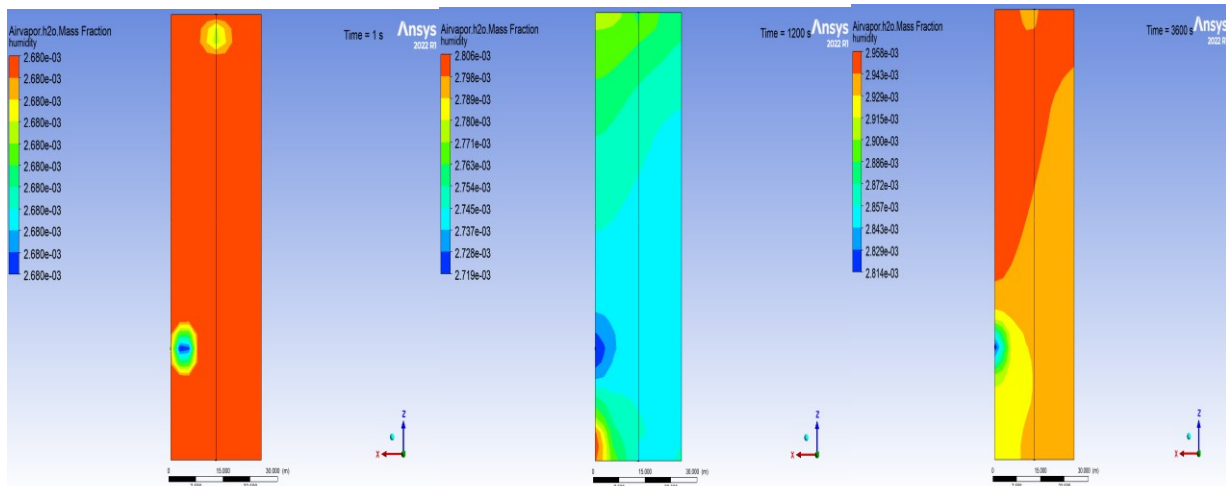
Figure 4-28 Evaporation Streamline in concrete

As seen in Figure 4-28, which is at t=0 seconds, the contour indicates a nearly an almost even humidity level (depicted by the orange colour indicating 0.0062 as a mass fraction of the air-vapor combination) spanning most of the area. This uniformity is a result of no evaporation having occurred in the simulation up to the point. Nevertheless, there are distinct areas close to both inlets where the contour exhibits a range of colours (yellow, green, blue). These areas represent the infusion of humidity from the external atmosphere, which enters the room through the inlets.

At 1200s, across the entire room, signifying in the boost in the total humidity figures. The dispersion of water vapor, ensuring from evaporation, seems to be uniformly spread across the room, the contour further demonstrates that the near the inlets presents elevated humidity levels, aligning the previously provided explanation.

At the simulation time, 2400s and 3600s, the contour consistently illustrates a slow decrease in humidity gradients from the inlet to the outlet. Yet, a key takeaway from the contour's legend is the remarkable increase in the room's maximum humidity value compared to the simulation's starting point. This development signifies that the evaporation process has caused an overall enhancement in the room's air humidity level, leading to a higher level of moisture saturation.

In this simulation, it's crucial to mention that hot air is introduced into the system via the inlet with a mass flow rate of 9 kg/s. The hefty mass flow rate generates turbulence in the flow, leading to variations or inconsistencies in the colour contour at specific times. Despite this, a constant observation throughout the simulation is the superior humidity values near the inlet compared to

the outlet. This disparity in humidity levels between the inlet and outlet remains a consistent feature of the system.

Figure 4-29 shows the distribution of humidity contours in the surface representation. In the figure, the evaporation process takes place and humidity in indoor air increase along with the capture of water vapor. After the evaporation, the water to vapor fraction throughout the building seem to be uniformly distributed.
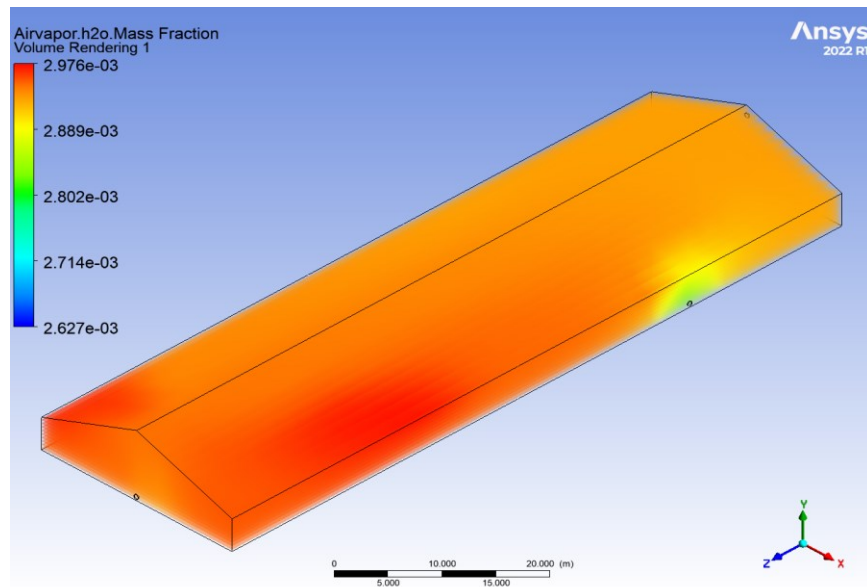
Figure 4-29 Distribution of water vapor throughout the building after hot air supplement

Figure 4-30 illustrates the significant rise in the gradient temperature. Following periods, the temperature goes down due to higher amount of water vapor in the room. This surge in water vapor is lined to evaporation, which in tun cause the air temperature to drop. In addition, the temperature undergoes variation because of the warming impact of the hot air inlet and escalating humidity brought about by the evaporation of water vapor.
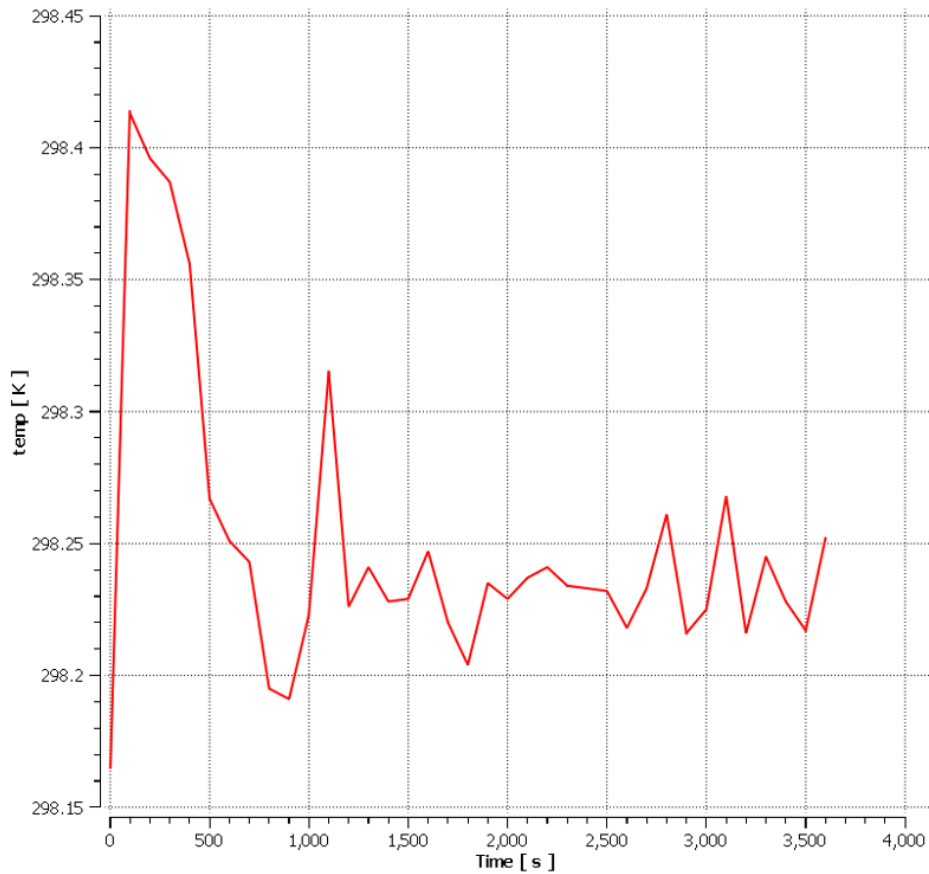
Figure 4-30 Temperature distribution inside farm

Figure 4-31 at simulation t=600s, the gradient vector of the water vapor mass fraction has grown more complex due to turbulent flow inside the room. Several vectors from the inlet and span the room, while others arise from the evaporation of the water film and diffuse into the nearby environment. In contrast, vectors can be observed moving towards the room's outlet on the opposite side. This occurrence emphasizes the need to account for the turbulence within the flow when examining water vapor distribution.

At t=3600s, the water vapor gradients in the room showed a significant rise. Nevertheless, the flow's turbulent characteristics resulted in more chaotic contours. Near the inlet, small areas denoted by blue vectors were amongst other vectors exhibiting higher contours.
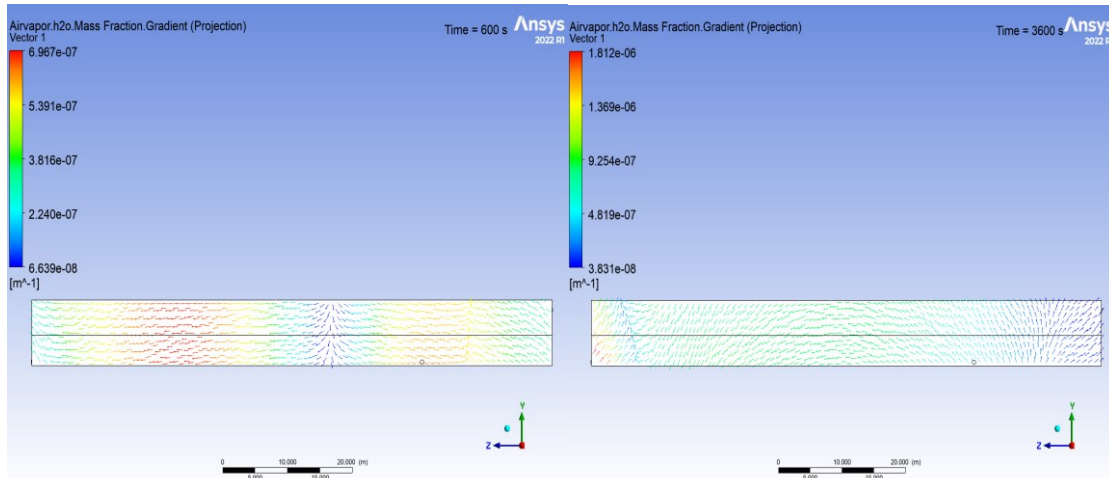
Figure 4-31 Projection of water vapor, vector plots

Figure 4-32 illustrates the changing mass flow rate at the outlet overtime. At the onset of the simulation, the amount and concentration of water vapor within the room is low, thus more air is compelled to exit the room due to a pressure differential. As the simulation time progresses, the mass flow rate at the outlet slowly increases and fluctuates. Nonetheless, it's worth nothing that the mass flow rate at the outlet is never steady due to turbulent characteristics of the fluids.
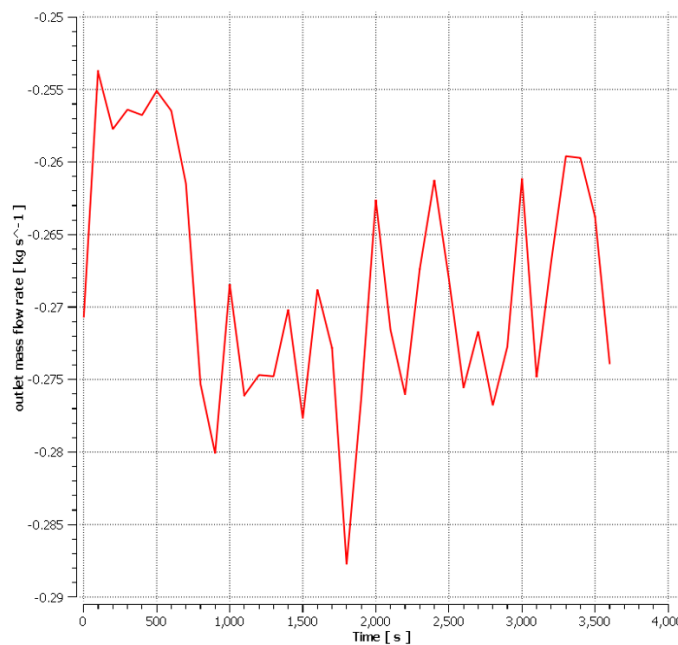
Figure 4-32 Outlet mass flow rate from the farm at given condition

Figure 4-33 shows a steady rise in the concentration of water vapor in the room as time goes on. This increase in water vapor can be tracked back to two main sources: the evaporation of the water film located on the concrete's top surface, and secondly, the infusion of hot air through the inlet, which also bears a small quantity of vapor. The evaporation process is the primary driving force behind the escalating concentration of water vapor in this simulation.
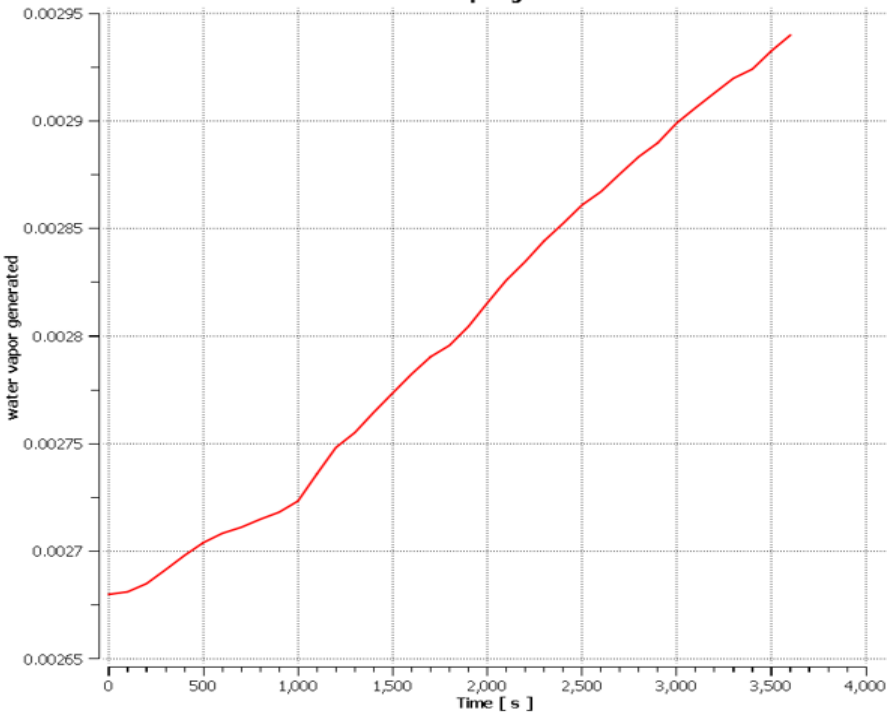
Figure 4-33 Water vapor generated during drying process

4.6.2   Helioscope Result

The solar production in Inderoya poultry farm is analyzed. It could be integrated either with a heat pump system to get maximum COP, providing hot water generated from solar as a source. It can also be supplied to the grid in case it cannot be fully utilized on the farm. The weather dataset is taken from 10km away from the poultry farm. The average operating ambient temperature is 9.4 °C with an average operating cell temperature of 13.3°C with 4566 hours operation. The new poultry farm (nyttfjos) has the potential to produce 145.1 MWh energy having the total collector irradiance 734.7 kWh/m^2. A fixed tilt racking is used during the simulation. However, a rotating racking can be provided to produce maximum electricity. A Tilt of 10°C is provided due to inclination of roof. The transposition model and temperature model used are Perez model and Sandia model respectively. The module used in the installation is TSM-PD14320(Trina Solar) and Sunny Tripower 24000TL-US(SMA). The strings used are 10AWG made of copper. The module DC plate for new and old farm is 211.2 kW and 99.8 kW respectively. Figure 4-34 illustrates the system losses and concludes that shading plays a vital role in low performance in energy production.
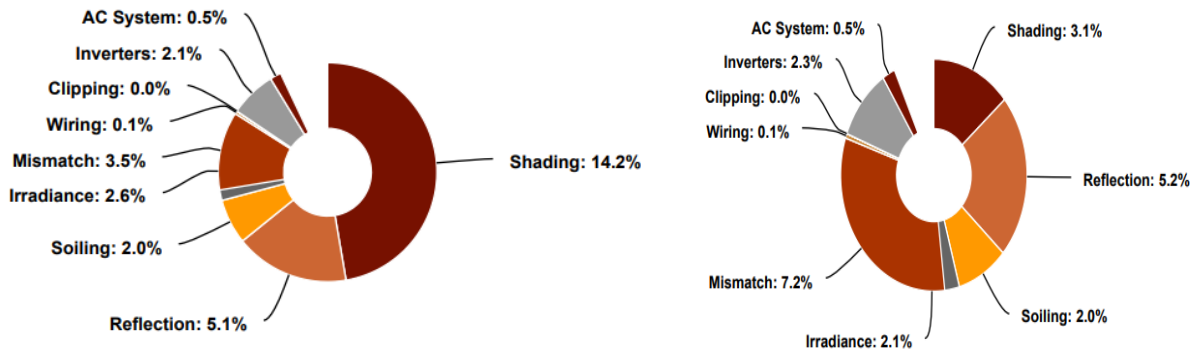
Figure 4-34 System losses in new poultry farm(left) and old poultry farm (right)

Annual energy production for new and old poultry farms is found to be 145.1 MWh and 73.91 MWh respectively. The highest production is in the month's May and June when the orientation of the panels is kept landscape and horizontal. December is the month with lowest production because of solar irradiation. The monthly production of energy in both the poultry farms is

illustrated in Figure 4-35 and Figure 4-36. Energy production in May, June and July is above 20 MWh for new poultry farm.
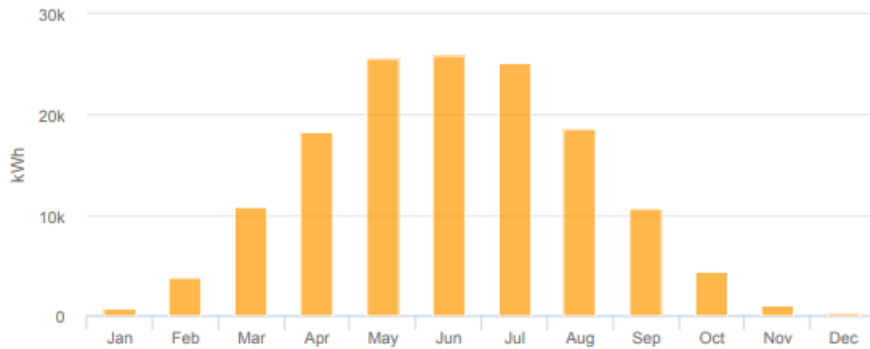
Figure 4-35 Monthly production for new poultry farms
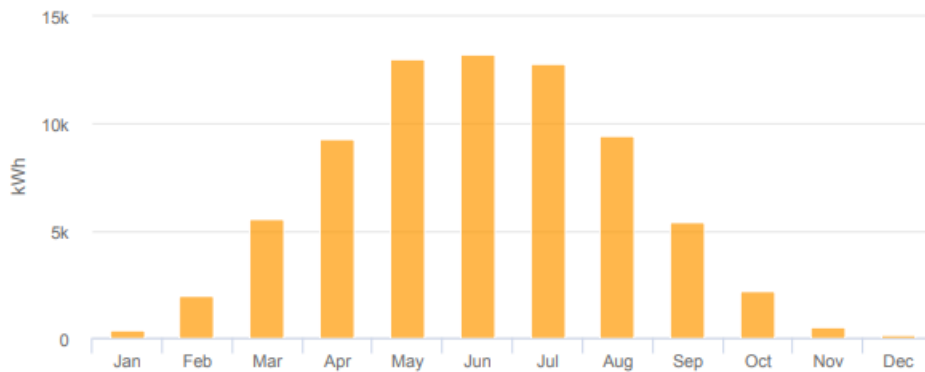
Figure 4-36 Monthly production for old poultry farm

5 Discussion

The chapter on results elucidates all critical discoveries in a comprehensive and articulate manner. It delivers a summary, focusing on the main insights derived from the study. The technical assessment of these results is delivered with a broader scope, augmenting the depth of understanding provided by literature review in the context of this research work.

➢ From the results to determine the heat production from chicken, the sensible and latent heat is determined. The weight of chicken increases along with the weight and found to be in the range of 8-10 W, while they are kept in the farm. However, the amount of heat production from chicken depends on metabolic state, water consumption or intake, daily activities, temperature in surrounding etc.

➢ The ventilation rate of the Norsk Regulation and Arbor management guide for healthy chicken's varies significantly. The ventilation rate needed is more compared to arbor management guidelines which results in more air exchange per hour that ultimately affects the energy consumption. Hence, the system is designed to cope with the challenge of high energy demand in buildings. Likewise, the ventilation rate plays a vital role in managing the concentration of CO_2 and ammonia inside the farm. Higher CO_2 and ammonia concentration than 3000 ppm and 25 ppm result the death of the chicken barns. Hence, the concentration of air exchange is most to produce the healthy chickens.

➢ The heat pump system is designed after the data readings from the sensor installed on the farm from August 2022. During the coldest days in December and February, the capacity needed to cover the energy demand in the farm is 156 kW. A 120-kW heat pump with CO_2 as a refrigerant is designed to fulfill the demand for heating. Here, the system uses CO_2 as a refrigerant, but a propane can also be used to provide heating solution to building since the maximum temperature range demand to heat building is 45°C. However, propane as a refrigerant is less reliable from safety perspective as well as high monitoring is needed to

perform system. Since this system is for poultry farm located at countryside in Trondheim, Norway, the availability of safety approach and expertise are limited. Moreover, highly skilled, and trained manpower are needed to install propane system handling. Although, a risk analysis showed that there is very less risk factor was analyzed in the study by Colbourne and his team [43] . Beyer et al. [44] and Hymes et al. [45] the fire event doesn't occur easily in R-290 or hydrocarbons, as there are certain conditions that need to be fulfilled. These conditions are refrigerant leakage, mixture of refrigerant with air within flammability limit (2-8% of HCs in air), ignition source must be more than 0.25 mJ or temperature above 440 °C. If one of these events does not occur at once, then the fire event won' take place.

➢ Each component of the P & ID diagram is selected from the manufacturer carefully. This can make a significant difference in the output of the system. The cooling demand at steady state is 99 kW. Likewise, expansion tank installation can be done in different positions upright or downward the pipes. The integration of HRV and FCU makes one perfect HVAC unit for the hot and cold air supply. The HVAC load is calculated to be 120 kW which was checked HVAC manual J calculation. The designed system not only provides the heat and cooling solution, but it has equal importance to perform drying of the concrete floor and humidify and dehumidify air at according to the necessity. At present, the drying of the poultry farm between each insert takes place 4-6 days. The designed system is calculated to dry the whole poultry farm in less than 24 hours, if the 2 cm thick water film lies above the concrete floor in the farm. During the calculation for drying time, all the airflow throughout the poultry farm is considered as turbulent flow. However, for the mixed analogy, the average mass transfer coefficient could be different. Because the length of the surface considered is 80 m, but the hot airflow is laminar for some distance and then only turbulent flow starts. Hence, this can make some differences in the result obtained.

➢ The designed HP system for both using air and water as source (Option I) and 2nd uses water as a source. Increase in evaporation temperature can lead to an increase in the COP of heat pump. In option I, the two evaporators, the suction regulating valve is very

important to maintain pressure. For the dynamic load, increase in source load results in high COP of the heat pump ranging from 3.74 to 4.5 at various inputs. At steady state, with source evaporator 99 kW, the option I showed higher COP (4.5) rather than option II. However, water being a source, the COP of system depends on source temperature. In case, the air temperature is different, and humidity can also result in the change in COP of the system. The source evaporator receives air from exhaust of the farm through heat recovery unit which can also result in high COP due to increase in source temperature.

➢ Both option I and option II can be used as dehumidification units, supplying hot air to the poultry farm. Both options give adaptability for heating the ambient air. The drying system is designed optional, one is the heat pump system itself can produce hot air and perform complete drying system. However, the other option could be integrating duct mounted dehumidifier to remove the moisture after drying. Integrating duct mounted dehumidifier to remove the moisture needs additional investment and power consumption. Hence, option I is more suitable to implement on the farm although system could be considered.

➢ The theoretical calculation for drying the water film of 2 cm is evaluated. Supplying air at low velocity at 1m/s at a temperature of 50 °C gives drying time is 23 hr. supplying higher velocity can make significant decrease in drying time. A ANSYS Fluent is used to see the evaporation process inside the concrete floor and see the water vapor generated. At air velocity from two inlets at 9 kg/s, the outlet mass flow rate resembles the theoretical calculation but since the simulation was done until 3600s further behavior is not predicted. However, it shows that drying with a heat pump results in significant reduction of drying time. Notably, the drying must be performed with windows and doors closed. The supply air must be supplied from two FCU to ensure uniform distribution of hot air.

➢ Annual energy production for new and old poultry farms is calculated 145.1 MWh and 73.91 MWh respectively. The module DC plate for new and old farms is 211.2 kW and 99.8 kW. This energy production could be further increased using parabolic panels that have more solar energy capturing potential, but it is not possible because of slanting angle of roof. The integration of solar energy production with heat pump could result in high

efficiency of the system. In case of excess energy production supplying to the electric grid is possible.

6   Conclusion

The main aim of the research work was to study the literature and see the benefits of using heat pump systems over fossil heating systems. Those were analyzed in depth and concluded that the heat pump is the best for heating solution as well as to grow healthy chickens. Heat production from the chicken is very uncertain ranging from 7-20 Watt, since they depend on so many factors like degree of freedom for chicken, activity level, food, and water consumption rate etc. Hence, the sensible and latent heat of the chicken has been analyzed to get the significant numbers for heat production. Understanding of the current heating system is key to replacing fossil free (heat pump) systems with the maximum utilization of the available components that already exists in the farm. Sensors were used to log data to study the energy consumption of the farm and its different units. An uncertainty analysis of the data logged in was performed. The analysis performed on uncertainty of the sensor shows that the energy consumption measured in the farm is ±0.41% of the measured value. Likewise, the pt1000 temperature sensor and flow meter sensor uncertainty has been analyzed. Understanding the maximum energy consumption, the new heat pump system is proposed (suggested) that can perform all the required tasks to maintain temperature including humidity level that best suits for chicken barns. A full system describing every component used in the system is designed. Every component including storage tank and residence time of the liquid separator is given in the calculation. The full P&ID gives an overview to explain the heating and cooling demand of the farm. Likewise, the drying system with heat pump and combination of it with integrated dehumidifier is analyzed. A 120-kW heat pump system is designed based on the starting of energy consumption, capacity required during cold days, and based on the simulation of the poultry farm performed by software IDA ICE in the summer report of the SINTEF during starting of the project. The dimensioning of the heat pump ranges from 40-70% of the full capacity. A 120 kW is designed with multiple options, making it Option I and Option II. Option I use parallel evaporators (using air / water as source), whereas option II uses single evaporator using city water as a source. Option I could be used for dual scenario. The option I have more COP ranging from 4 to 4.6, as found in simulation from software called Dymola. Likewise, option II gives COP of 3.6 at the same capacity

measured for option I. Hence, Option I is the most applicable one than option II. Option I with parallel evaporators, bypass valve gives high COP. Alongside, both the systems had a potential to produce hot water ranging from 75-85 °C. In addition, the drying time with heat pump is theoretically calculated. The drying time supplying 50 °C of hot air with uniform distribution throughout the surface of 2000 m^2 gives drying time of 23 hours at air velocity of 1 m/s. Likewise, increasing the velocity of air resulted in increase in mass transfer coefficient from 0.0097 m/s to 0.1192 m/s starting from velocity 1 m/s to 20 m/s. However, the moisture capture from the wet floor is better at low velocity air supply since, the relative humidity of air at exit in drying is 100% with exit temperature 25 °C at velocity 1 m/s. Hence, velocity of air at slow movement can be useful for energy saving and better output rather than supplying high velocity hot air. Annual energy production from solar panels installed in slanted roof of new and old poultry farms gives out 145.1 MWh and 73.91 MWh respectively. The module DC plate for new and old farms is 211.2 kW and 99.8 kW. The shows that high monthly energy production from solar is during May, June, and July whereas the least is for December.

7   Further Recommendation

This chapter highlights the suggestion for improvement and further work. Most of the points below are related to the extension of the work.

➢ This design of the system for heating and drying poultry can be tested using another refrigerant such as R717 and R290.

➢ Sizing of the heat pump is done according to the measurement of data during the cold winter based on energy demand for heating. However, the sizing can vary according to the air flow rate which could be taken into consideration.

➢ A thermal storage system is not implemented in dymola simulation yet. This must be done to study the internal temperature of storage tank in each layer.

➢ The theoretical analysis is examined for drying process. However, practical analysis is yet to be done after the installation of the system. The variation between theoretical, simulation and experimental data can be compared.

➢ Energy production from both PV cells is calculated. However, production ways like implementing panels according to timer of sunrise and sunset/rotating panels might increase the production.

➢ Economic analysis to calculate investment cost, payback period, NPV (Net present value) etc. could be done after designing each component of the system.

8 References

1. Nations, F.a.A.O.o.t.U. *Poultry species*. 2023; Available from: https://www.fao.org/poultry-production-products/production/poultry-species/en/.
2. Poore, J. and T. Nemecek, *Reducing food's environmental impacts through producers and consumers.* Science, 2018. **360**(6392): p. 987-992.
3. B.V., M.U., *Norway increases poultry production*, in *POULTRY WORLD*. 2023.
4. SSB, N. *Statistics Norway*. 2023; Available from: https://www.ssb.no/en/jord-skog-jakt-og-fiskeri/jordbruk/statistikk/kjotproduksjon.
5. Bradstreet, D., *Poultry And Egg Production Companies In Norway*. 2023.
6. Ireland, S.E.A., *Energy Efficiency on Poultry Farms*. 2023.
7. Heidari, M., M. Omid, and A. Akram, *Energy efficiency and econometric analysis of broiler production farms.* Energy, 2011. **36**(11): p. 6536-6541.
8. Kharseh, M. and B. Nordell, *Sustainable heating and cooling systems for agriculture.* International journal of energy research, 2011. **35**(5): p. 415-422.
9. Choi, H., et al., *Effect of heating system using a geothermal heat pump on the production performance and housing environment of broiler chickens.* Poultry science, 2012. **91**(2): p. 275-281.
10. Kwak, H.Y., et al., *Thermoeconomic analysis of ground-source heat pump systems.* International journal of energy research, 2014. **38**(2): p. 259-269.
11. MA Agriculture Ltd, a.M.A.G.c., *Air-source heat pumps power poultry shed*. 2023.
12. Bokkers, E., H. Van Zanten, and H. Van den Brand, *Field study on effects of a heat exchanger on broiler performance, energy use, and calculated carbon dioxide emission at commercial broiler farms, and the experiences of farmers using a heat exchanger.* Poultry science, 2010. **89**(12): p. 2743-2750.
13. Singh, R.P. and D.R. Heldman, *Introduction to food engineering*. 2001: Gulf Professional Publishing.
14. Strommen, I., et al. *Low temperature drying with heat pumps new generations of high quality dried products*. in *Proceeding in 13th International Drying Symposium (IDS2002)*. 2002.
15. Hartmann, N., C. Glueck, and F. Schmidt, *Solar cooling for small office buildings: Comparison of solar thermal and photovoltaic options for two different European climates.* Renewable Energy, 2011. **36**(5): p. 1329-1338.
16. Franco, A. and F. Fantozzi, *Experimental analysis of a self consumption strategy for residential building: The integration of PV system and geothermal heat pump.* Renewable Energy, 2016. **86**: p. 1075-1085.
17. Bee, E., et al. *Air-source heat pump and photovoltaic systems for residential heating and cooling: Potential of self-consumption in different European climates*. in *Building Simulation*. 2019. Springer.
18. Bakker, M., et al., *Performance and costs of a roof-sized PV/thermal array combined with a ground coupled heat pump.* Solar energy, 2005. **78**(2): p. 331-339.
19. Wang, E., et al., *Performance prediction of a hybrid solar ground-source heat pump system.* Energy and Buildings, 2012. **47**: p. 600-611.
20. Freeman, T., J. Mitchell, and T. Audit, *Performance of combined solar-heat pump systems.* Solar energy, 1979. **22**(2): p. 125-135.

21.   HALBHAVI, N., *The benefits of using water-source heat pumps*, in *Consulting Specifying engineer*. 2023.

22.   Midttømme, K., et al. *Geothermal Energy Use in Norway, Country Update for 2015-2019*. in *Proceedings, World Geothermal Congress*. 2020.

23.   Erbach, G., *At a glance Using the Montreal Protocol for climate action*. 2016.

24.   Mujumdar, A.S., *Drying technology in agriculture and food sciences*. 2000: Science Publishers, Inc.

25.   Qui, S., M. White, and R. Galbrith. *Thermal Energy Storage System Design and Optimization*. in *ES/FuelCell2013, ASME 2013 7th International Conference on Energy Sustainability, Paper*. 2013.

26.   *DOWTHERM Q*. Product Technical data, 1997.

27.   Nordell, B. *Underground thermal energy storage (UTES)*. in *International Conference on Energy Storage: 16/05/2012-18/05/2012*. 2013.

28.   Coleman, H.W. and W.G. Steele, *Experimentation, validation, and uncertainty analysis for engineers*. 2018: John Wiley & Sons.

29.   Deaton, J. and F. Reece, *Respiration in relation to poultry house ventilation*. Poultry Science, 1980. **59**(12): p. 2680-2685.

30.   Pedersen, S. and K. Sällvik, *Climatization of animal houses-heat and moisture production at animal and house level 4th report of CIGR working group*. Research Centre Bygholm, Danish Insitute of Agricultural Sciences, Horsens, Demark, 2002.

31.   Stroem, J., *Heat loss from cattle, swine and poultry as a basis for the design of environmental control system in livestock buildings [Denmark]*. SBI-Landbrugsbyggeri (Denmark). no. 55., 1978.

32.   Gates, R.S., D.G. Overhults, and S.H. Zhang, *Minimum ventilation for modern broiler facilities*. Transactions of the ASAE, 1996. **39**(3): p. 1135-1144.

33.   Alchalabi, D., *Environmental management of the poultry house*. Poultry International, 2003. **42**(3): p. 26-31.

34.   Klimaservicesenter, N., *Kunnskap for et klimarobust samfunn*. 2023.

35.   Incropera, F.P., et al., *Principles of heat and mass transfer*. (No Title), 2013.

36.   Indeed. *The Manual J Calculation: What It Is and How To Use It*. 2023 04.05.2023]; Available from: https://www.indeed.com/career-advice/career-development/manual-j-calculation.

37.   Vacker, *Dehumidifier Capacity Calculation*. 2023.

38.   Industrial, S. *Steel 18 D 17.3 H 17.9 W Inline Duct Fan*. 2023; Available from: https://www.spsindustrial.com/steel-18-d-17-3-h-17-9-w-inline-duct-fan-6kvy8?fbclid=IwAR2nuOdMhKSXMWjqhriHN6appxp66emnQ21FbmPNYoIiC0CdN_iJ9a0eBis.

39.   Labs, F. 2022; Available from: https://helioscope.aurorasolar.com/.

40.   Trademark, J., *Anaconda (Notebook)*. 2023.

41.   Kylling, N., *Measured datas in chicken farm, Trondheim*. 2023.

42.   Aviagen, *Arbor Acres broiler management handbook. Broiler performance objectives*. 2014.

43.   Colbourne, D. and K. Suen, *Comparative evaluation of risk of a split air conditioner and refrigerator using hydrocarbon refrigerants*. International Journal of Refrigeration, 2015. **59**: p. 295-303.

44.   Beyler, C.L., *Fire hazard calculations for large, open hydrocarbon fires.* SFPE handbook of fire protection engineering, 2016: p. 2591-2663.
45.   Hymes, I., W. Boydell, and B. Prescott, *Thermal Radiation: physiological and pathological effects*. 1996: Institution of Chemical Engineers.
46.   Aviagen. *"Arbor Acres Broiler Management Guide.".* 2009; Available from: https://eu.aviagen.com/assets/Tech_Center/AA_Broiler/AA-BroilerHandbook2018-EN.pdf.

9 APPENDIX I

The ventilation rate according to the arbor management [46] shows that the ventilation rate for the chicken required can be calculated using the reference values listed in Table 15. Table provides a basic guidance on ventilation rates per bird at temperatures between -1 and 16 °C, through these rates may slightly decrease or increase at lower and higher temperatures, respectively. Ventilation should maintain recommended maximum levels for relative humidity (RH), carbon monoxide, carbon dioxide, and ammonia. Specific ventilation needs may vary depending on factors such as breed, sex, and individual poultry house conditions. They should also be adjusted according to the environmental conditions, bird behavior, and total bird weight. Monitoring bird behavior and distribution can serve as an indicator of ventilation adequacy.

Table 15 Ventilation Rates and Calculations

Live Weight (kg)	Live Weight (lbs)	Minimum Ventilation Rate (m³/hr)	Minimum Ventilation Rate (ft³/min)
0.05	0.11	0.080	0.047
0.10	0.22	0.141	0.083
0.15	0.33	0.208	0.122
0.20	0.44	0.258	0.152
0.25	0.55	0.305	0.180
0.30	0.66	0.350	0.206
0.35	0.77	0.393	0.231
0.40	0.88	0.435	0.256
0.45	0.99	0.475	0.280
0.50	1.10	0.514	0.303
0.55	1.21	0.552	0.325
0.60	1.32	0.589	0.347
0.65	1.43	0.625	0.368
0.70	1.54	0.661	0.389
0.75	1.65	0.696	0.410
0.80	1.76	0.731	0.430
0.85	1.87	0.765	0.450
0.90	1.98	0.798	0.470
0.95	2.09	0.831	0.489
1.00	2.20	0.864	0.509
1.10	2.43	0.928	0.546
1.20	2.65	0.991	0.583
1.30	2.87	1.052	0.619
1.40	3.09	1.112	0.654
1.50	3.31	1.171	0.689
1.60	3.53	1.229	0.723
1.70	3.75	1.286	0.757
1.80	3.97	1.343	0.790
1.90	4.19	1.398	0.823
2.00	4.41	1.453	0.855
2.20	4.85	1.561	0.919
2.40	5.29	1.666	0.981
2.60	5.73	1.769	1.041
2.80	6.17	1.870	1.101
3.00	6.61	1.969	1.159
3.20	7.05	2.067	1.217
3.40	7.50	2.163	1.273
3.60	7.94	2.258	1.329
3.80	8.38	2.352	1.384
4.00	8.82	2.444	1.438
4.20	9.26	2.535	1.492
4.40	9.70	2.625	1.545

Table 16 Minimum Ventilation rate required for Old Poultry farm

Number of days	Alive birds	Weight[g]	Minimum ventilation rate[m3/hr]
0	13000	34	442
1	12 596	34	442
2	12 594	48	906
3	12 586	51	944.2
4	12 574	67	1148.5
5	12 574	84	1366.54
6	12 568	104	1613.7
7	12 567	127	1859.28
8	12 564	149	2093.79
9	12 562	175	2371.07
10	12 562	202	2656.86
11	12 562	235	2967.77
12	12 562	273	3325.78
13	12 559	312	3681.79
14	12 558	352	4023.08
15	12 557	392	4364.31
16	12 552	430	4671.85
17	12 546	478	5055.03
18	12 546	540	5542.82
19	12 545	578	5837.94
20	12 542	636	6269.48
21	12 542	676	6560.46
22	12 542	756	7135.39
23	12 540	818	7572.9
24	12 539	879	7992.98
25	12 537	942	8415.58
26	12 536	1 011	8871.288
27	12 534	1 089	9373.36
28	12 530	1 147	9744.64
29	12 524	1 209	10137.61
30	12 522	1 267	10495.5
31	12 518	1 330	10882.52
32	12 512	1 405	11340.56
33	12 505	1 452	11613
34	12 504	1 503	11915
35	12 501	1 572	12322
36	12 496	1 680	12943
37	12 485	1 793	13578.75

38	12 483	1 849	13894
39	12 482	1 888	14112
40	12 477	2 022	14854.74
41	12 472	2 066	15087.5
42	12 469	2 080	15159.81
43	12 466	2 317	16434.05
44	12 463	2 324	16467.61
45	12 458	2 451	17131.8
46	12 456	2 529	17532

Table 17 Minimum Ventilation rate for New Poultry farm (area = 2000m^2)

Number of days	Alive birds	Weight[g]	Minimum ventilation rate[m3/hr]
1	25000	35	1700
2	24 094	45	1850
3	24 089	52	1831.42
4	24 085	63	2101.65
5	24 081	80	2518.87
6	24 077	99	2985.06
7	24 070	122	4481.83
8	24 063	144	4930.5
9	24 061	168	5420.94
10	24 060	195	5972.89
11	24 058	228	5557.39
12	24 060	195	5972.89
13	24 056	228	5557.39
14	24 055	337	7460.89
15	24 051	378	8131.55
16	24 047	456	9350
17	24 045	501	10175
18	24 043	549	10757
19	24 041	603	11557.4
20	24 041	654	12268.6
21	24 041	667	12449
22	24 041	676	6560.46
23	24 041	752	13622.5
24	24 041	811	14425.8
25	24 039	868	15178
26	24 038	939	16097
27	24 030	1 004	16968

28	24 025	1 118	17706
29	24 020	1 186	17703
30	24 020	1 189	19162
31	24 017	1 239	19799
32	24 015	1 315	20700
33	24 015	1 388	21363
34	24 007	1 463	22420
35	24 006	1 503	22875
36	24 004	1 557	23489.71
37	24 004	1 660	24664
38	24 003	1 732	25436
39	23 997	1 812	25900
40	23 990	1 878	26200
41	23 983	1 951	26500
42	23 969	2 008	26832
43	23 960	2 049	27000
44	23 948	2 127	27232
45	23 931	2 158	27600
46	23 911	2 230	28000

In the graph, the energy uncertainty (in green line) over time represents the standard deviation of the energy production from the Monte Carlo simulations. Thus, energy uncertainty values provide the estimation for the variation in energy production due to uncertainties in the mass flow rate and temperature measurements. The graph in Figure 9-1 illustrates the energy variation uncertainty for the 89 days in the poultry farm for sensor1. The average energy uncertainty over time is 1.66 kJ/s.
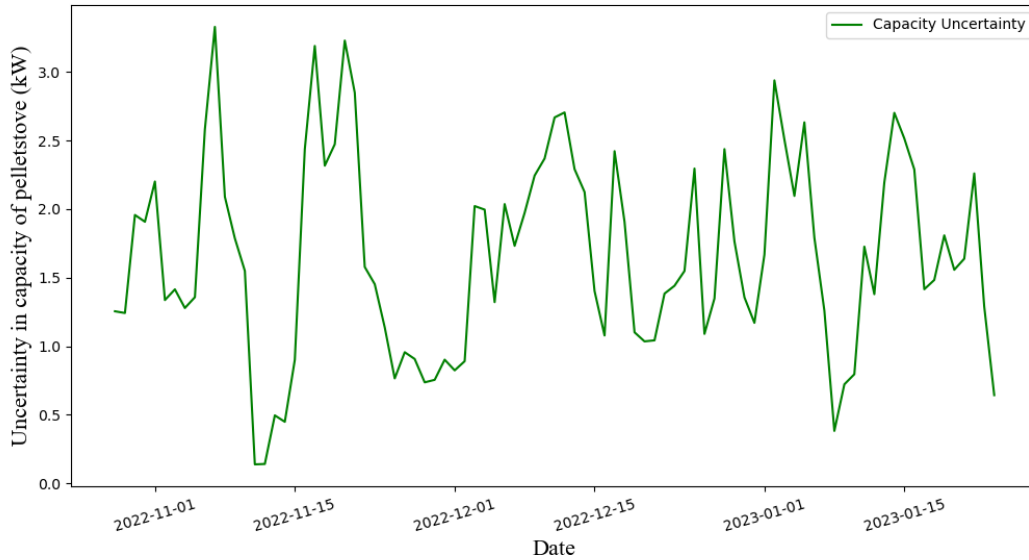
Figure 9-1 Energy production uncertainty variation

Figure *9-1* demonstrates relative uncertainties, revealing how the uncertainties are spread over the range of time. The histogram (in blue) shows the frequency distribution of relative uncertainties. The error distribution (in red) represents the normalized frequency of these uncertainties. The average relative uncertainty is 2.10%, illustrating the shape of the uncertainty distribution.
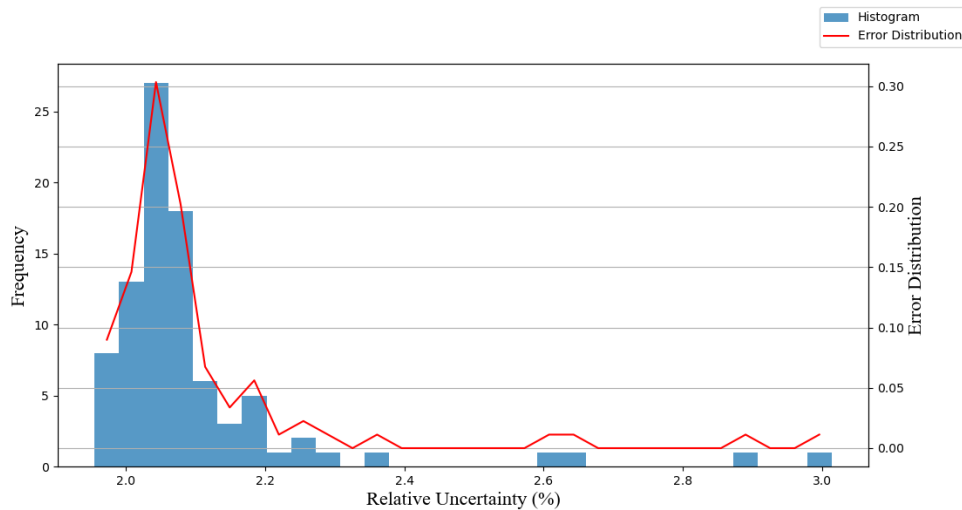
Figure 9-2 Histogram and error distribution of Relative Uncertainty

Likewise, the uncertainty of the sensor measured by other sensors E2, E3, E4, E6 and E7 is given respectively.

Likewise, volumetric flow rate measured with the flow meter of class 2 accuracy gives the uncertainty as Tabulated below:

Volumetric flow rate at units	Random error	System error	Overall uncertainty
District heating (Fjernvarme)	0.08	0.01	0.08
Floor heating (GulvvarmeE2)	0.00	0.00	0.00
Floor heating (Gulvvarme E2.1)	0.00	0.00	0.00
Heat recoveryE3(varmegjenvinning)	0.00	0.00	0.00
Fan coil unit	0.61	0.00	0.61

Hence, the overall system uncertainty of the flow meter is ±0.61%.

The temperature sensor PT1000 gives the total uncertainty of sensor as Tabulated as follows:

Supply Temperature at units	Random error	System error	Overall uncertainty
District heating (Fjernvarme)	0.08	0.01	0.08
Floor heating (GulvvarmeE2)	0.00	0.00	0.00
Floor heating (Gulvvarme E2.1)	0.00	0.00	0.00
Heat recoveryE3(varmegjenvinning)	0.00	0.00	0.00
Fan coil unit	0.61	0.00	0.61

Figure 9-3 Annual Production Report
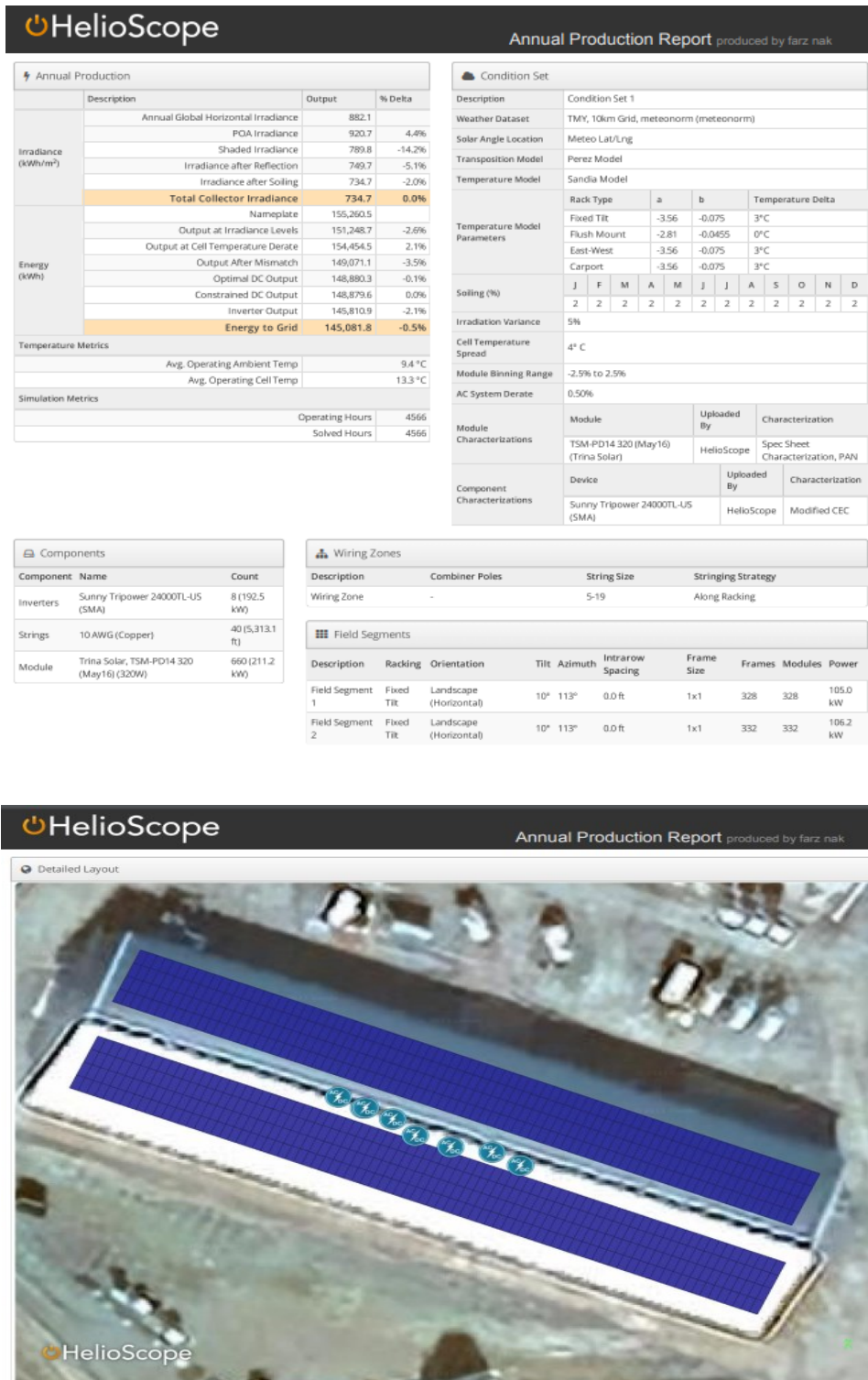
Figure 9-4 Annual Production Report

⚡ Annual Production

	Description	Output	% Delta
Irradiance (kWh/m²)	Annual Global Horizontal Irradiance	882.1	
	POA Irradiance	917.3	4.0%
	Shaded Irradiance	889.0	-3.1%
	Irradiance after Reflection	843.0	-5.2%
	Irradiance after Soiling	826.1	-2.0%
	Total Collector Irradiance	**826.1**	**0.0%**
Energy (kWh)	Nameplate	82,517.9	
	Output at Irradiance Levels	80,758.0	-2.1%
	Output at Cell Temperature Derate	82,019.6	1.6%
	Output After Mismatch	76,101.4	-7.2%
	Optimal DC Output	75,990.8	-0.1%
	Constrained DC Output	75,990.4	0.0%
	Inverter Output	74,280.3	-2.3%
	Energy to Grid	**73,908.9**	**-0.5%**

Temperature Metrics

Avg. Operating Ambient Temp	9.4 °C
Avg. Operating Cell Temp	13.8 °C

Simulation Metrics

Operating Hours	4566
Solved Hours	4566

☁ Condition Set

Description	Condition Set 1
Weather Dataset	TMY, 10km Grid, meteonorm (meteonorm)
Solar Angle Location	Meteo Lat/Lng
Transposition Model	Perez Model
Temperature Model	Sandia Model

	Rack Type	a	b	Temperature Delta
Temperature Model Parameters	Fixed Tilt	-3.56	-0.075	3°C
	Flush Mount	-2.81	-0.0455	0°C
	East-West	-3.56	-0.075	3°C
	Carport	-3.56	-0.075	3°C

	J	F	M	A	M	J	J	A	S	O	N	D
Soiling (%)	2	2	2	2	2	2	2	2	2	2	2	2

Irradiation Variance	5%
Cell Temperature Spread	4° C
Module Binning Range	-2.5% to 2.5%
AC System Derate	0.50%

	Module	Uploaded By	Characterization
Module Characterizations	TSM-PD14 320 (May16) (Trina Solar)	HelioScope	Spec Sheet Characterization, PAN

	Device	Uploaded By	Characterization
Component Characterizations	Sunny Tripower 24000TL-US (SMA)	HelioScope	Modified CEC

🗀 Components

Component	Name	Count
Inverters	Sunny Tripower 24000TL-US (SMA)	4 (96.2 kW)
Strings	10 AWG (Copper)	20 (1,998.6 ft)
Module	Trina Solar, TSM-PD14 320 (May16) (320W)	312 (99.8 kW)

⁂ Wiring Zones

Description	Combiner Poles	String Size	Stringing Strategy
Wiring Zone	-	5-19	Along Racking

▦ Field Segments

Description	Racking	Orientation	Tilt	Azimuth	Intrarow Spacing	Frame Size	Frames	Modules	Power
Field Segment 1	Fixed Tilt	Landscape (Horizontal)	10°	111°	9.4 ft	10x1	15	150	48.0 kW
Field Segment 2	Fixed Tilt	Landscape (Horizontal)	10°	111°	4.8 ft	9x1	18	162	51.8 kW
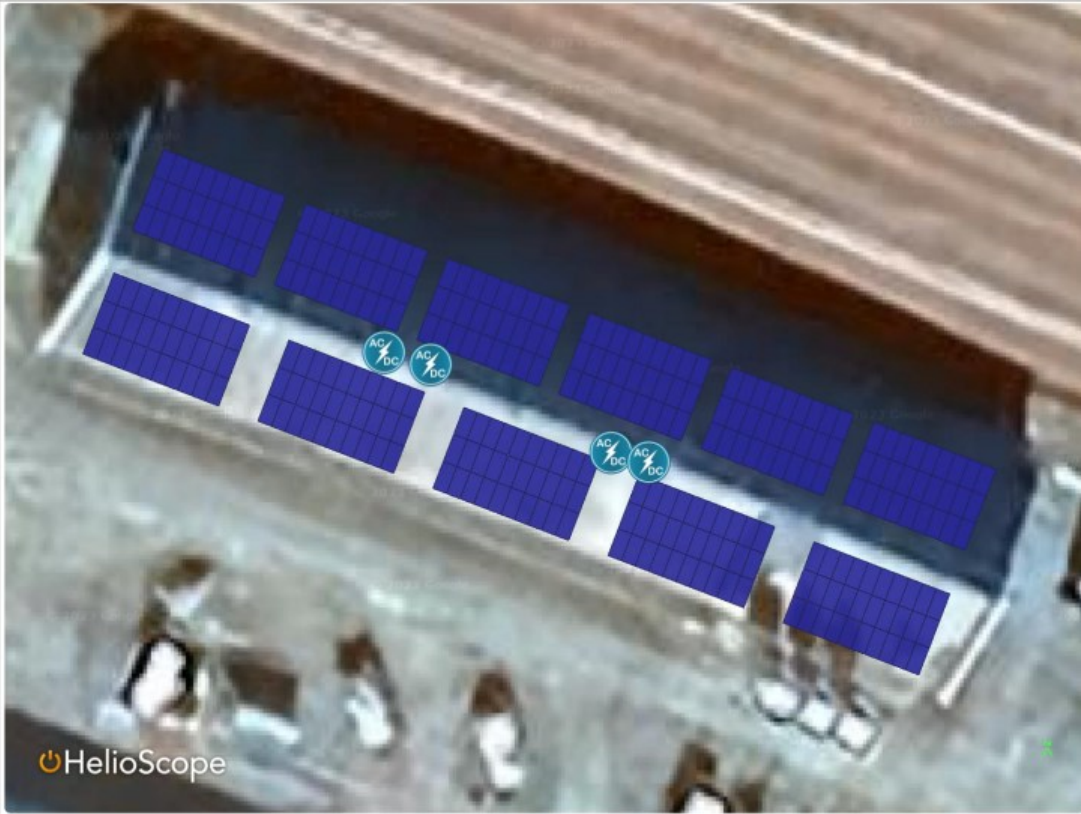
Development of a fossil-free heating system for chicken barns based on heat pumps and thermal storage

Saroj THAPA[a], Håkon SELVNES[b], Armin HAFNER[a]

[a] Norwegian University of Science and Technology
Trondheim, 7491, Norway, saroj.thapa@ntnu.no, armin.hafner@ntnu.no, engin.soylemez@ntnu.no
[b] SINTEF Energy Research
Trondheim, 7465, Norway, hakon.selvnes@sintef.no

ABSTRACT

This paper investigates the potential of renewable heating and cooling systems to mitigate the environmental footprint of the burgeoning poultry industry. Current energy consumption in poultry farms, primarily through pellet boilers, was analyzed with an error margin of 0.41%. A new heat pump system is proposed to replace the existing broiler that provides heating in poultry house. The study further evaluated a 120-kW CO_2 heat pump, focusing on various configurations. The most effective configuration was found to be a system featuring an FGBV and parallel evaporators, achieving a COP of 4 to 4.6. Conversely, using city water as a source achieved a steady state COP of 3.6. Efficiency was assessed via drying time calculation for a 2 cm water film on a 2000 m^2 concrete surface, demonstrating that slower airflow yields more effective drying and potential energy savings. The drying time in the poultry farm is 23 hours when 1 m/s hot air is uniformly distributed at 50 ℃ throughout the area. These findings suggest CO_2 heat pump systems potential to enhance sustainable solutions.
Keywords: COP, Global warming potential, refrigerant, heat pump

1. INTRODUCTION

The global poultry industry plays a vital role in food security, supplying significant amounts of meat and fertilizers for crop cultivation. However, despite chicken being a more environmentally meat source, the environmental footprint associated with its production is substantial. The growing shifts towards poultry consumption, such as that observed in Norway, further intensify the industry's environmental impact. Current heating practices in poultry farms, often reliant on fossil fuels, are neither cost-effective nor sustainable.

As the European Union progresses toward its carbon reduction goals, the transition from traditional heating systems to renewable ones is becoming increasingly imperative. Poultry farms, contributing notably to greenhouse gas emissions, are the prime sector for introducing such transitions. With the predicted increase in energy consumption due to advancing mechanization and automation in farms, it becomes essential to incorporate renewable, energy-efficient heating and cooling systems. These systems promise improved temperature, humidity, and air quality control within farms, thus optimizing poultry growth conditions and enhancing productivity (Poore & Nemecek, 2018).

Energy production for poultry farming is a multi-faceted process, significantly affecting the sector's environmental impact and economic viability. It largely encompasses heating, cooling, and ventilation systems necessary to maintain optimal growth conditions for poultry. Conventionally, these energy requirements have been met through fossil fuel-based systems like propane heaters or bio-pellets, which while effective, also contribute to greenhouse gas emissions. Increasingly, farms are recognizing the potential of renewable energy sources, such as solar power and biogas, to meet these demands in a more sustainable manner. Photovoltaic cells are installed on farm roofs to capture solar energy, and biogas can be produced through the anaerobic digestion of chicken manure. This not only helps reduce carbon emissions but also cuts down energy costs. Furthermore, innovative solutions like heat pumps and thermal energy storage, using phase change materials (PCM), are being more energy efficient. These systems can excessively store excess heat generated during non-peak hours and use it during periods of high demand, ensuring consistent temperature control while optimizing energy consumption. As such, the shift towards renewable and

efficient energy production methods in poultry farming is crucial for its sustainable growth and reduced environmental impact (Liu et al., 2022).

2. CASE STUDY OF THE DEMO FARM

This section focuses on a general overview of concept implemented in poultry farm, uncertainty analysis of measurement equipment, fossil-free heating systems, and study of uncertainty in measurement equipment. To design any specific system, it is necessary to study the climatic condition of that place. The poultry farm is based in Inderøy, Trondheim where temperature ranges from -20 ℃ to 28 ℃. The climate registration centre is Maere III which is located nearest to the farm as shown in Figure 1.
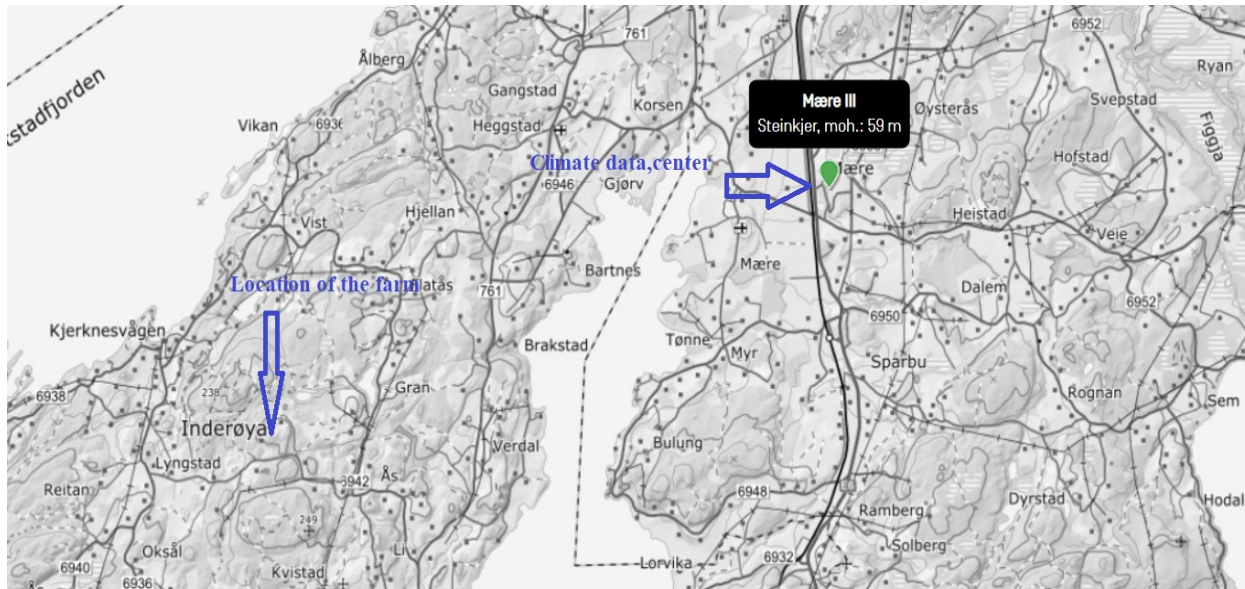

Figure 1 Climate centre and poultry farm location in Trondheim

The consideration of extreme weather during the designing process is important to assure the longevity of the designed system. Air can be used as a source for fossil-free heating systems whose temperature is at 2.5 ℃ to 14.5 ℃ and whose mean relative humidity ranges from 72-86% for the past 12 months. The poultry farm in the location has the following dimensions as shown in Table 1.

Table 1 Dimension of Poultry farm

Types of farms	Dimension(m^2)	Volume of farm(m^3)	No. of chickens
New Poultry	80x25	10890	25000
Old Poultry	64x16	5575.7	1300

The sensors are fitted at different locations to measure the energy consumption of the poultry farm. The uncertainty analysis indicates that systematic errors need to be rectified to a recognized or accurate value. This can be accomplished by adjusting the various sensor of the system. Calibration is a process that entails comparing the data obtained from different sensors in the system to a calibration benchmark of known precision. The poultry farm consists of a series of sensors to measure the thermal energy demand at different units. The features and accuracy of different sensor in the facility in the poultry farm are as follows:

Table 2 Features and accuracy of different sensors in the facility

Sensor Type	Type	Accuracy Class	Measuring range	Accuracy
Temperature	pFlow	Class B		±(0.3+0.005T) ℃
Power	Split-core current Transformer	Class 1	-20 to 55℃	Class 1
Volumetric mass flow	pFlow	Class 2	-10℃ to 60℃	±2%
Datalogger(eGaugePro Specifications)	ANSI C12.2		-30 to 70℃ 80% humidity up to 31℃	0.5%

The sensor gives the uncertainty for energy consumption based on the accuracy of the data logger. The data has a trial number of 2194 which is measured every 10 minutes in the poultry farm. The data are logged in from 01.0.3.2023 (Time = 01:03) to 16.03.2023 (Time = 06:23). In the measurement, the thermal energy meter, flow meter, and temperature sensor recorded energy consumption in kWh, the volumetric flow rate is m^3/h, supply and return temperature in ℃. The uncertainty of the sensors for energy consumption is listed as follows:

Table 3 Uncertainty or error at different conditions of energy consumption

Energy consumption at units	Random error	System error	Overall uncertainty
District heating (Fjernvarme)	0.16	0.06	0.2
Floor heating (GulvvarmeE2)	0.01	0.00	0.01
Floor heating (Gulvvarme E2.1)	0.01	0.00	0.01
Heat recoveryE3(varmegjenvinning)	0.02	0.00	0.02
Fan coil unit	0.16	0.03	0.17

Hence, the uncertainty of energy consumption measured is ±0.41%.

3. METHODOLOGY

3.1.1. Uncertainty analysis

Measurement typically involves quantifying a physical attribute numerically. Key considerations of this process include the physical quantity being measured, the method of measurement, the most suitable device or measurement, the desired level of precision, and the procedures for processing the data. Given that nearly all measurements carry some degree of error and uncertainty, it is crucial to set realistic expectations for the

accuracy of the results that align with what can realistically be achieved. Hence, there are three types of errors: Gross errors, systematic errors, and random errors (Coleman & Steele, 2018).

The estimation of the uncertainty levels is done using different methods:

For simple measurements, the equation of measurement is as follows (Coleman & Steele, 2018):

$$\bar{x} = \sum x/n$$

Eq. 1

The level of uncertainty in individual measurements can be determined based on several measurements taken (represented by 'n'), each individual measurement value (denoted by 'x'), and the mean of these measurements (also represented by 'x̄'). This uncertainty is typically communicated via the standard deviation represented by the symbol 's'.

$$S = \sqrt{\frac{\sum(x - \bar{x})^2}{n - 1}}$$

Eq. 2

The total error can be given by:

$$U_R = \pm\sqrt{U_T^2 + U_S^2}$$

Eq. 3

Where U_R is always specified by the manufacturer of the meter.

Most physical measurements are complex in nature, implying that the result is dependent on the measurement of multiple variables that are then incorporated into a mathematical equation. As a result, the uncertainty associated with the final measurement result is influenced by multiple distinct factors. When directly measured quantities are denoted as u, and N is the resultant value from the compounded measurements, each u is measured with an associated degree of uncertainty, denoted as Δu.

$$N \pm \Delta N = f(u_1 + u_2 + \cdots, u_n \pm \Delta u_n$$

Eq. 4

Assuming that the uncertainty of the individual measurement is independent, for example not measured with the same meter or method the resultant error can be estimated as follows. Replacing ΔN by U_R.

$$U_R = \pm\sqrt{\left(\frac{\partial f}{\partial u_1}.\Delta u_1\right)^2 + \cdots + \left(\frac{\partial f}{\partial u_n}.\Delta u_n\right)^2}$$

Eq. 5

3.1.2. Calculation to estimate drying system

To estimate the drying time, and behavior of system during drying following parameters were the analyzed. It was analyzed on the basis that 50 ℃ of hot air with average air flow rate at different velocities. is uniformly distributed throughout the area of 2000 m². The thickness of the water film above the concrete was assumed to be 2 cm. The steps followed during the calculation of drying time are as follows:

- Properties of air are obtained at a temperature of 50 ℃, using the air properties from Table A.4. (Incropera et al., 2013) These properties, which include air density, specific heat capacity, and thermal conductivity, are critical subsequent calculations in methodology.

- Properties of saturated water vapor: The properties of saturated water vapor are determined from Table A.6 (Incropera et al., 2013) at a given temperature. The parameters like specific volume, the heat of vaporization, thermal conductivity etc. are obtained.

- Reynold's number was calculated using the standard formula as follows:

$$RE_N = \frac{uL}{\vartheta}$$
<div align="right">Eq. 6</div>

Where, RE_N is the Reynold number, u is the velocity of air, L is the length of surface to dry, and ϑ is the kinematic viscosity.

- Determine the Schimdt number: The Schimdt number, which is a dimensionless number, describing the ratio of momentum diffusivity(kinematic viscosity) to mass diffusivity was calculated.

$$Sc = \frac{\vartheta}{D_{AB}}$$
<div align="right">Eq. 7</div>

Afterward, heat and mass transfer analogy are utilized to find the Sherwood number. The heat and mass transfer are assumed to be turbulent throughout the length of concrete surface.

<div align="right">Eq. 8</div>

$$Sh_l = h_m L / D_{AB} = (0.037 Re^{4/5} - 871) Sc^{1/3}$$

Where, Sh_l is the Sherwood number and h_m is the average convective mass transfer coefficient.

Likewise, mass flow rate of water evaporation per unit plate is calculated using the following equation.

$$n_A = h_m L (\rho_{AS} - \emptyset \rho_{A\infty})$$
<div align="right">Eq. 9</div>

This gives an evaporation rate per unit length for different air velocities.

Afterward, humidity is added to the air after hot air supply to the air, and humidity leaving the surface is calculated accordingly from the psychometric chart. This can help to estimate the drying time of the surface throughout the total area of the poultry farm.

4. RESULTS

4.1.1. Design of heat pump layout for poultry farm

The existing system in a poultry farm has a pellet boiler which produces a lot of CO_2 production and has the potential for high global warming. This study highlights the replacement of conventional pellet boiler systems with new heat pump systems using natural refrigerants, For instance, R744. The capacity of the heat pump is 120 kW to meet the heating and cooling capacity. This will significantly reduce the GWP and help to maintain a clean and healthy environment. The new layout of the poultry farm is given below.

The Figure 2 is the layout for the proposed new system that can be implemented after the case study. This heat pump system is fossil free heating using electricity and high environmentally friendly. This system is designed from the inspiration of system layout Gullo et al. (Gullo et al., 2017).
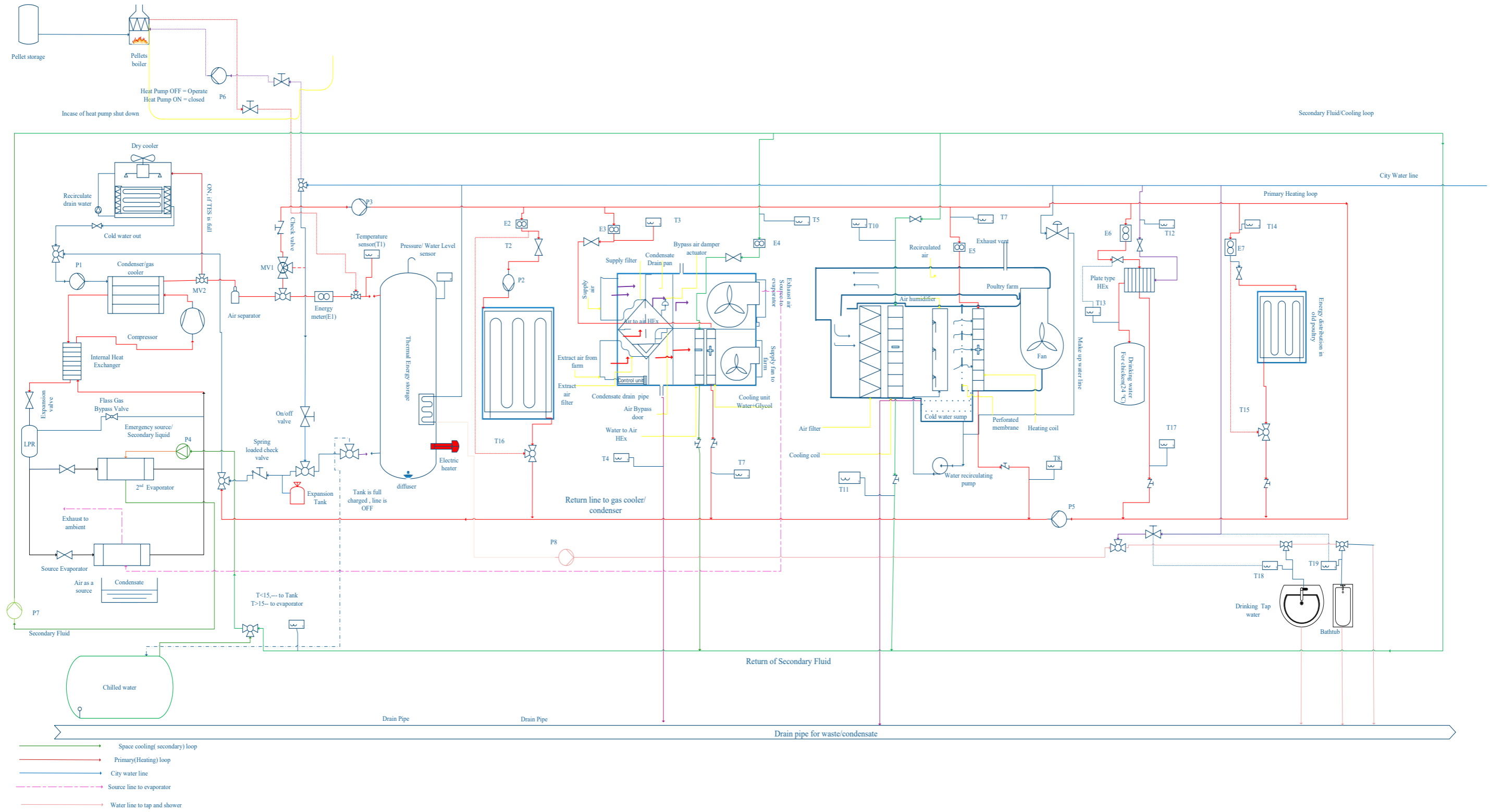
Figure 2 New proposed heat pump system for a poultry farm (zoom it for high quality and better resolution of every components in each units)

Bypass duct

Exhaust air from farm, activated in normal operation

Supply Air Inside farm

Sensor control unit

Upper exhaust from farm to duct in Operation when dehumidifier is not activated and drying is not needed

Recirculating pump

Drain Pan

Water sump

To drain Pipe

11470

8037mm

Humidifier

Mixed air

Machine Room closet

Perforated Membrane

Drying activation, dehumidifier activated

To evaporator
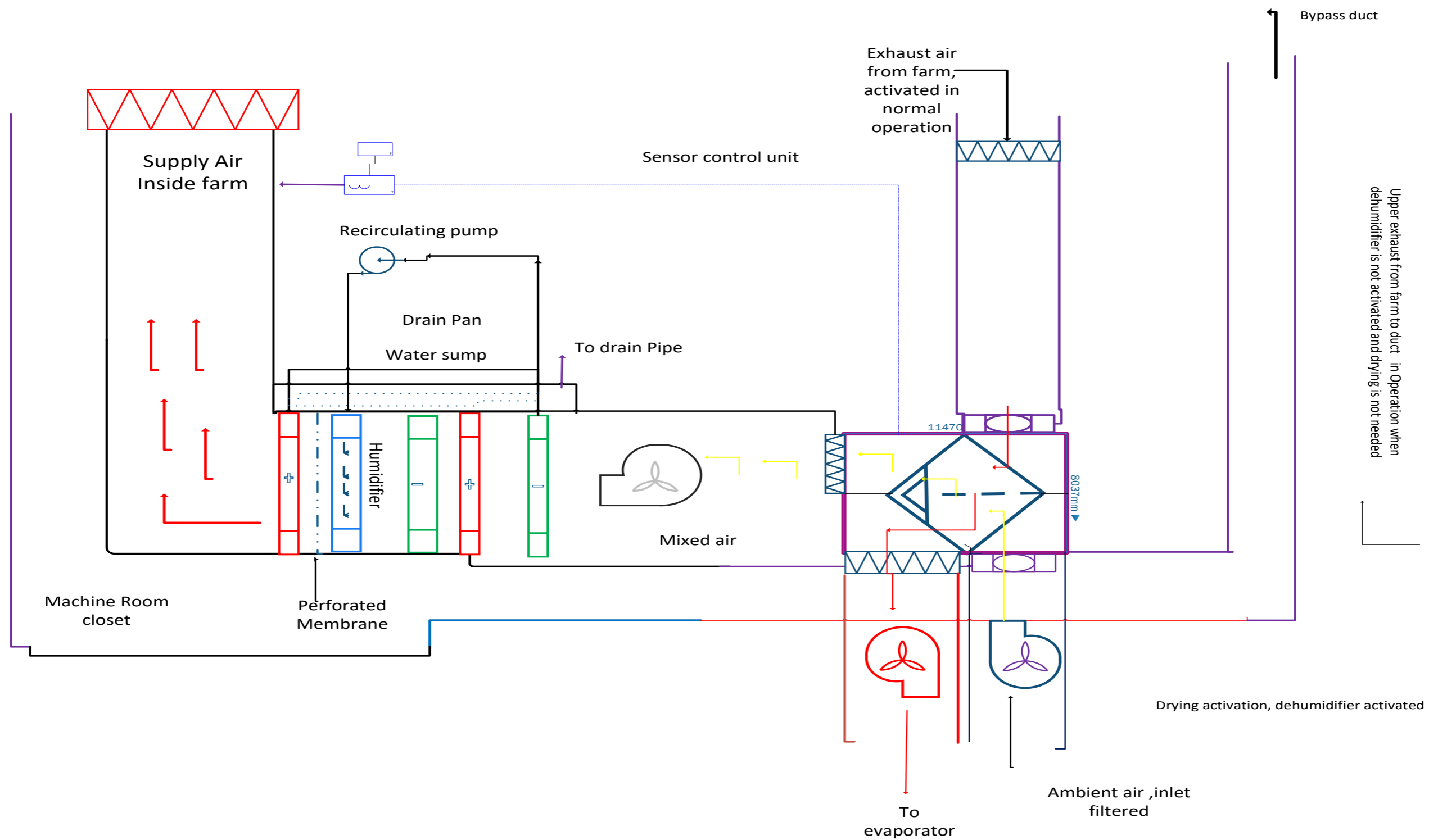
Ambient air ,inlet filtered

Figure 3 HVAC integration (Combined Heat Recovery and Fan Coil Unit)

Working mechanism for winter: The heat pump cycle designed for the poultry farm as shown in Figure 2 incorporates the two evaporators, a flash gas bypass valve, an internal heat exchanger, a compressor, a gas cooler, pressure regulating valves, a humidification and dehumidifying unit and storage tank. In this layout, the first evaporator takes air as a source, while the second evaporator exchanges heat between city water and the refrigerant to produce chilled water. The flash gas bypass valve (FGBV) bypasses vapor refrigerant from the low-pressure receiver(LPR). Both the lower refrigerant (suction to the compressor) and the higher temperature refrigerant (return line from the gas cooler) pass through the internal heat exchanger unit. The compressor compresses the refrigerant, which then passes through a gas cooler, delivering high-temperature and high-pressure refrigerant in transcritical mode. After the gas cooler, the return line of the refrigerant passes through the internal heat exchanger and an expansion valve, which reduces its pressure and temperature. Pressure-regulating valves are added on the suction sides of both evaporators, connected in parallel. The humid air from the HRU is used as a source in this layout, producing condensate when used as a source in the evaporator. This condensate is collected in a drainpipe. City water is supplied to the gas cooler via a three-way valve and is then pumped into the gas cooler. The gas cooler produces hot water at temperatures ranging from 80-85 ℃. An air separator is placed at the outlet after heating water in the gas cooler to remove air pockets and prevent cavitation. The primary heating loop supplies hot water to the floor heating tubes, the HRU, FCUs, and the farm drinking water system. The FCU and HRU include humidifiers, heating coils, and cooling coils. When heating demand is low, the hot water from the gas cooler is stored in a stratified tank. The drinking water temperature for chickens is maintained at 24 ℃ by exchanging heat between the primary heating line and city water using the Plate heat exchanger. The return line from all units is supplied back to the cooler for further heating. Heating and cooling are controlled according to the requirements inside the farm. When hot air with less humidity than requirement is present, the air is further humidified with the help of a humidifier connected to the city water line. The condensate produced is a sump and is recirculated with the help of a pump. This comprehensive heat pump cycle design ensures optimal temperature and humidity conditions for the poultry farm.

Working mechanism for summer: During summer conditions, the heat pump system adapts to provide adequate cooling and maintain optimal temperatures and humidity levels in the poultry farm. Here is the system that operates in summer conditions.

- Reduced heating demand: As the heating demand decreases during the summer, the hot water produced by the gas cooler is stored in the stratified tank for later use when needed. This storage helps balance heating and cooling demands throughout the day or during changing weather conditions.

- Cooling via FCUs: The Fan coil unit is utilized to provide by circulating cooled water or glycol solution through the coils. The cooled air is then distributed throughout the poultry farm to maintain comfortable temperatures for the chickens. This process helps to counteract the heat generated by chickens and any other external heat entering the facility.

- Evaporative cooling: the evaporators in the system can also contribute to cooling. As the refrigerant evaporates and absorbs heat from the secondary loop (chilled water), it helps lower the temperature of the circulating fluid, which can be used for cooling purposes in the facility.

The dry cooler is integrated into a heat pump system. When a dry cooler is integrated into a pump system with a fully charged storage tank, it effectively prevents overheating and maintains efficient operation. The control system continuously monitors the storage tank temperature, and the dry cooler using a three-way valve. The dry cooler consists of a heat exchanger with fined tubes or coils and a fan system, that dissipates excess heat from the hot water to the ambient. Consequently, cooled water returns to the system, and excess heat is released into the environment. Once the storage tank temperature drops below the predefined threshold, the control system deactivates the dry cooler, returning the hot water flow to its normal path. This ensures the heat pump system continues to operate efficiently without necessary heat loss, effectively excess heat with the help of the dry cooler.

4.1.2.   Thermodynamic modeling of the Proposed system

The performance modeling of the proposed heat pump system above was conducted by Dymola (Dynamic modeling library, version 2022, Dassault Systems) using Modelica language. The evaporating pressure was set to 39.69 bar and condensing temperature at 96 bar. Two commercial Modelica libraries were utilized for the simulations, namely TIL-suite 3.10.0 and TILMedia 3.10.0 which is provided by Thermo Gmbh. The proposed model is simulated for two types. The first option could be using parallel evaporators and the second one is using a single evaporator (water as source , instead of humid air). Those two models were implemented and compared. The simulation model for the 1st option with the parallel evaporators is shown below:
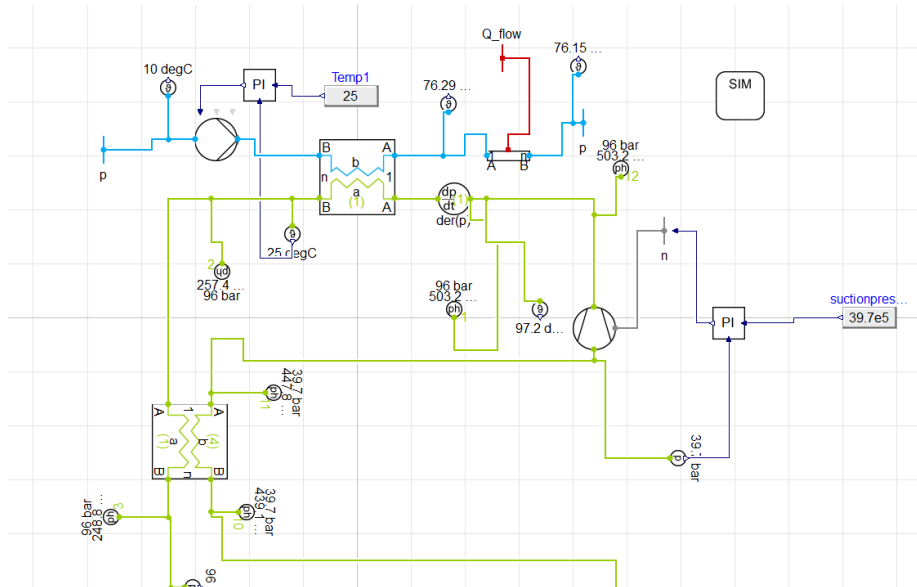

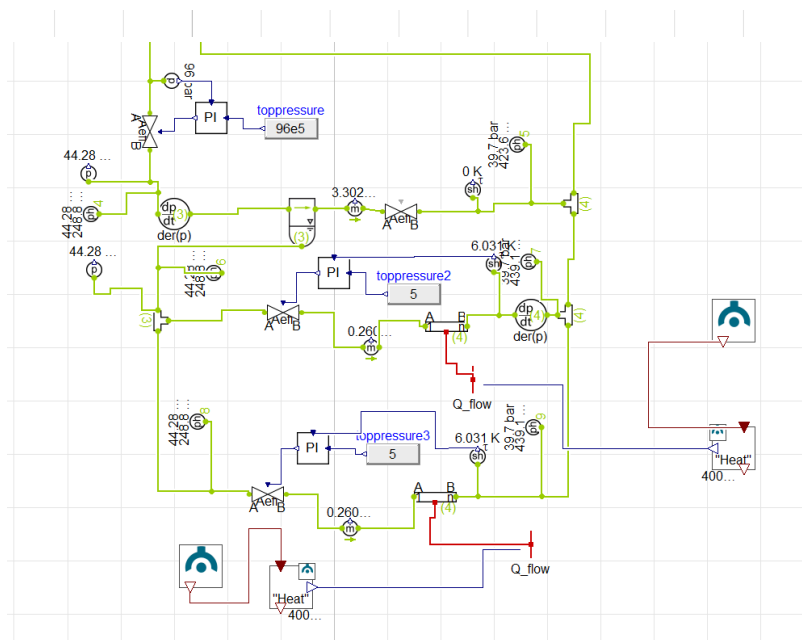Figure 4 High pressure side after simulation for 100000s

Figure 5 Low pressure side after simulation

Components implemented in the model: The components implemented in the model are as follows:

- **Evaporator:** The evaporator is used for a heat source. A steady state the system is designed to take heat source of 99 kW. The evaporator has a heat transfer coefficient of 4000 W/m²K. Hot moist air at the exhaust of the poultry farm is given as an input source.

- **Compressor:** The pressure ratio is 2.42 while compressing the CO_2 from 39.69 bar to 96 bar. The compressor used in the system is a piston compressor. The isentropic efficiency is calculated to be 0.7 which gives the volumetric efficiency of 0.85. Characteristics of the compressors needed are as follows:

Compressor Type	Piston
Volume of flow inlet to the compressor	17.82 m³/h
Enthalpy at compressor outlet	483,26 kJ/kg
Stroke volume/ displacement volume of the compressor	20.97 m³/h
Shaft power	24,68 kW
Isentropic compressor capacity	17,27 kW

A Dorin compressor for the CD series can be used in the system to fulfill the demand on the farm. The compressor operates in transcritical mode with operating up to 110 bars. The displacement of these compressors ranges from 1,12 to 80 m³/h (50 Hz, single stage).

- **Liquid receiver/Separator:** The fluid line from the internal heat exchanger is expanded from 96 to 39.6 bar through the expansion valve. The two-phase separation takes place in the tank. The gas in the tank is passed from the top of the tank whereas liquid line is further taken to evaporator. The evaporator can be single or multiple depending upon the requirement and system. The liquid droplets settle in the tank using the following:

$$F_g = \frac{M_p(\rho_l - \rho_v)g}{g_c \rho L}$$ Eq. 10

Where, F_g is the gravity force, M_p is the mass of droplets, g is the gravitational constant, ρ_l is liquid density and ρ_v is the vapor density, and g_c= gravitational constant/ (gravitational force- Vessel material stress[2])

Hence, the vertical terminal velocity is determined by:

$$U_T = K \sqrt{\frac{\rho_l - \rho_g}{\rho_v}}$$ Eq. 11

Where, U_T is the vertical terminal Velocity and k is the separator values.

The refrigerant use in the system is R744, with a density of 1.98 kg/m^3. The mass flow rate at steady state is 0.5 kg/s, compressor capacity is 24 kW. Assume that the separator efficiency is 0.8 and a residence time of 5 seconds. The separator mass is 2.5 kg. The separator volume needed is calculated as 1.58 m^3.

- Expansion tank : The purpose of an expansion tank in a hydronic system with a heat pump is to accomodate the expansion and contraction of the water in the system as it heats up and cools down. When water is heated, it expands and can cause an increase in pressure in the system. Here, if we assume that the minimum temperature of water is 20°C and maximum temperature is 100°C along with corresponding pressure at 1 bar and 3 bars respectively. The volume of water throughout the system is 5 m^3 with a 4 m^3 storage tank. The tank is made up of stainless steel whose volume is 0.25 m^3 but, with a safety factor of 1.5 it must be 0.37 m^3.

At the 1st state, the pressure at the high-pressure side was recorded to be 503.2 kJ/kg. Following this, at state 2, the gas cooler's influence on the system could be seen as the enthalpy dropped to 257.4 kJ/kg after the gas cooler at 96 bars. This stage further involved a temperature transformation where cold water, initially at a temperature of 10 °C, was heated up to 76.29 °C. The heated water was then directed to a thermal storage tank, which was represented as a tube in the simulation. At the 3rd point, the enthalpy was observed to decline marginally to 248.8 kJ/kg. Remarkably, this same enthalpy value was maintained across three different points-state points 4,6 and 8. These observations were recorded after the refrigerant was guided through the expansion valve. Another key process involved the routing of the refrigerant past a bypass valve to junction 4, where a mass flow rate of 3.302e-07 kg/s was noted. In this stage, two evaporators are depicted as tubes in the simulation, displaying a mass flow rate of 0.261 kg/s. These evaporators played a crucial role in producing cold water in one evaporator and other evaporators are taken as a source. Moving to state points 5,7,9 and 10, a consistent pattern of enthalpy measurement was noted. The enthalpy remained at 447.8 kJ/kg. The conclusion of this cycle was marked by the compressor outlet's temperature, which was recorded at 97.2 °C.
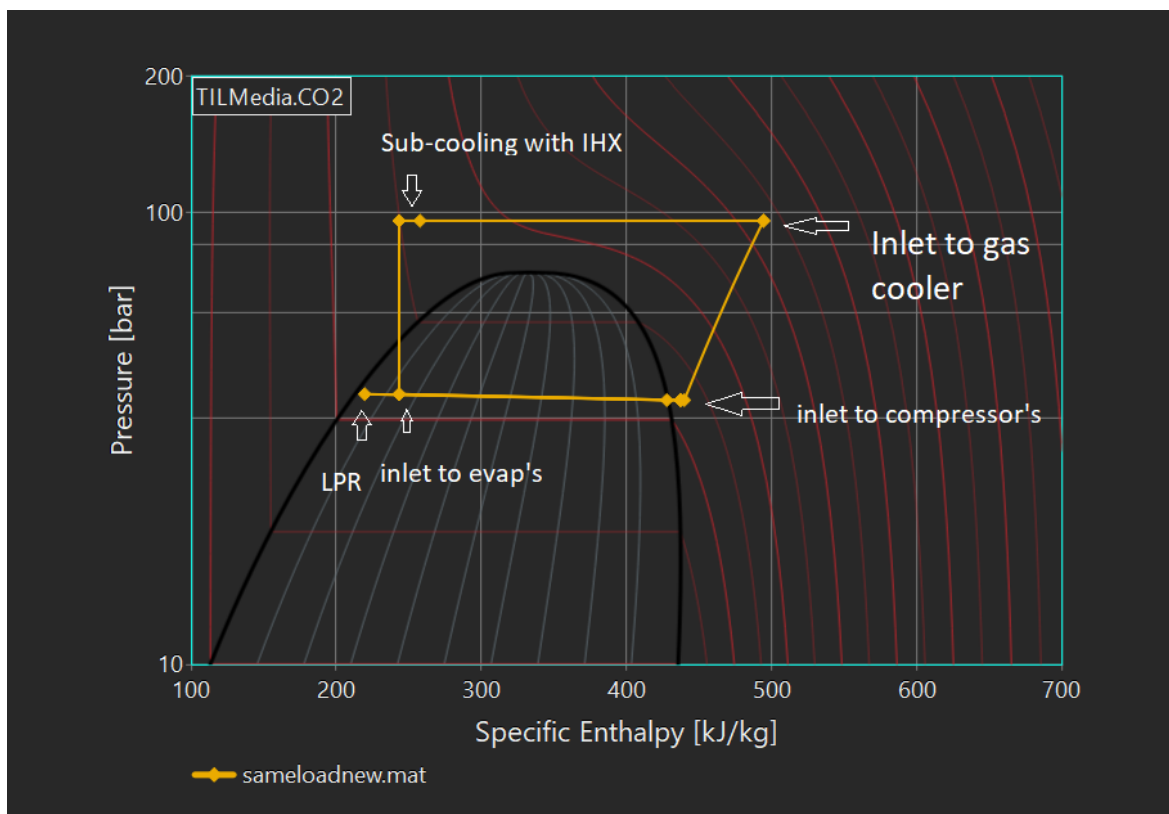

Figure 6 P-h diagram for proposed layout thermodynamic modelling

Figure 7 shows the cold-water at 20°C being heated by the VLE fluid. The VLE fluid shows the gliding behavior inside the gas cooler. The exit at the compressor is approximately 100 °C which transfers the heat to cold water. The city water temperature rises to 85°C when heated at the gas cooler which is further sent to different energy distribution units or thermal storage tank in case energy demand is less. The pitch point is approximately 6 K.
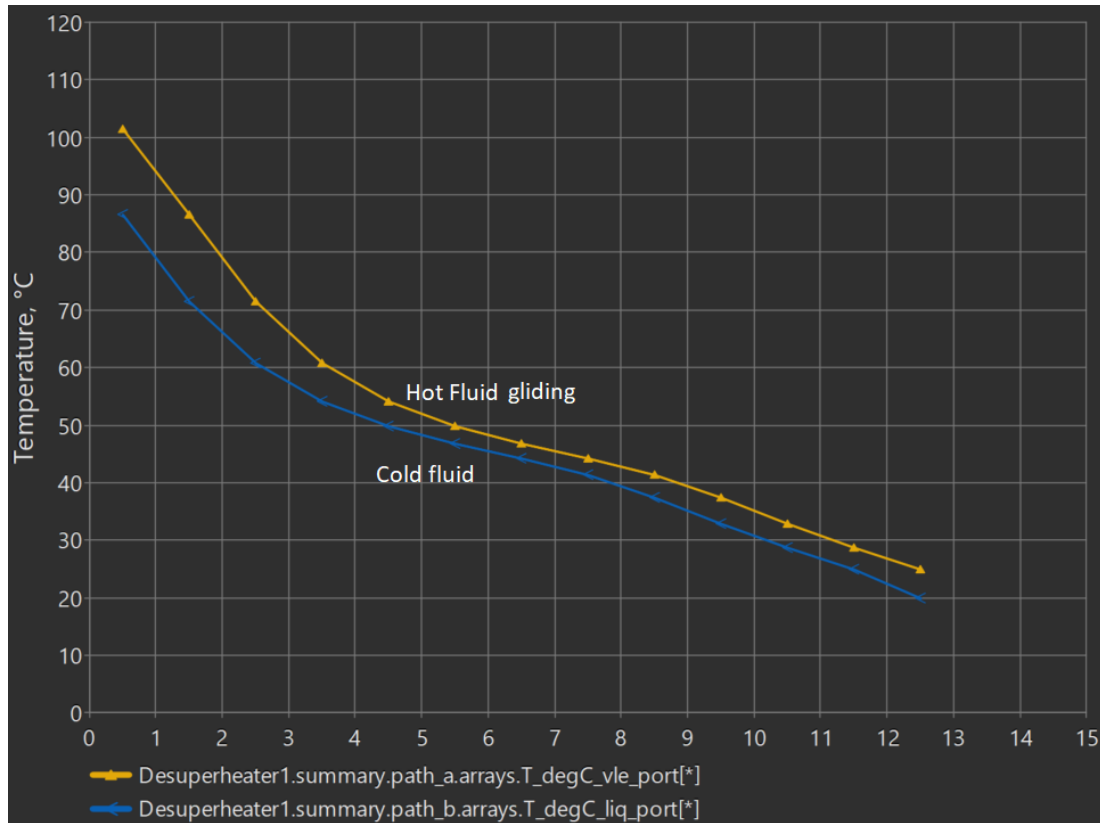

Figure 7 Counterflow of hot and cold fluids inside gas cooler

In the analysis of variable load in parallel evaporators, distinct load levels were evaluated, including 8.75 kW, 17.5 kW, 20 kW, and 49.5 kW. A notable increase in COP was observed, as illustrated in Figure 8 . In these parallel evaporators, the upper evaporator can be used to chill down water and lower to take air as a source. Each of these levels was simulated for a duration of 6000 seconds. Consequently, throughout the variable load study, the total simulation time reached 24000 seconds. This dynamic load variation exhibited a COP range between 3.74 to 4.5.
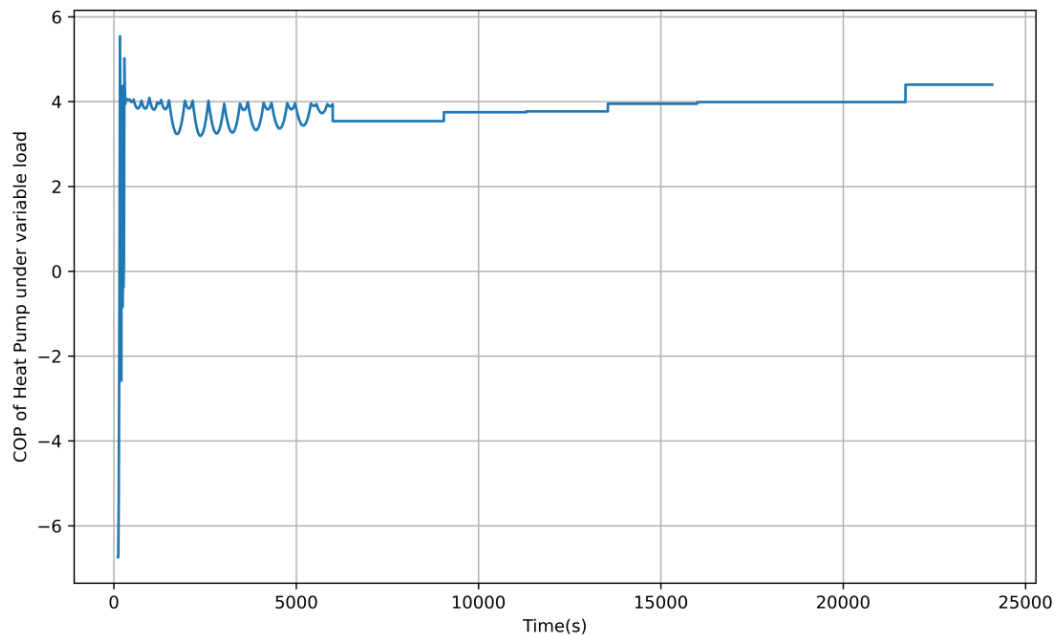
Figure 8 COP of heat pump under variable load

Likewise, if water is considered as a source and only a single evaporator is used, the COP of the system when only a single evaporator is used rather than humid air is 3.6.

4.1.3.   Drying with heat pump

Figure 9 illustrates two distinct trends related to the heat and mass transfer processes along an isothermal surface of 80m length at a fixed temperature of 50 °C and relative humidity of 13.1%.

The plot between the mass transfer coefficient and between dry air velocity gives that as air velocity amplifies the moisture-carrying potential of the air is increased. This observation is consistent with the theory that convective mass transfer coefficient with air velocity. With the increasing velocity of air, from 1 to 20 m/s, there is a notable increase in the mass transfer coefficient from approximately 0.0097m/s to 0.1192 m/s. This indicates an almost 12-fold increase in the mass transfer coefficient with a 20-fold increase in the air velocity. This non-linear correlation suggests the effect of air velocity. This non-linear correlation suggests that the effect of air velocity on the mass transfer coefficient may be more complex than a straightforward linear relationship and could have been influenced by other factors like turbulence, boundary layer thickness, etc.

The plot shows the increasing trend between air velocity and evaporation rate per unit area. This trend underscores the role of air velocity in intensifying the rate of evaporation. The evaporation rate increases from 0.000867 kgH_2O/m^2.s at 1 m/s to 0.00892 kgH_2O/m^2.s at 20 m/s. Similar to the mass transfer coefficient, the evaporation rate shows an approximately tenfold increase with a 20-fold increase in air velocity.
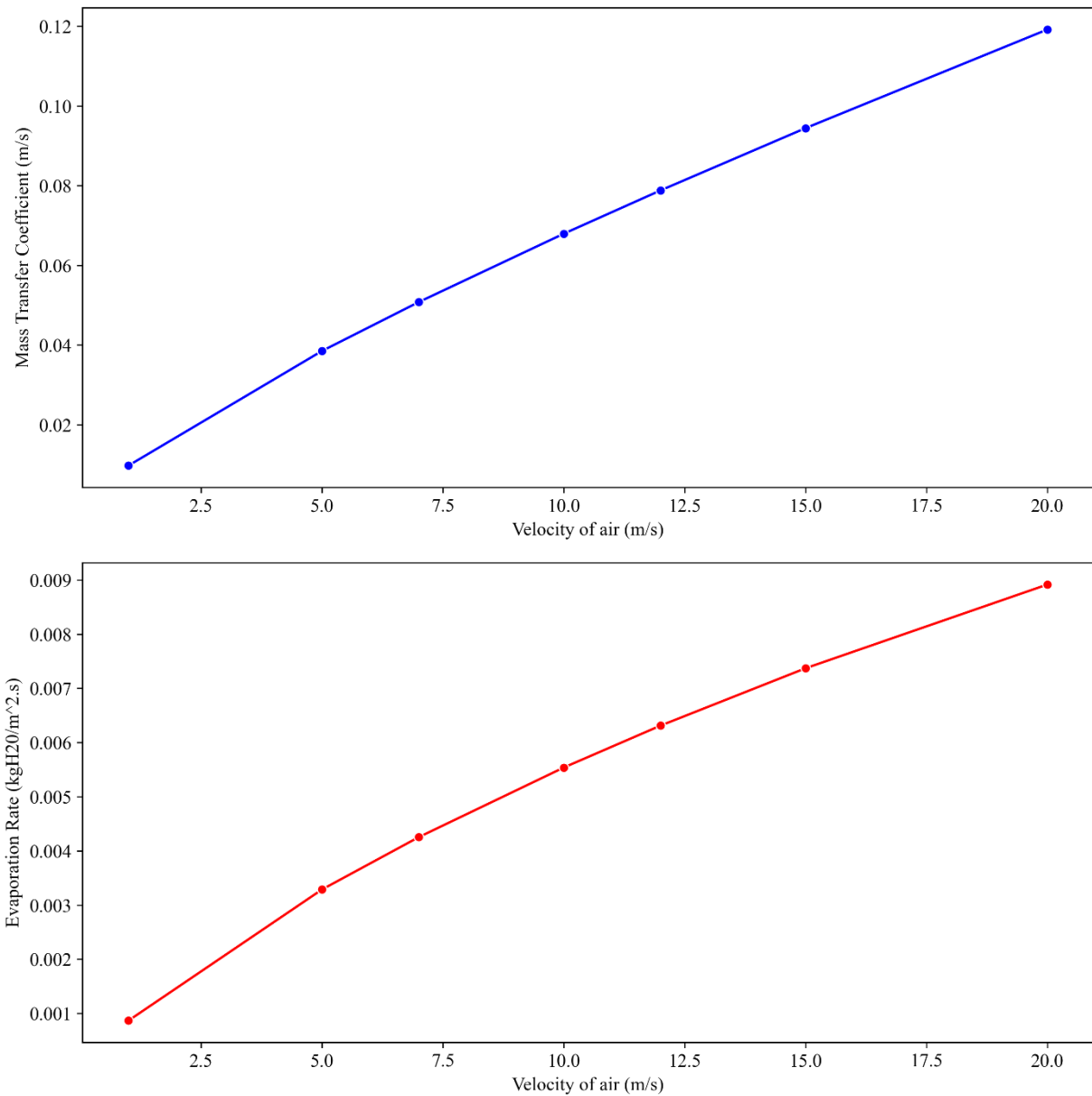
Figure 9 Mass transfer coefficient, evaporation rate with respect to velocity

Figure 10 demonstrates that the drying time with air velocity 1m/s is 23 hr. Supplying air at 5, 7, 10, 12, 15, 20 m/s gives a drying time of 6, 4.59, 3.43, 2.96, 2.47, 1.95 hrs. respectively. Likewise, the drying time decreases as the velocity of hot air increases at the inlet of the farm. It is assumed that the hot air is uniformly distributed throughout the farm. During the calculation, we have floor heating in the poultry farm and is believed that the water in the floor is heated to 50°C during this drying process. However, there can be still problems while applying practically.
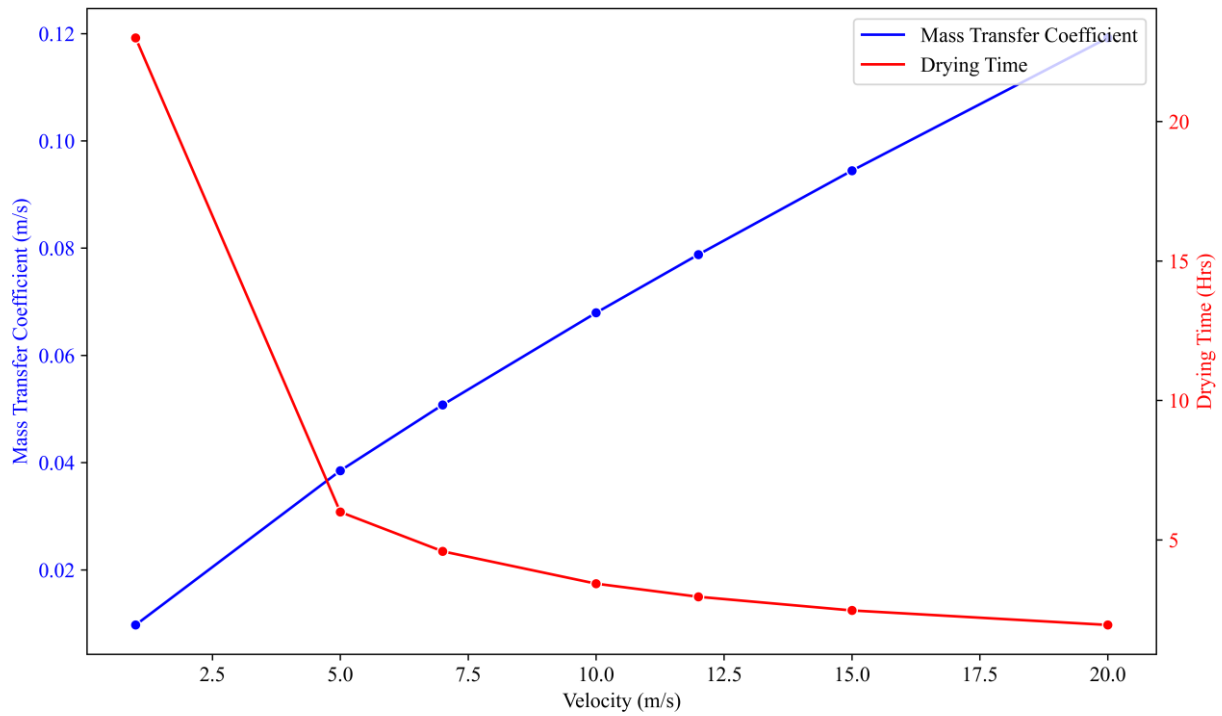
Figure 10 Drying Time at different velocities of air supply

5. CONCLUSION

In this study, the analysis performed on the uncertainty of the sensor shows that the energy consumption measured in the farm is ±0.41% of the measured value. Likewise, the temperature sensor and flow meter sensor's working characteristics and features have been analyzed. A 120-kW heat pump system is designed based on the starting of energy production during cold days. A heat pump is simulated with parallel evaporators, and a single evaporator using Dymola. This results that a parallel evaporator arrangement with FGBV performs better than a single evaporator. A COP measured for the layout with parallel evaporators gives COP of 4.5 and COP for a single evaporator as a source gives COP of 3.6. Hence, a parallel evaporator with FGBV provides the best solution for heating chicken farms rather than using city water as a source at 15 ℃ in this case. Likewise, the system examines the drying of the concrete surface with the heat pumps. The drying time is calculated theoretically using different formula and methodologies assuming that 2 cm thick water is above the concrete in an area of 2000 m². The drying time supplying 50 ℃ of hot air with uniform distribution throughout the surface, gives the drying time of 23 hours at air velocity of 1 m/s. Likewise, increasing the velocity of air resulted in an increase in mass transfer coefficient from 0.0097 m/s to 0.1192 m/s starting from velocity 1 m/s to 20 m/s. The moisture capture from the wet floor is better at low-velocity air supply since the relative humidity of air at exit in drying is 100% with exit temperature 25 ℃. Hence, the velocity of air at slow movement can be useful for energy savings and better output rather than supplying high velocity hot air.

ACKNOWLEDGEMENTS

REFERENCES

Coleman, H. W., & Steele, W. G. (2018). *Experimentation, validation, and uncertainty analysis for engineers*. John Wiley & Sons.

Gullo, P., Hafner, A., & Cortella, G. (2017). Multi-ejector R744 booster refrigerating plant and air conditioning system integration–A theoretical evaluation of energy benefits for supermarket applications. *International Journal of Refrigeration*, *75*, 164-176.

Incropera, F. P., Dewitt, D. P., Bergman, T. L., & Lavine, A. S. (2013). Principles of heat and mass transfer. *(No Title)*.

Liu, Z., Deng, Z., Davis, S. J., Giron, C., & Ciais, P. (2022). Monitoring global carbon emissions in 2021. *Nature Reviews Earth & Environment*, *3*(4), 217-219.

Poore, J., & Nemecek, T. (2018). Reducing food's environmental impacts through producers and consumers. *Science*, *360*(6392), 987-992.